Investigation on the Performance of Solar Thermal-Powered Vapor Absorption Refrigeration System Integrated with Phase Change Material for Vaccine Storage

Daniel Merga Bekele

A Thesis Submitted to

the Department of Mechanical Engineering

School of Mechanical, Chemical and Materials Engineering

Presented in Partial Fulfilment of the Requirement for the Degree of Master of Science in Thermal Engineering

Office of Graduate Studies

Adama Science and Technology University

November, 2022

Adama, Ethiopia

Investigation on the Performance of Solar Thermal-Powered Vapor Absorption Refrigeration System Integrated with Phase Change Material for Vaccine Storage

Daniel Merga Bekele

Advisor

Dr. Addisu Bekele

A Thesis Submitted to

the Department of Mechanical Engineering

School of Mechanical, Chemical and Materials Engineering

Presented in Partial Fulfilment of the Requirement for the Degree of Master of Science in Thermal Engineering

Office of Graduate Studies

Adama Science and Technology University

November, 2022

Adama, Ethiopia

DECLARATION

I hereby declare that this Master Thesis entitled "**Investigation on the performance of solar thermal-powered vapor absorption refrigeration system integrated with phase change material for vaccine storage**'' is my original work. That is, it has not been submitted for the award of any academic degree, diploma or certificate in any other university. All sources of materials that are used for this thesis have been duly acknowledged through citation.

Daniel Merga Bekele ______________________ ________________

Name of student Signature Date

RECOMMENDATION

I, the advisor of this thesis, hereby certify that I have read the revised version of the thesis entitled "**Investigation on the performance of solar thermal-powered vapor absorption refrigeration system integrated with phase change material for vaccine storage**'' prepared under my guidance by Daniel Merga submitted in partial fulfilment of the requirements for the degree of Master of Science in thermal engineering. Therefore, I recommend the submission of revised version of the thesis to the department following the applicable procedures.

Dr. Addisu Bekele	____________________________	__________________________
Advisor	Signature	Date

APPROVAL PAGE

I, the advisor of the thesis entitled "**Investigation on the performance of solar thermal-powered vapor absorption refrigeration system integrated with phase change material for vaccine storage**" and developed by **Daniel Merga,** hereby certify that the recommendation and suggestions made by the board of examiners are appropriately incorporated into the final version of the thesis.

Dr. Addisu Bekele	____________________	______________
Advisor	Signature	Date

We, the undersigned, members of the Board of Examiners of the thesis by **Daniel Merga** have read and evaluated the thesis entitled "**Investigation on the performance of solar thermal-powered vapor absorption refrigeration system integrated with phase change material for vaccine storage**'' and examined the candidate during open Défense. This is, therefore, to certify that the thesis is accepted for partial fulfilment of the requirement of the degree of Master of Science in Thermal Engineering

Chairperson	Signature	Date
Internal Examiner	Signature	Date
External Examiner	Signature	Date

Final approval and acceptance of the thesis is contingent upon submission of its final copy to the Office of Postgraduate Studies (OPGS) through the Department Graduate Council (DGC) and School Graduate Committee (SGC).

Department Head	Signature	Date
School Dean	Signature	Date
Office of Postgraduate Studies, Dean	Signature	Date

ACKNOWLEDGEMENT

First of all, I would like to thank the almighty God for everything. Next, I would like to express my deep and sincere gratitude to my advisor Dr. Addisu Bekele for his continuous genuine support, advise and sharing his immense knowledge. Also, I would like to thanks Dr. Gezahegn Habtamu for his encouragement and friendship during my master's study as well as thesis work. Additionally, I would like to extend my warmest gratitude to my MSc course teachers. I am extremely grateful to my parents for their love, prayers and preparing me for my futures. Finally, my thanks go to all the people who have supported me to complete this thesis work directly or indirectly.

ABSTRACT

A vapour absorption refrigeration system is a type of refrigeration system that uses thermal energy as a source of power. This study has investigated the performance of a solar thermal-powered vapour absorption refrigeration system integrated with phase change materials for vaccine storage based on the required refrigeration capacity of Mukiye Haro rural health center. This system contains parabolic trough solar collector and single-effect vapour absorption refrigeration system with NH_3-H_2O as the working fluid where ammonia is refrigerant and water is absorbent. This study is developed first by determining the cooling capacity of the selected area, design the major components of both parabolic trough solar collector and single-effect vapour absorption refrigeration system, constructing the prototype by integrating phase change materials and lastly, experimentally tested the prototype. From the data collected, 8707.5cm^3 cold chain capacity is required and based on the required capacity the cooling capacity is calculated to be 0.26 kW. Maximum coefficient of performance of the system is determined from analyses made between varies absorber and generator temperature for constant condenser and evaporator temperatures. According to the analysis, the maximum coefficient of performance of 0.66 is obtained at 75 and 25℃ generator and absorber temperatures respectively, for a constant condenser temperature of 30℃ and a refrigerant temperature in the evaporator coil of -2℃ to keep the evaporator temperature at 5℃. Also, the coefficient of performance was calculated from the experimental result using the average temperature of system components recorded during the experiment and its value was 0.6. Parabolic trough solar collector is designed and fabricated for delivering the required energy of 0.39 kW to the generator and the average outlet temperature, useful energy gain and thermal efficiency of parabolic trough solar collector in representative day of the month in the year is 78.4℃, 0.414 kW and 73 % respectively. Finally, the phase change material stored in the generator continuously the system at required temperature for three hours after the outlet solar collector temperature is reduced below the required temperature in the system.

Keywords: Vapour Absorption Refrigeration system, Ammonia-water, Parabolic trough collector, Vaccine storage, Solar thermal, PCM.

TABLE OF CONTENTS

CONTENTS PAGES

LIST OF TABLES

LIST OF FIGURES

ABBREVIATIONS

Symbols	**Descriptions**
BWG	Birmingham Wire Gauge
COP	Coefficient of Performance
DC	Direct Current
DTP	Diphtheria-Tetanus-Pertussis
HX	Heat Exchanger
LHS	Latent Heat Storage
LMTD	Logarithmic Mean Temperature Difference
LPD	Litre Per Day
PCM	Phase Change Materials
PCV	Pneumococcal Conjugate Vaccine
PTC	Parabolic Through Collector
PTSC	Parabolic Through Solar Collector
PV	Photovoltaic
SHS	Sensible Heat Storage
TT	Tetanus Toxoid
VAR	Vapour Absorption Refrigeration
VARS	Vapour Absorption Refrigeration System

NOMENCLATURES

Symbol	Descriptions	Units
Q_{cond}	Conduction Heat transfer	kW
Q_{conv}	Convection Heat transfer	kW
Q_{rad}	Radiation Heat transfer	kW
A_b	Blockage Area	m^2
A_e	Surface area of evaporator	m^2
A_e	Effect of aperture area	m^2
A_f	Geometric factor,	-
A_{gc}	Area of generator coil	m^2
A_l	Aperture area lost	m^2
D_e	Equivalent diameter of the shell	m
G_s	Mass velocity	m/s
Q_{ba}	Heat transfer through back of refrigerator	kW
Q_{bo}	Heat transfer through bottom of refrigerator	kW
Q_d	Heat transfer through the refrigerator door	kW
Q_e	Heat transfer rate in evaporator	kW
Q_{ls}	Heat transfer through left side of refrigerator	kW
Q_{rs}	Heat transfer through right side of refrigerator	kW
Q_t	Heat transfer through top of refrigerator	kW
U_o	Overall Heat transfer coefficient.	$W/m^2.K$
d_{st}	Diameter of storage tank.	m
l_{HEc}	Length of heat exchanger coil	m
l_c	Condenser coil length	m
l_e	Evaporative coil length	m
$\dot{m}$	Mass flow rate of ammonia	Kg/s
x_w	Concentration of water in ammonia	-
C	Concentration ratio	-
To	Outside side air temperature	℃
V	Free stream velocity	m/s
Agt	Area of generator tube	m^2

Hwe	Hot water exits from generator	℃
Hwi	Hot water inlet to generator	℃
Nu	Nusselt number	-
Re	Reynold number	-
$Thwe$	Temperature of hot water exit from generator	℃
$Thwi$	Temperature of hot water inlet to generator	℃
Ta	Ambient temperature	℃
Tav	Temperature of ammonia vapour exit generator	℃
Tg	Generator temperature	℃
Ti	Inside temperature in refrigerated space	℃
Tss	Strong solution temperature inlet generator	℃
Vhw	Velocity of hot water	m/s
mss	Mass of strong solution	kg
mws	Mass of weak solution	kg
x	Quality of fluid flow	-
λ	Circulation ratio	-

GREEK SYMBOLS

Symbols	Descriptions	Units
ϕ	Latitude angle	(°)
ω	Hour angle	(°)
σ	Stefan-Boltzmann constant	W/ $m^2.K^4$
ν	Kinematic viscosity	m^2/s
μ	Dynamic viscosity	Pa. s
θz	Zenith angle	(°)
θ	Angle of incidence	(°)
δ	Declination angle	(°)
γ	Surface azimuth angle	(°)
α	Solar altitude angle	(°)
Ψ	Rim angle	(°)
θ_f	Melt fraction	%
η_{th}	Thermal energy efficiency	%
η_0	Optical efficiency	(%)
γ_s	Solar azimuth angle	(°)

CHAPTER ONE

INTRODUCTION

1.1 Background of the Study

Solar energy is radiant energy produced by the sun. Sun is a big ball of heat and light resulting from nuclear fusion in its core, and its nuclear reaction releases energy that travels outwards to the surface of the Sun. Every day, the sun radiates or sends out an enormous amount of radiant and heat energy. Sun radiates more energy in one second than people have used since the beginning of time (Abdin *et al*.,2013). Heat and light are two forms of solar energy that reach the Earth. The major applications of solar energy can be classified into solar thermal systems, which converts solar energy into thermal energy, and photovoltaic (PV) systems, that converts solar energy into electrical energy.

Solar energy received by the earth through radiation can be absorbed by the solar collector, which convert it to heat energy that can be efficiently utilized for various systems and applications. Solar energy can be used for a variety of things, including: heating water for domestic, commercial and industrial applications; heating air for comfortable space and drying crops; distilling brackish or saline water for drinking, pumping water, powering air conditioning, refrigeration, and ice-making machines and generating power (Yadav and Agrawal, 2018).

However, these sources of energy are available only from sunrise to sunset or are limited to some hours per day. But in many applications, continuous power is required to work efficiently, like in storing vaccines and medicines in refrigerants. Hence, energy storage is needed to compensate for the mismatch between the solar energy available and the required power for refrigeration to work efficiently during the unavailability of solar energy. This energy can be stored in electric (electrical batteries) or thermal form. Among these, the energy stored in the battery has a limited lifespan, use materials with limited availability and have a high maintenance cost. Whereas, energy stored in thermal form or phase change material (PCM) is less expensive and has a lower environmental impact (Hernandez and Roldan, 2021).

1.2 Refrigeration

Refrigeration is the process of removal of heat from a selected environment to cool down or maintain at the required temperature by dissipating heat to the surrounding. It is a very important unit operation that touches most of our daily lives in its applications. A refrigeration system is constructed from different components, which are connected in a sequential order to produce the desired refrigeration effect in the cooling system. Based on operating system component, type of refrigerant used and source of power, the refrigeration system can be classified into three categories: mechanical refrigeration which uses a compressor to compress the refrigerant in the system, absorption refrigeration which uses thermal energy sources and steam jet refrigeration which powered by steam produced in the boiler (Chandra and Arora, 2012).

A vapour absorption refrigeration system (VARS) is an economical type of refrigeration system that uses thermal energy as a source of power. These sources of energy can be solar energy, geothermal energy, process steam plants, waste heat from cogeneration and natural gas when available at a low price. This system contains an absorber and generator connected as one cycle which are integrated with pump and heat exchanger, replacement of the compressor in a vapour compression refrigeration system, in addition to a condenser, evaporator and expansion valve to cool the substance in the evaporator. Accordingly, the vapour absorption refrigeration system has an advantage over the vapour compression refrigeration system because work input is low and the source of power is more available.

Because of its abundance and low cost, a solar-powered vapour absorption refrigeration system is superior to other sources. Based on the method by which solar energy can be utilized for refrigeration purposes, it can be divided into the solar electric method, solar thermal method, and solar mechanical method. The solar electric method is the one that directly converts energy from the sun to direct current (DC) by using an array of solar cells known as photovoltaic panels, whereas the solar mechanical method uses energy from the sun to drive the compressor (Karl, 2014).

The solar thermal method is the one that used heat rather than electricity which can utilize more of the incoming sunlight than the PV system. In a solar collector over 95% of the incoming solar radiation is absorbed whereas, in a PV collector 65% of incident solar radiation is lost (Sinha and Karale, 2013). To transfer energy between components and refrigerated space the integration of solar collector, thermal storage tank, refrigeration system, and heat exchanger are very important.

The importance of solar thermal refrigeration systems is greatest, especially in rural areas where electricity is unavailable. So, this study investigated a solar thermally powered vapour absorption refrigeration system for vaccine storage based on the determined cooling capacity from Mukiye Haro rural health center.

1.3 Statement of the Problems

In Ethiopia, vaccine storage in the rural health center is a big challenge. This is because of poor or unstable power supply, a lack of fuel for generators, insufficient cold boxes, insufficient ice packs for cold temperature maintenance, and insufficient refrigerators. As a result, vaccine has been transported from towns. Vaccines need to be continuously stored between 2 to 8°C, from their production to administration up to beneficiaries. However, many vaccines are wasted during transportation because of vaccines are sensitive to environmental change and light, that causes reach the vaccine to inappropriate temperature and affect the vaccine puissance. So, to maintain vaccine quality, it must be protected from extreme temperatures because once lost, vaccine potency cannot be regained. To do this, vapour absorption refrigeration systems powered by solar energy, which are environmentally friendly are developed in this study based on the required refrigeration capacity of Mukiye Haro rural health center. This system works by receiving heat from the solar energy, using ammonia-water refrigerant absorbent which are environmentally friendly and also use phase change material for the time of fluctuation and unavailability of solar energy to maintain the vaccine at required temperature without interruption.

1.4 Objectives of the Study

1.4.1 General Objective

The main objective of this study is to analyze the performance of a solar thermal-powered vapor absorption refrigeration system integrated with phase change materials for vaccine storage in the case of Mukiye Haro rural health center.

1.4.2 Specific Objectives

The specific objective of this studies is to:

- ✓ Determine the refrigeration capacity required for vaccine storage in Mukiye Haro rural health center.
- ✓ Design a single-effect vapour absorption refrigeration system that uses NH_3-H_2O refrigerant- absorbent for the determined refrigeration capacity
- ✓ Analyse the performance of single-effect vapour absorption refrigeration system

- ✓ Design the solar collector based on the required generator temperature in the system.
- ✓ Develop the prototype of the designed single-effect vapour absorption refrigeration system
- ✓ Test the performance of single-effect vapour absorption refrigeration system integrated with and without phase change material.

1.5 Conceptual Framework

Refrigeration is the process of removing heat from a selected environment to cool down and maintain at the required temperature. A vapour absorption refrigeration system is one type of refrigeration system that uses heat energy as a source of power from different sources. The solar power vapour absorption refrigeration system is the one that receives heat from the sun and contains a solar thermal collector, generator, absorber, condenser, evaporator, expansion valve, and mini pumps to cool a substance in the system. The working principle can be classified into hot water circuits and refrigerant circuits. In a hot water circuit, the available cold water is first filled in the storage tank, then the parabolic trough solar collector is placed in the open atmosphere in the correct way of the tracking system, then water in the storage tank is pumped into the receiver tube of the solar collector to receive heat from the solar radiation reflected from the parabolic trough solar collector and finally, recirculated into the storage tank. In a refrigerant circuit, ammonia solution is filled in the absorber tank, the strong solution of ammonia in the absorber is pumped to the generator, the solution is heated in the generator by heat from the solar collector, and ammonia (refrigerant) turns to vapour quickly because it has a lower boiling temperature than the absorbent. Eventually, if the inlet temperature to the generator is high, absorbent (water) will also turn into vapour and enter to the system, that causes reduce the efficiency and may be damage the systems. So, the rectifier attached at the top edge of the generator that rectifies the water vapour from ammonia vapour and sends water back to the generator by cooling it. The absorbent was dropped into the absorber, passing through the heat exchanger by reducing its temperature. Additionally, in this system, phase change material is added at the bottom of the generator in order to maintain the fluctuation of solar energy and is used as heat storage for the time when solar energy is not available. The large pressure, high-temperature pure ammonia vapour enters the condenser through connected pipe and releases heat into the environment and completely converts into liquid. After condensation, the liquid ammonia is passed to the expansion valve, where the pressure of the refrigerant reduces significantly and it becomes very cold liquid ammonia. This liquid refrigerant enters the evaporator through a connecting pipe to the evaporator coil and absorbs heat from the substance in the evaporator. The substance in the evaporator cools down by losing heat to the liquid refrigerant. Finally, the liquid refrigerant converts into saturated vapour and enters the absorber. This entire cycle was repeated again and again.

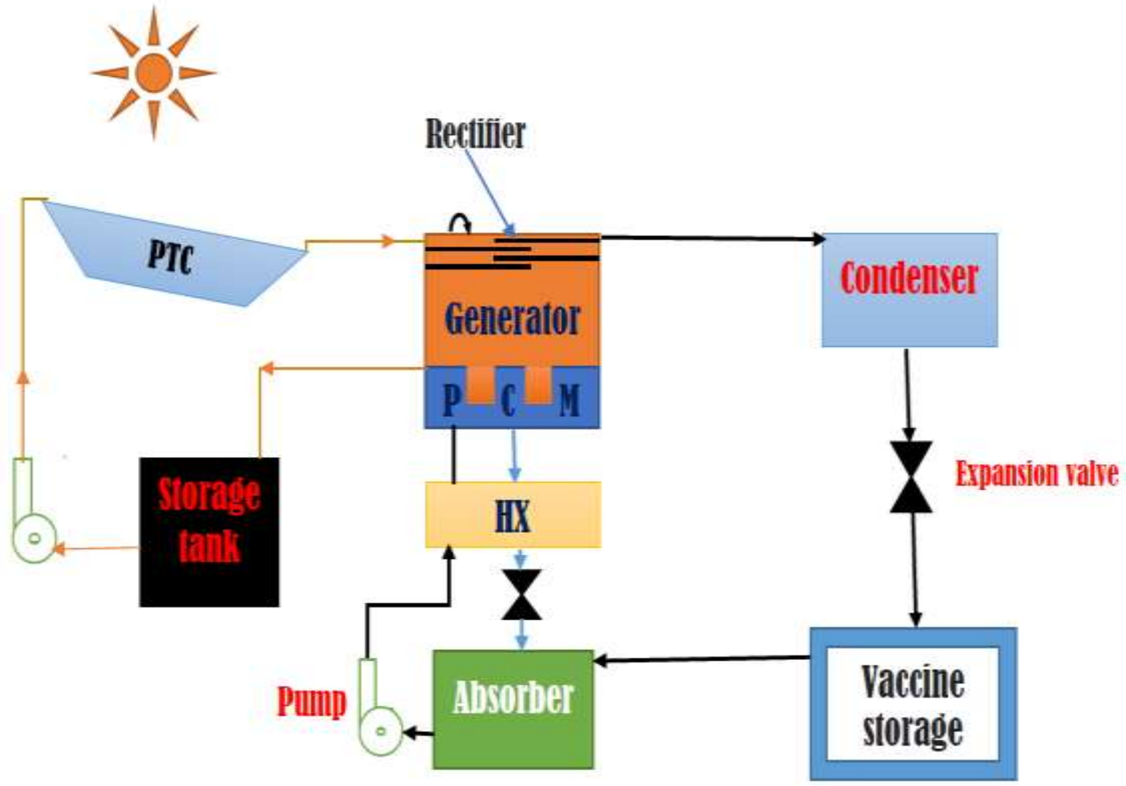

Figure 1.1 Schematic diagram of solar thermal collector integrated with VAR system.

1.6 Significance of the Study

Successful implementation of the study primarily solves the problems of rural health centres to store vaccines at the required temperature. It also increases the storage time of the vaccine for a long time, including at night by using phase change materials. Generally, it reduces the death of children in rural areas by maintaining the temperature of the refrigeration system that stores vaccines.

1.7 Scope and Limitation of the Study

This study was focused on the performance analysis of solar-powered vapour absorption refrigeration systems for vaccine storage in the rural health centre. The analysis has been done by determining the required refrigeration capacity for selected rural health, study the solar potential, design the solar collector required for determined refrigeration capacity based on the solar potential and design the vapour absorption refrigeration system based on refrigeration capacity. It also includes analyses the system performance, develop and test the prototype of solar powered vapour absorption refrigeration system. Finally, investigate the impact of phase change material on a vapour absorption refrigeration system. While doing this thesis, the material unavailability and the disproportionality of the cost given vs material cost can be raised as limitations.

1.8 Organization of the Study

This thesis is organized with 7 chapters. The first chapter introduces the concept of solar energy, refrigeration system and solar powered refrigeration system integrated with phase change materials. The second chapter includes literature reviews on vapour absorption refrigeration system, parabolic trough solar collector and phase change materials. It also includes literature summary and research gap. The third chapter presents the methods and material used in this study in order to develop the system, the fourth chapter describes the design components of both vapour absorption refrigeration system and parabolic trough solar collector. The fifth chapter includes the fabrication process of solar powered vapour absorption refrigeration system integrated with phase change materials. The six chapter contains result and discussion and the last chapter composed, conclusions and recommendations.

CHAPTER TWO

LITERATURE REVIEW

2.1 Introduction

This chapter contains: definitions, classifications and previews work on vapour absorption refrigeration system, solar collectors and phase change materials. Also, it includes summary of literature review and research gap from the previous work on solar thermal powered refrigeration system.

2.2 Vapour Absorption Refrigeration System

Vapour absorption refrigeration (VAR) system is a type of refrigeration system which uses energy in the form of heat rather than electricity in a vapour compression refrigeration system. This heat energy can be from solar energy, geothermal energy, waste heat from cogeneration, and natural gas that are available at a low price. Hence it is an economical type of refrigeration. This system consists of five main components, namely generator, absorber, condenser, evaporator and heat exchanger which are connected in a sequential order to produce the desired refrigeration effect in the cooling system.

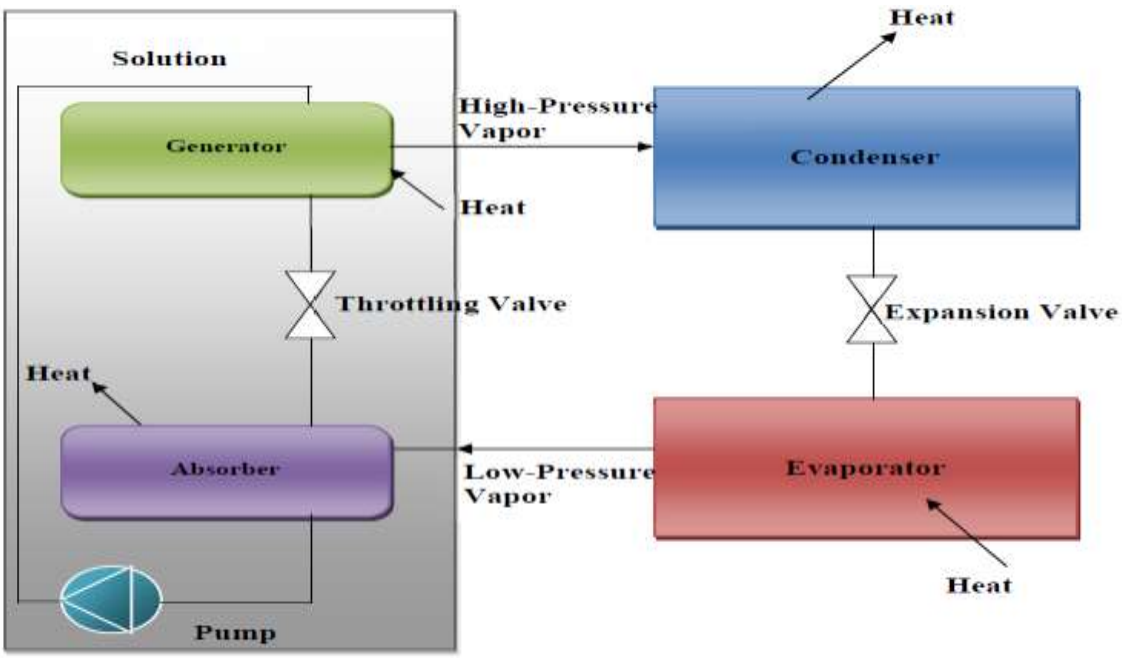

Figure 2.1 Basic absorption refrigeration system (Karl, 2014).

2.2.1 The basic components of Vapour Absorption Refrigeration System

Vapour absorption refrigeration system have different components in order to cool the substance in the system.

1, Generator: is one of the components of vapour absorption refrigeration system that deliver the refrigerant vapour to the rest of the system by separating the refrigerant from the solution. In this system the refrigerant absorbent solutions pumped from the absorber are falls on horizontal tube which contains a high temperature generated from the external source either from solar, geothermal or west heat then heat is transferred between them, and finally the refrigerant vaporized from the solution and move to the condenser. From different types of heat exchanger cross flow type is selected for our system due to the way of heat is transferred from generator coil to the refrigerant absorbent solution is cross flow type heat exchanger.

2, Condenser: it is an important device used to remove heat from refrigerant vapour discharged the generator until it condenses into saturated liquid. The heat from the hot vapour refrigerant in the condenser is removed first by transferring heat to the wall tube of condenser and next from the tube wall to the cooling medium**.** The cooling medium may be air, water or combination of the two. In our system natural convection air cooled condenser are selected because of simple construction and less cost and also fouling effect is low. The natural convection type condensers are can be classified as plate surface type and finned tube type. Both of them are used for small refrigerator where the refrigerant carrying tube is attached to the outer wall of the refrigerant.

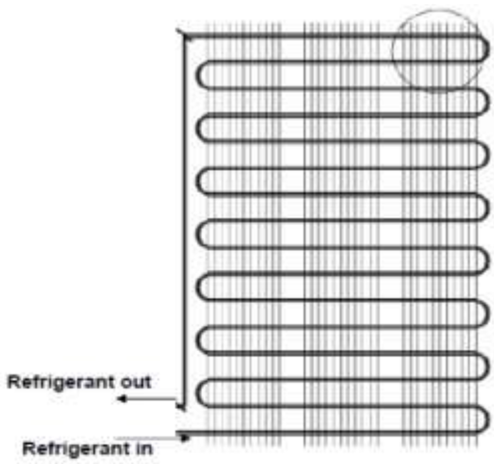

Figure 2.2 Schematic of a wire-and-tube type condenser used in small refrigeration systems (Jejaw and Getnet,2021)

3, Evaporator: It is a part of refrigeration system where refrigeration effect is takes place by absorbing heat from materials to be cooled**.** The refrigerant exits the condenser passes in the expansion valve by reducing its temperature and pressure, then it enters into evaporator coil. Based on the construction type evaporator can be classified as bare tube, finned tube, shell and tube, shell and coil, tube in tube and plate evaporator. For our system natural convection bare tube coil evaporator are selected because of simple construction, easy to clean and defrost.

4, Absorber: It is a heat exchanger where refrigerant and absorbent are mixed. Also, the weak solution flow back from the generator and the refrigerant vapour produced in the evaporator was mixed in the absorber.

5, Solution heat exchanger: is a device that exchange heat between the strong solution having low temperature pumped from the absorber and weak solution that have high temperature dropped from the generator. The installation of this heat exchanger has many advantages for the system includes minimize heat loss, reduce the load on the collector and increase the coefficient of performance of the system.

How the system works

The working principle of vapour absorption refrigeration system can be clarified by the figure 2.1 above. Absorbent and refrigerant are mixed first in the absorber, then the strong solution formed are pump to the generator by the help of pump where the refrigerant and absorbent are separated by the high temperature external heat from either solar, geothermal or west heat from industry. In generator after heat is exchange between the external heat and the absorbent refrigerant solution, the refrigerant vapour is formed and goes to the condenser, whereas the weak solution having high contents of absorbent are dropped to the absorber passing the heat exchanger. The refrigerant vapour goes to the condenser are changed into liquid by releasing heat to the environment, also it continues to reduce temperature and pressure in the expansion valve up to evaporator to give the cooling effect in the evaporator. The absorbent dropped into the absorber is again mixed with the vapour formed in the evaporator by absorbing heat from the substance to be cooled and the system circulate.

2.2.2 Classification of Vapour Absorption Refrigeration System

Vapour absorption refrigeration system can be classified based on thermodynamic cycle, source of power and type of refrigerant used to achieve cooling effect in the system

1, **Depends on thermodynamic cycle**

Based on the operation of the thermodynamic cycle and the way the solution regenerates vapour absorption refrigeration system can be divided into three categories: single-effect, double-effect, and triple effect vapour absorption cycles. Also based on their performance it can be classified into: -single, double, and triple effects which are having 0.6 to 0.8, 1.0 to 1.2 and 1.4 to 1.6 respectively.

A, Single effect vapour absorption refrigeration system

It is a vapour absorption refrigeration system having single heat exchanger and generator where heat is added for the system. Its working principle is same with the above described.

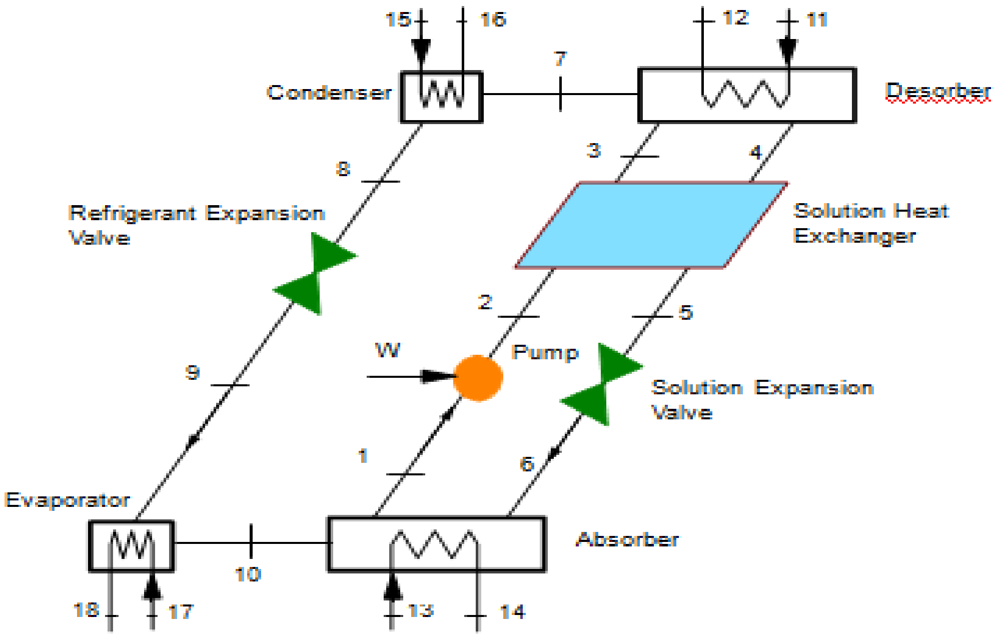

Figure 2.3 Schematic diagram for single effect VAR system (Kanabar and Ramani, 2018).

B, Double effect vapour absorption refrigration system

This system consists of high temperature generator and lower temperature generator,condenser,two solution heat exchanger,absorber, evaporator,water circulating pump,three throattling valve. The input energy required coefficient of performance was higher than the single effect.

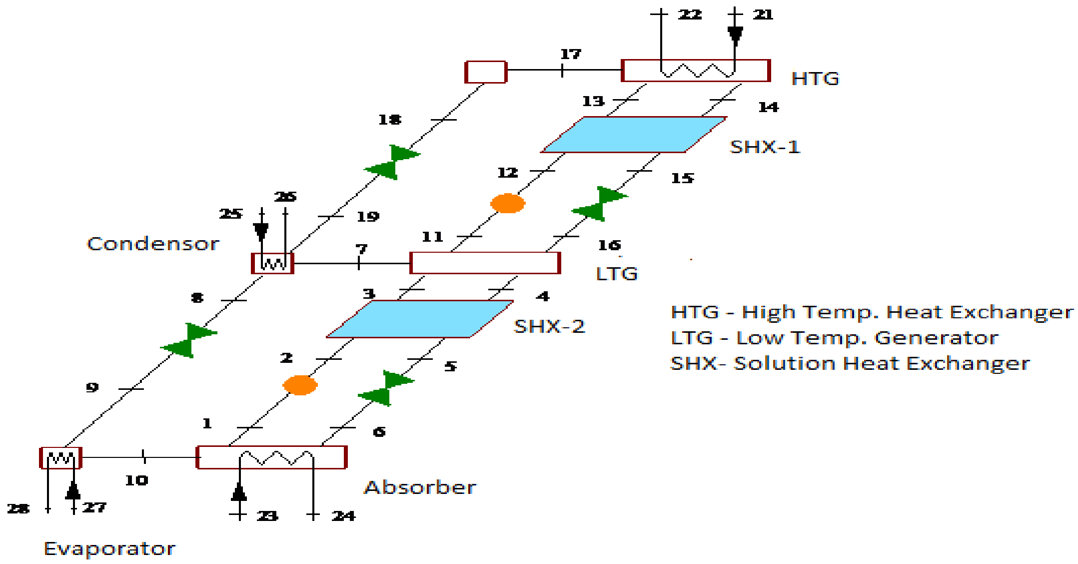

Figure 2.4 Schematic Diagram for Double Effect VAR System (Kanabar and Ramani, 2018).

C, Triple effect or multi effect vapour absorption refrigeration system

It has one additional generator on the double effect and if the source temperature is higher this system is better to obtain high COP.

Reviewed literatures under these topics

Solanki and Pal (2020) investigated a triple effect vapour absorption refrigeration system of 100 kW cooling capacity using a parabolic trough collector. The system has three generators: -high, medium, and low-temperature generator to concentrate a dilute LiBr which is received from the absorber in addition to other vapour absorption refrigeration system components. It is used in industrial applications for cooling purposes by receiving input heat energy around 140-180°C from a solar collector to cool the system effectively. From the experimental result, evaporator temperature is maintained in the range of 6.4-8.9°C in the year the experiment was performed.

Wang *et al.,* (2018) analysed the thermal performance of a double effect LiBr-H_2O absorption cooling system using a parabolic trough solar collector. The system consists of a parabolic solar collector, heat storage subsystem and double effect LiBr-H_2O absorption having a high and low-pressure generator, high and low-temperature exchanger, two reducing valves, and two refrigerant expansion valves. In addition to the power from the solar collector, heat-conducting oil is added to the system to increase the input energy for generators.

Al-Ugla (2015) developed solar air conditioning in Saudi Arabia to accommodate a 24-hour uninterrupted daily cooling load. The system used LiBr-H_2O absorbent refrigerant, three storage systems, and four hybrid storage systems to cool the 5-kW absorption chiller. To cool the system at the required temperature two solar collectors are used, where the first one is the flat plate collector, which provides solar energy for the generator at day time and the second one is the evacuated tube collector, which provides energy to the storage tank in the system for night operation when there are insufficient solar insulations. The storage tank in the systems is a heat storage tank, cold storage tank, and refrigerant storage tank which is powered from the second collector to cool the system effectively.

Pongtornkulpanich *et al.,* (2008) designed and installed a solar-driven 10-ton LiBr-H_2O single-effect vapour absorption cooling system in Thailand. The overall system consists 72 m^2 roof-mounted evacuated tube solar collector, hot storage tank, heat backup system, and fan coil units to produce chilled water. The system works by receiving heat energy from the solar collector, the refrigerant liberated from the solution by supplying heat at the generator and producing a cooling effect in the evaporator. Finally, the chilled water in the evaporator is about 7℃.

Syed *et al.,* (2005) investigated solar energized, single effect (LiBr-H_2O) vapour absorption refrigeration system for 35kW nominal cooling capacity in Madrid during the summer season. The system consists of a 49.9 m^2 flat plate collector, 2 m^3 storage tank and heat exchanger in addition to other components of the VAR system. Primary hot water was circulated through the flat-plate collector panels and heated up to 90 ℃ by the incidence of solar energy on the copper absorber plates. The heat produced was transferred to a storage tank via a plate heat exchanger, then goes to the generator to vaporize the refrigerant and lastly, the refrigerant vapour circulates in the system to give the low temperature in the room. From the reviewed work of literatures, the single effect vapour absorption refrigeration system is the simplest and used one generator only. Also, it can easily construct and the energy required for the generator can harvested from lower energy source. So, for this study single effect vapour absorption refrigeration system are selected.

2, **Depends on the external source of energy/source of power/**

Based on the external source of energy vapour absorption refrigeration system can be classified into:

A, Solar powered vapour absorption refrigeration system

B, Non-solar powered vapour absorption refrigeration system

A, Vapour absorption refrigeration system powered by solar energy

Vapour absorption refrigeration system used different types of energy sources to heat the refrigerant in the generator to cool the substance in the system. It uses waste heat from the industry, solar energy, geothermal or other sources as energy input. From that, solar energy is the most abundant, clean, and eco-friendly source of energy.

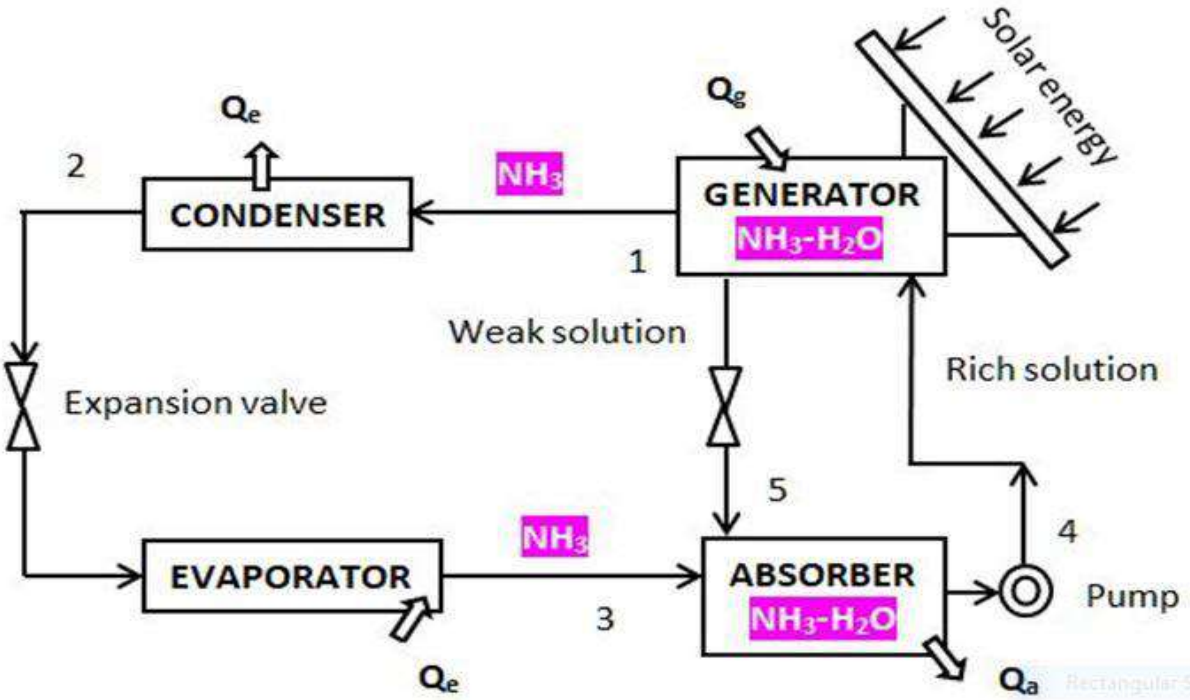

Figure 2.5 Schematic assembly of solar-powered ammonia-water vapour absorption refrigeration system (Oni, 2018).

Depending on the methods by which solar energy was utilized for refrigeration purposes it can be divided into the solar electric method, solar thermal method, and solar mechanical method.

a) **Solar Electric Method**

In this method, the energy from the solar is directly converted to DC by an array of solar cells known as Photovoltaic panels. A part of this current is used to drive the compressor of the refrigerator and the others are stored in the lead-acid battery. The major components of a solar PV system are a solar charge controller, battery bank, inverter, auxiliary energy sources and loads.

b) Solar Mechanical Method

In this Solar Mechanical Method, the compressor is driven by mechanical power which is generated from solar energy. In this system, the Rankine cycle is considered the heat power cycle. The system consists of the integration of a solar collector, storage tank, expander, heat exchanger, condenser, and pump to work effectively for required purposes. The Rankine cycle efficiency can increase by increasing the expander temperature and rotating the solar collector into the sun's positions.

c) Solar Thermal Method

The solar thermal method is the one that used heat rather than electricity which can utilize more of the incoming sunlight than the PV system. This source of energy is harvested from the solar radiation using solar collectors. In a solar collector over 95% of the incoming solar radiation is absorbed whereas in a PV collector 65% of incident solar radiation is lost (Sinha and Karale, 2013). To transfer energy between components and refrigerated space the integration of solar collector, thermal storage tank, thermal refrigeration system and heat exchanger are very important.

Reviewed literatures under this topic

Hashim and Kassim's (2021) studied solar powered vapour absorption refrigeration system with LiCl-H_2O refrigerant absorbent bubble pump for water cooling system experimentally. The system contains a parabolic trough solar collector, condenser, evaporator, absorber, and water-cooling system. It is also modified by adding a separator on the top of the generator where strong solution and water vapour are separated. From the experiment, the result shows collector efficiency increases as the water through the collector receiver increase and the maximum temperature obtained in the generator and absorber are 87 and 17℃ respectively in July. Also, the system can work efficiently for a generator temperature between 86 to 71℃.

Almultashi *et al.,* (2021) analysed the effect of using ethyl ether-acetaldehyde solution in a solar-driven absorption chiller integrated with a parabolic trough solar concentrator experimentally for a cooling capacity of 0.5 kW. In these experiments, by using vapour absorption refrigeration system components ethyl-ether-acetaldehyde solution is compared with lithium bromide-water solutions. The results show that ethyl ether –acetaldehyde solution requires less hot water (78°C) from the solar collector and produce more chilled water temperature (7°C) in the evaporator, while the lithium bromide-water solution requires more solar energy (90°C) and the temperature of chilled water the in the evaporator is high (16°C) when compared with the above solution. So, the coefficient of performance improves from 0.64 to 0.78 by using ethyl ether-acetaldehyde.

Devarajan *et al*., (2021) analysed the effect of the integration of solar collectors on the performance of solar-powered ejector systems. Scheffler concentrator and flat plate collector are two solar collectors which have 2.7 and 5 m^2 collecting areas simultaneously coupled with the storage tank of 15 L capacity. The system contains an ejector in place of the absorber in addition to other main components of vapour absorption refrigeration systems with R134a and tetrafluoromethane refrigerants. The ejector has a nozzle section, mixing section, throat section, and diffuser section which are specifically used to reduce the pressure of refrigerant from the generator. From the study, the effect of integration of solar collectors produces higher generator temperature closer to 200°C and the COP of the system increased from 0.22 to 0.47.

Ghyadh *et al*., (2020) designed and fabricated a vapour absorption refrigeration system using a parabolic trough solar collector for a cooling system. The components of vapour absorption refrigeration systems are: - parabolic trough solar collector, condenser, evaporator, generator, capillary tube, storage tank, absorber, and pumps. The system uses a water-methanol solution, where methanol is refrigerant and water is absorbent to cool the substance in the evaporator. As the result shows temperature is varied based on solar radiation in different months. In this study 85°C in July is the maximum temperature of the generator which increases the performance of the system and reduces the evaporator temperature in the range of 9.8 -15.8°C.

Bose and Modi (2020) studied the exergy analysis and cost optimization of solar plate collectors for a two-stage absorption refrigeration system using water-lithium bromide as working fluids. The system contains a two-stage absorption system, two water-lithium bromide solutions where one is high pressure and others low pressure, two throttling valves, condenser, evaporator, and also absorber, evaporator, and generator having high pressure and low pressure each of them. The source of power for high and low-pressure refrigerators are FPC-2 and FPC-1, respectively.

Natnale (2019) investigated solar vapour absorption refrigeration system integrated with phase change material using numerical methods for industrial applications. The system consists of an evacuated heat pipe collector, water-lithium bromide refrigerant-absorbent, and latent heat as thermal energy storage to give the required cooling system. Bekas chemical PLC and Ah-Wan food complex were the selected industry for the study to produce chiller capacities of 186.66 and 245 kW respectively. Finally, the result showed that 242 units of heat pipe evacuated tube collector with 4.917m height and 3.278m diameter storage tank is required for Bekas chemical PLC and 310 units of evacuated tube collector with 5.334m height and 3.556m diameter storage tank is needed for Ah-Wan food complex to produce the required chilling capacity.
Yadav and Saikhedkar (2017) developed the simulation modelling of a VAR system using a parabolic disc and an evacuated tube collector working in a conjugate system. The system uses NH_3-H_2O solution where ammonia is refrigerant and water as an absorbent to develop the system and performance analysis of two solar collectors. To increase the performance, the disc type collector is adjusted manually according to sun tracking, whereas the evacuated tube collector is inclined at 45^0 in the experiments. Finally, the result shows as the collector area increases the efficiency of the generator increase, this shows the COP of the cycle became increases.

Rasul and Murphy (2006) designed and studied solar powered vapour absorption refrigeration system for vaccine storage in remote desert areas away from the electrical national grid. This system used aqua ammonia solution for absorbent refrigerant where the volume of cabinet is $0.6\times 0.3 \times 0.5$ m and insulated by 0.05 m of fiberglass. The cylindrical concentrator solar collector having 1.5×0.5 m aperture area and 0.05 m pipe diameter at the centre are used to give the required power input to the system. The system performance was analysed by using MATLAB and Excel software and finally the coefficient of performance was ranged between 0.5 and 0.65.

Gandhi and Arakerimath (2016) studied vapour absorption refrigeration systems for cooling purposes using a flat plate collector. The system contains a solar water heating system circuit and vapour absorption refrigeration system circuit. This experimental study used ammonia-water solution for the refrigerant and absorbent to circulate the system. From the experimental study, the result shows maximum temperature drop in the evaporator, and the coefficient of performance increased by 0.62.

Mohanty and Padhiary (2015) analysed the thermodynamic performance of a vapour absorption refrigeration system using an evacuated tube solar collector as a source of energy and LiBr-H_2O solution where water is a refrigerant. This solar-powered vapour absorption refrigeration system contains four major system condenser, evaporator, absorber, and generator. Also contains an expansion valve, heat exchanger, and pump to circulate refrigerant to cool substances in the evaporator at required temperatures. Finally, from the result obtained, the generator temperature is 90℃ and absorber temperature is 40℃ which is enough to give the required temperature (5°C) in the evaporator.

Shukla *et al*., (2015) studied the coefficient of performance derivation and thermodynamic calculation of NH_3-H_2O vapour absorption refrigeration system for cooling purposes. This system uses a rectifier in addition to four main components of the VAR system in between condenser and generator to purify ammonia vapour in the generator. To calculate the COP of the system, thermodynamics properties like enthalpy, mass flow rate, flow ratio, heat, and mass transfer are analysed by applying mass and energy balance for each component. Finally, after the design and analysis of each component, the COP of the system is approximately 0.598.

Raja and Shanmugam (2012) reviewed the approach to minimize the cost of a solar-assisted absorption cooling system using LiBr-H_2O solution in absorber and water as a refrigerant. The main components of solar-assisted VAR systems for cooling systems are the coupling of the solar field which is the source of power, absorption cooling system, and heat storage tank. Analysis of initial and operating coast is used to understand comfort demands and the environmental impact of the system. Initial cost, operating cost, and maintenance cost were analysed in this study. Finally, it is concluded that cooling systems using LiBr-H_2O as working fluid in VAR system are suitable for domestic purposes and the cost analysis can be improved by placing the generator inside the insulated storage tank to reduce heat loss, putting hot water storage tank above the solar collector ad using vacuum pressure of the cooling circuit to increase boiling of water in the generator.

B, Vapour absorption refrigeration system powered by non-solar energy

Not only solar energy, there are also many types of renewable energy used in the refrigeration system. This includes geothermal energy, waste energy from the industry, biomass energy, exhaust gas from engine of vehicles and boats are the common ones. In this system the working principle is the same with solar powered refrigeration system, the only difference is the external energy source and the way heat is transferred to the refrigerant.

Reviewed literatures under this sub topics.

Manojprabhakar *et al.,* (2014) fabricated and tested vapour absorption refrigeration system powered by engine waste heat using ammonia water refrigerant- absorbent solution. The system contains 95℃ generator temperature,40℃ condenser temperature,8℃ evaporator temperature and 165℃ engine exhaust temperature. Also, 72gm of ammonia with 0.133kg mass of water for refrigerant and the actual and theoretical coefficient of performance was 0.22 and 0.39 respectively.

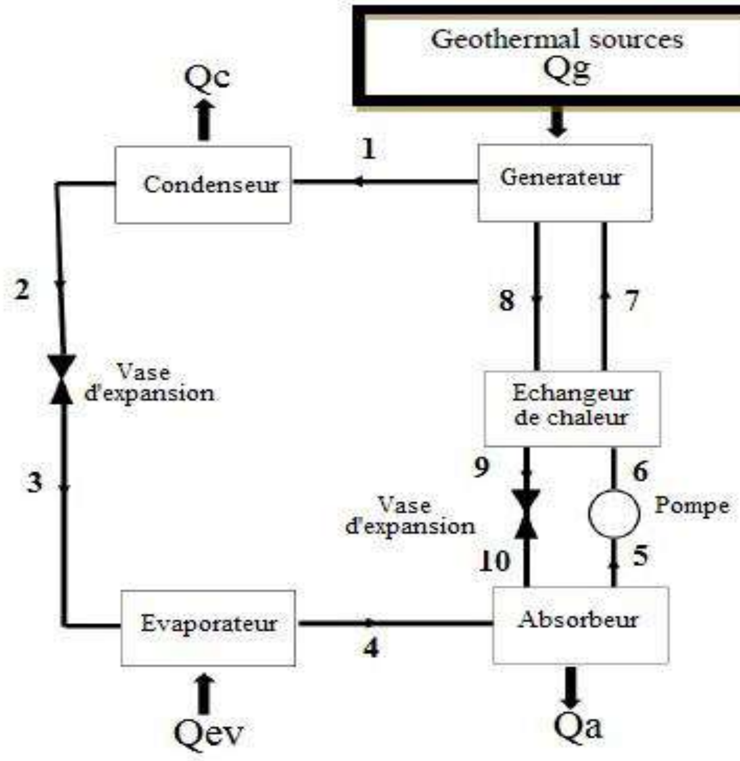

Figure 2.6 Non-solar powered vapour absorption refrigeration system (Ketfi *et al*., 2015)

Tetemke *et al*., (2021) analysed vapour absorption refrigeration systems powered by geothermal energy for cool drinking water at Dilla University, Ethiopia. The source of this geothermal energy is the Gedeo and Guji zone which are about 359 and 375 km from Addis Ababa to the south of Ethiopia and their average measured temperature is approximately 54 and 88.25 ℃ respectively. The system uses ammonia-water as refrigerant-absorber pair comprised of components of condenser, absorber, generator, pump, evaporator, heat exchanger, and expansion valve for cooling purposes. By using the above system, the drinking water temperature of Dilla University is reduced from 37 to 16℃ within 16 hrs.

Horuz and Callander (2004) investigated the performance of commercially available vapour absorption refrigeration systems experimentally using an aqua-ammonia solution with water as absorber and ammonia as a refrigerant to produce a rated cooling capacity of 10 kW chilled water for air conditioning. The system contains a solution-cooled absorber in addition to other common components of the vapour absorption refrigeration system: condenser, absorber, expansion valve, generator, and evaporator that is used as a heat exchanger in other units for transfer heat to the strong solution before entering to the generator to reduce external heat required. The input energy of the system is from hot combustion gases flowing around the lower finned part of the generator and providing the energy input for the system.

Bangotra (2017) designed and analysed generator for vapour absorption refrigeration system for automotive air conditioning. The generator was designed for 3.5kW cooling capacity which required to evaporate refrigerant with pressure of 20 bar and 95°C temperature. This system used exhaust gas from internal combustion engine as a source of power and ammonia water solution for refrigerant. Finally, it concludes that the diesel engine can be considered as potential source of energy and their coefficient of performance was 0.85.

From the reviewed work of literature on solar and non- solar powered, the solar powered have advantages because it's available almost all of the day, in all place and also the way of harvesting is not much complex. Whereas the others are limited to some place and it is difficult to harvest it. However, the vaccine storage is needed in all rural health center were unavailability of electricity. For this reason, this study used solar thermal powered vapour absorption refrigeration system.

3, Depends on type of refrigerants

The vapour absorption refrigeration system cycle uses a refrigerant-absorbent solution rather than pure refrigerant as the working fluid. This absorbent refrigerant is mixed in absorber and it can be a strong solution or a weak solution depending on the amount of refrigerant in the solution. The refrigerant-absorbent solution passing through the solution pump is referred to as a strong solution, being relatively rich in the refrigerant. The solution returning from the generator to the absorber contains only a little refrigerant and is therefore referred to as a weak solution. The absorbent acts as a secondary fluid to absorb the primary fluid which is the refrigerant in its vapour phase (Kurem and Horuz, 2001). In vapour absorption refrigeration system NH_3-H_2O and LiBr-H_2O are the two most common refrigerant absorbent solution where ammonia is the refrigerant earlier and water is the refrigerant in the later one. There is also other refrigerant absorbent like LiCl-H_2O, Ethyl ether-acetaldehyde and others.

Overview literatures for this topic

Lima *et al*., (2021) reviewed a vapour absorption refrigeration system based on ammonia as a refrigerant for different absorbents. The synthetic refrigerant fluids used in mechanical refrigeration have an environmental impact and need high electric power. Due to these uses absorption systems should be rising that have more efficient, pollutant-free to the environment. Vapour absorption refrigeration system usually used either LiBr-H_2O or NH_3-H_2O refrigerant-absorbent pair as working fluids having some disadvantages such as corrosion problems, low operating pressure for LiBr-H_2O, crystallization, toxicity problems, high operating pressures for the pair NH_3-H_2O need for an extra component (rectifier) and need for high temperatures for the mixture separation process in the generator, and limitations to operate with solar energy as a driving source.

Kumar and Arakerimath (2015) reviewed and compared various parameters which can affect the efficiency of NH_3-H_2O and LiBr-H_2O. Ammonia-water refrigerant-absorbent pair is frequently used in VAR systems which have a broad range of working temperature and pressure. Because NH_3 possesses high latent heat of vaporization, and extremely low freezing temperature (-77°C) resulted in an improved performance at low-temperature applications.

Kurem and Horuz (2001) studied the comparison of ammonia-water and water-lithium bromide solution in vapour absorption refrigeration system based on the coefficient of performance (COP), maximum and minimum system pressures, and cooling capacity. Vapour absorption refrigeration system widely uses water-lithium bromide solution with water as refrigerant and ammonia-water solution with ammonia as the refrigerant.

The ammonia-water vapour absorption refrigeration system has been used at low temperatures for process cooling in large-capacity industrial applications. The disadvantage of this system is ammonia vapour leaving the generator contains a small amount of water vapour that affects the system by increasing the temperature of the evaporator and reducing the refrigerating effect. To prevent this problem, additional component like analyser and rectifier is needed which are added on the top of generators.

For this study NH_3-H_2O refrigerant absorbent solution are selected. Because the application area of this study (vaccine storage) required the temperature interval 2-8°C, which are easily maintained by this refrigerant absorbent.

2.3 Solar Collector

Solar collector is a special kind of heat exchanger that receive solar energy, convert into thermal energy and transfer into the fluid (usually air, water or oil) flowing through the collector. The basic principle of solar collector is received solar radiation, absorbed by its surface and increasing the temperature of the surface; part of this heat is transferred to the heat transfer fluid and others are lost to the environment.
Based on the operating temperature and their motion, solar collectors are classified into: non-concentrating or stationary and concentrating or sun tracking.

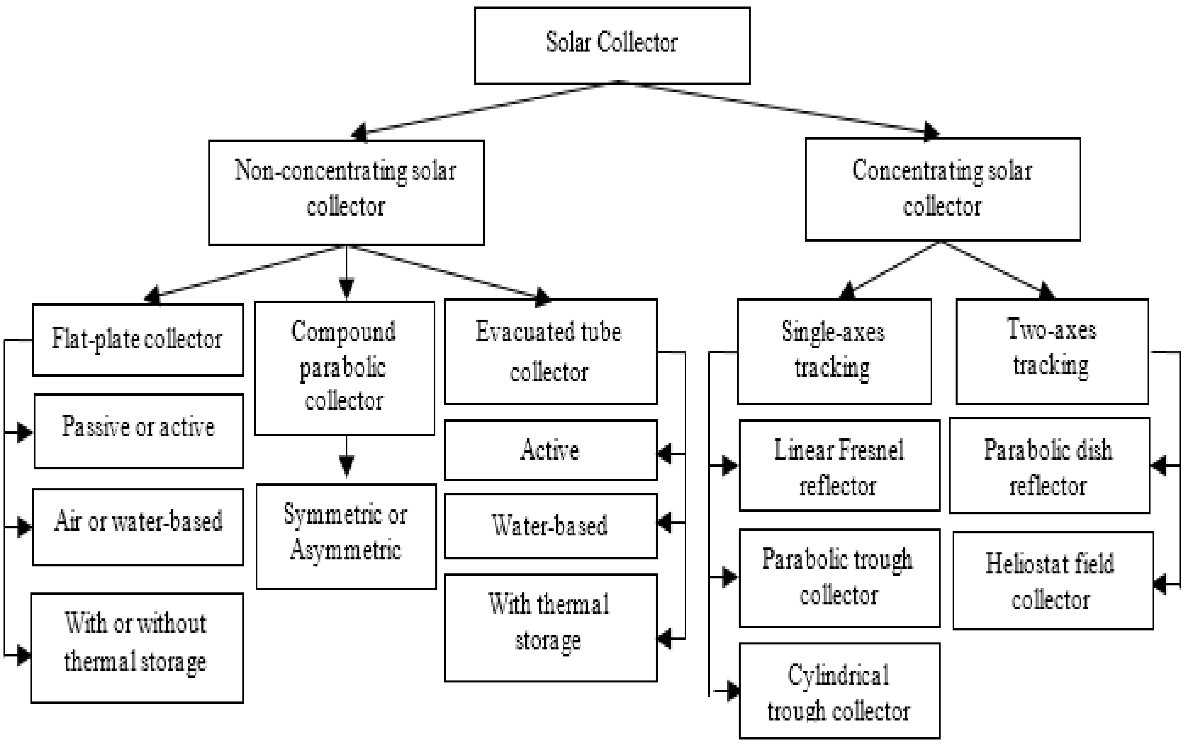

Figure 2.7 Classification of solar collectors (Fudholi and Sopian, 2018).

2.3.1 Classification of Solar Collectors

The solar collector can be classified based on their collecting characteristic, operating temperature range, type of transfer fluid they employ and the way in which they are mounted.

A, Based on the way of transportation of fluid

1. Passive system: Is a system that do not use pump in order to circulate the working fluid, it relies natural convection or gravitational force to circulate water or heat absorbing fluid through the system. It is less cost, more reliable and low maintenance requirement. However, it's efficient is significantly lower.
2. Active system: Is highly efficient system compared to passive and it can be classified into active open loop system, active closed loop system and drain back system.

Active open loop system: is also direct system, where the fluid pumped from the storage tank to the solar collector and enter into storage tank after heated. Mostly it uses water as working fluid.

Active closed loop system: it is indirect system and my uses antifreezes in addition to water as working fluid. This system used copper coil inside storage tank or outside the storage tank for heat exchange between the hot and cold fluids.

Drain back system: it is similar with closed loop system except the working fluid is water.

B, Based on collecting characteristics

Depending on the area and shape of collector, harvested solar energy is different.

1) Non-concentrating solar collector: These collectors are permanently fixed in position or same area is used for both interception and absorption of incident radiation. Flat plate collector, compound parabolic collector and evacuated tube collectors are categorized under this solar collector.

2) Concentrating solar collector: It is a type of collector, which have concave reflecting surfaces to intercept and focus the sun beam radiation to small receiving area. In this system working fluid can receive high temperature, high thermal efficiency, reflecting surfaces require less material and structurally simple. Also tracking system is required in order to get high thermal efficiency using either one tracking system or two tracking system.

C, Operating temperature range

Table 2.1 Operating temperature of different solar collectors (Zaki,1999).

Type of collector	Flat plate collectors	Evacuated collectors	Parabolic through collectors	Parabolic dish collectors
Concentration ratio	1	1	15-45	100-1000
Typical working temperature in °C	30-80	50-200	50-400	100-500
Diagram				

D, Mounting: is the way of solar collector is either adjustable or fixed at one position. Some collectors need tracking to increase absorption of daily solar radiation, which tracking system is either manually or automatically whereas others are stationary or fixed at one place.

E, Type of fluids: In solar collector, the energy harvested from the solar radiation is transferred into the fluid flow in the tube which attached on the absorber plate or concentrated to the collector plate. These fluids are mostly water or water ethyl-glycol.

The significant criteria of selection from solar thermal collectors for thermally operated vapor absorption systems include the operational temperature of heat supply to the generator, optical efficiency, thermal energy conversion per unit area, thermal losses to the environment, and cost. Additionally, estimation of the solar collector area should also account for the energy to be stored within thermal energy storage to be utilized during non-sunshine hours and periods of weak solar intensity (Sharma *et al.*, 2020). For this study open loop active system, parabolic trough solar collector is selected due to the temperature required in our system is belongs to this type and it have also many advantages likes: the area required for collector is less than flat plate collector, it uses single tube, the energy absorbed per unit area is maximum, can be achieved around 125 ℃ outlet temperatures and also low construction and maintenance cost.

2.3.2 Parabolic Trough Solar Collector

It is a linear focus, low-cost implementation concentrated solar collector, basically composed of parabolic trough shaped concentrator that reflect direct solar radiation into absorber tube where the fluid is heated up to the required temperature depending on the concentrator area, tracking system and supporting structure. Also, it is a high-performance solar collector to deliver high temperature with interval of 50 up to 400℃ and good efficiency for different applications (Kalogirou, 2013).

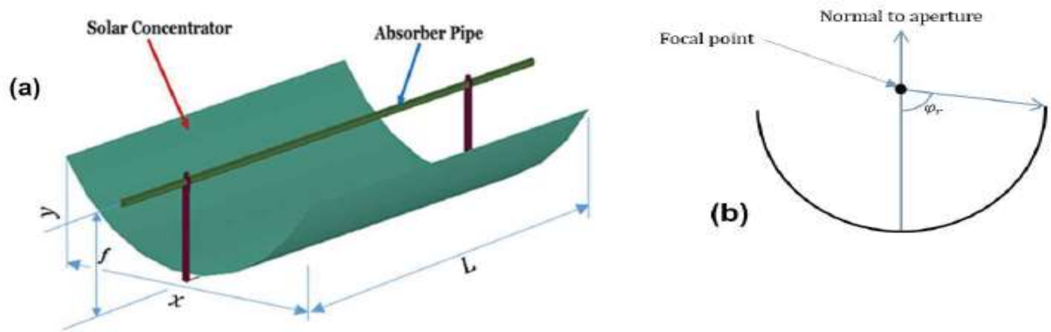

Figure 2.8 a) Parabolic Trough Solar Collector and B) Rim Angle Evaluation (Ibrahim, 2020).

Concentrator**: -** is a parabolic shape made of reflective material to converge sunlight into the focal line. The material selection for the concentrator is based on the reflectance property.

Receiver tube**: -** is the most crucial element in parabolic trough solar collector where the solar energy is converted to heat. It acts as receiver and transporter of the energy which is being concentrated at focal line of the reflecting surface It was made from steel or copper and coated with heat resistance black paints

Heat transfer fluid: **-** it is used to transfer the heat received by receiver. This fluid can water, oil or others based on the required temperature in the system.

Reflector**: -** is most important and costlier part of parabolic trough solar collector. Glass mirror, aluminium foil, ionized aluminium sheet and others are reflector materials.

Tracking system: **-** Parabolic trough is a line focusing concentrating device due to this one it needs at least one tracking system. This tracking system can be east-west alignment and north-south tracking system or north- south alignment and east-west tracking system. From the two north-south tracking system is better for experimental work and east-west tracking system is preferred for general use (Upadhyay, 2020).

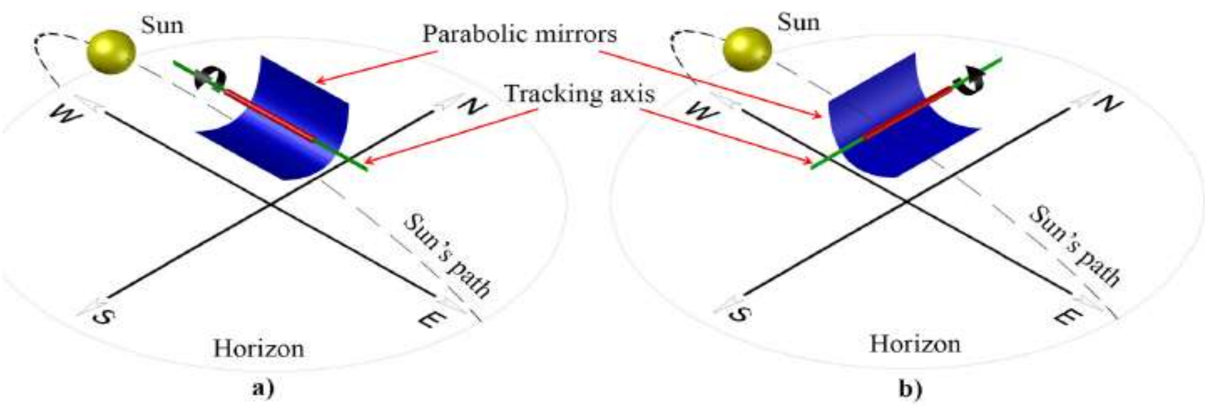

Figure 2.9 Common tracking methods a, north-south b, east-west (Tagle-Salazar *et al.*,2020)

Components of parabolic trough solar collector and its working principle

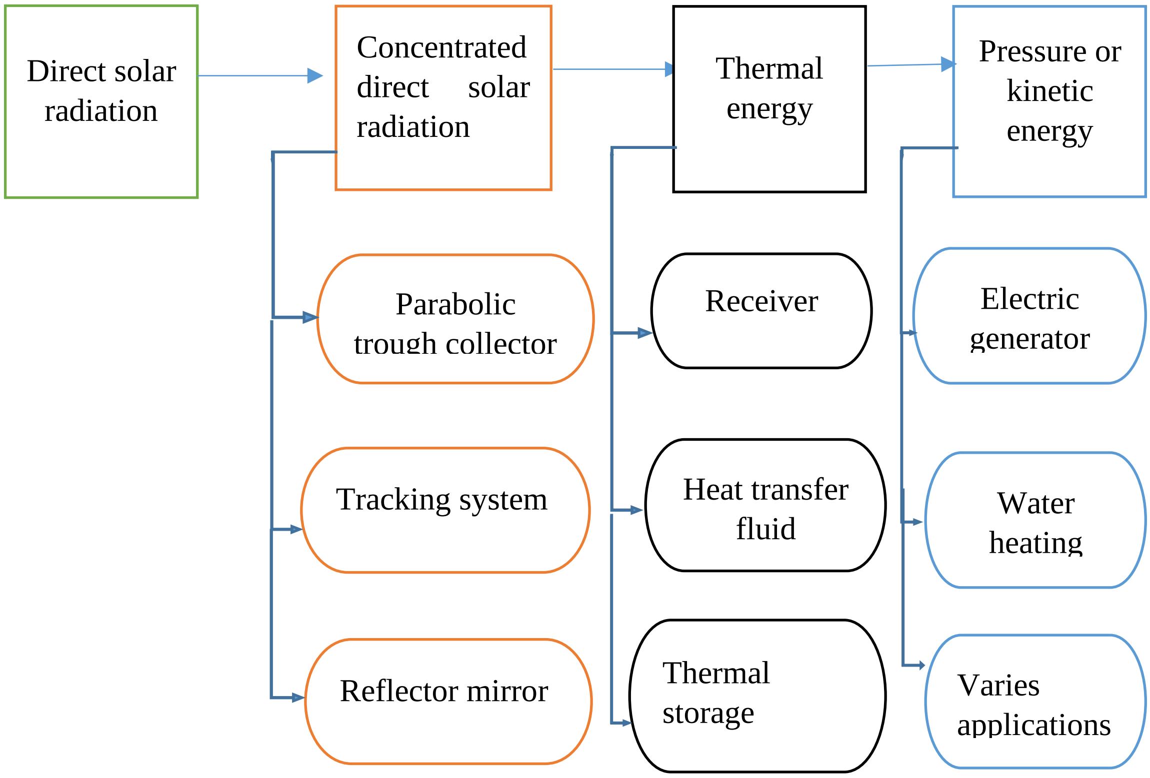

Figure 2.10 Components and working principle of parabolic trough collector

Reviewed paper related with parabolic trough collector.

Singh (2012) designed and fabricated parabolic trough solar collector for hot water generation. The system was constructed from aluminium sheet having 1.2m length, 1.2m aperture width, 0.3m focal length, 1.387 and 1.44 m^2 aperture area and collector area respectively. Also, the diameter of the pipe is 0.0325m, absorber pipe thickness is 0.001m and 11.3 concentration ratio. Finally, after the optical and thermal analysis the system efficiency is 0.1827.

Ramesh *et al.,* (2015) designed, fabricated and analysed the solar parabolic trough solar collector for water heating applications. The system consists of 32.5 and 31.5mm outside and inside copper tube receiver tube,38mm glass cover tube diameter, 1.545m^2 aperture area and aluminium sheet reflective material. The experimental work was performed for different solar radiation and ambient temperature, from the experiment the lower and higher temperature observed are 60 and 103℃, also the highest and lowest heat gain from the collector is 1500 and 450W respectively.

Çağlar (2016) designed parabolic trough solar collector using different reflective materials. 316-L chrome plate and aluminium composite panel are the selected reflecting material, parabolic trough solar collector having relatively large, efficient surface, harvesting the income solar radiation and concentrating into small receiver area. The system consists, 28mm copper tube absorber,1mm wall thickness,50mm of glass that covered the absorber with 2.3mm thickness. Finally, absorber tube with and without glass cover was analysed. From the analysis aluminium composite panel reflector and absorber tube covered by glass wall have high efficiency.

Tabassum *et al.,* (2019**)** designed and analysed solar parabolic trough solar collector experimentally for water heating applications. It focuses on analyses the performance of concentrating solar collector by changing the reflector material (aluminium sheet, aluminium foil and mirror film). The experiment was performed in Bangladesh which having 4-5kWh/m^2 solar radiation and 3.9m/s wind speed. The system consists of three parabolic trough collector and storage tank placed above the receiver pipe line which helps the heating fluid flows naturally without pumping system. The parameter used in these systems are: 0.914m aperture length, 0.508m aperture diameter, 100° rim angle, 0.104m focal length,0.013m receiver diameter,0.152m concentrator height, 0.612m linear diameter and

0.2L/min flow rate. The experimental result showed that from the three-reflector, mirror film has higher outlet water temperature, highest durability and 48% collector efficiency.

Torres *et al.,* (2020) designed and constructed solar parabolic trough using low-cost alternative materials. The system design contains the following parameters and assumption. It was experimentally tested in Brazil. Using 900W/m^2 solar beam radiation, 25℃ inlet fluid temperature and room temperature, water is a working fluid, 2.4m collector length, 22 and 20mm outer and inner diameter receiver tube made up of copper, galvanized steel covered with aluminium foil used as reflective surface also blank ink is used on the absorber to increase solar absorption. The result from the experiment showed the maximum outlet temperature from the collector reach 100℃ and the heat absorbed by the receiver was 1.2kW with 52.38% efficiency.

Itabiyi *et al.,* (2021) analysed parabolic trough collector for water heater experimentally. This work aimed to analyses the performance of parabolic trough collector using grey, black and uncoated receiver tubes made of galvanized iron. This work has advantages because parabolic trough solar collector is clean, cheaper and constructed from locally available. It was constructed from 2.1m collector length, 0.029 and 0.031m internal and external receiver tube respectively,1.2m aperture width, 90° rim angle, focal length of 0.03m,2.424m^2 aperture area and 10L water in the storage tank. The experimental result reveal that, black coated receiver tube has highly efficient and the maximum outlet temperature was 70℃.

Arunkumar and Ramesh (2022) studied experimental and numerical analysis of parabolic trough solar collector for water heating applications. In these system effect of absorber material was analysed by using coper tube and aluminium tube for absorber tube, also five different mass flow rates of water (0.0017, 0.0033, 0.0050, 0.0067, and 0.0083 kg/s) were analysed experimentally. The parameter used in the experiments are 15 and 13mm outer and inner absorber diameter respectively and 120mm collector length, in order to prevent heat transfer from the receiver tube 120mm lengh,50mm diameter and 4mm thickness borosilicate transparent glass tube was added in the system. From the experimental and simulation result for copper absorber tube, 763W useful energy is obtained by using solar irradiance(I) = 1024W/m^2, 0.0083 kg/s mass flow rate and 36.3℃ inlet temperature. Whereas 783W useful energy is obtained in aluminium absorber tube by using 1077 W/m^2 solar irradiance, 0.0083kg/s mass flow rate and 35.7℃ inlet temperature. Generally, for both copper and aluminium absorber tube as mass flow rate increase the outlet temperature decrease and also the inverse is true. So, 0.0017kg/s mass flow rate of water is preferred to get high outlet temperature.

2.4 Phase Change Material

In nature many energy sources are intermittent. To improve this, energy storage plays an important role to convert the available energy for non-availability time. Solar energy is one type of power full energy source that is available only during the day, and hence, its application requires efficient thermal energy storage for the sunshine hours. Many applications need energy storage to improve performance for the time of unavailability or shortage of energy. Hot and cold medical therapy, transportation and storage of perishable foods, medicine and pharmaceuticals products, solar power plants to store thermal energy during day time and reuse it during the latter part of the day are few application areas of phase change materials.

2.4.1 Classification of Phase Change Material

Depending on the requirements of storage temperature, phase change materials can be classified into:

A**,** Cold and Hot storage PCM.

Cold storage phase change materials are that store energy at low temperatures by received heat from the low-temperature substance, whereas hot storage stores high temperature from high-temperature sources to fulfil unavailability power by charging and discharging.

Table 2.2 Classification of PCM based on temperature interval (-20°C To 200°C) (Faraj *et al.*,2012)

Temperature range		Mode	Application
Specific temperature ranges of reviewed PCM applications (-20°C to 200°C)	Low (-20℃ *to* 5℃)	Cooling	Domestic refrigerator
			Commercial refrigerated products
	Medium-Low (5°C to 40°C)	Heating +Cooling	Building passive heating and cooling
		Cooling	Free cooling
			Solar absorption chiller
			Evaporative and radiative cooling
			Air conditioning system
	Medium (40°C to 80°C)	Cooling	Electric device
		Heating	Solar air heater
			Solar stills
			Solar domestic hot water
	High (80°C to 200°C)	Cooling	Solar absorption cooling
		Heating	On-site waste heat recovery
			Off-site waste heat recovery
		Power generation	Solar-thermal electricity generation

B, Latent heat, Sensible heat and Thermochemical storage PCM

Depending on the way of storage heat, thermal energy storage can also be classified as latent storage, sensible storage, and thermochemical storage.

Sensible heat storage stores heat by raising the temperature of a solid or a liquid by using its heat capacity. The amount of heat stored depends on the temperature change, the amount of storage material, and the specific heat of the storage medium. The other is latent heat storage which stores thermal energy when phase change takes place in the material. It is one of the most efficient ways of storing thermal energy because it provides a much higher storage density with a smaller temperature difference between storing and releasing heat, higher thermal storage capacity, thermal stability, relatively constant temperature during charging and discharging (Farid *et al*., 2004).

Also, the phase change material can be classified into: Organic, Inorganic and Eutectics based on the phase change material between solid and liquid

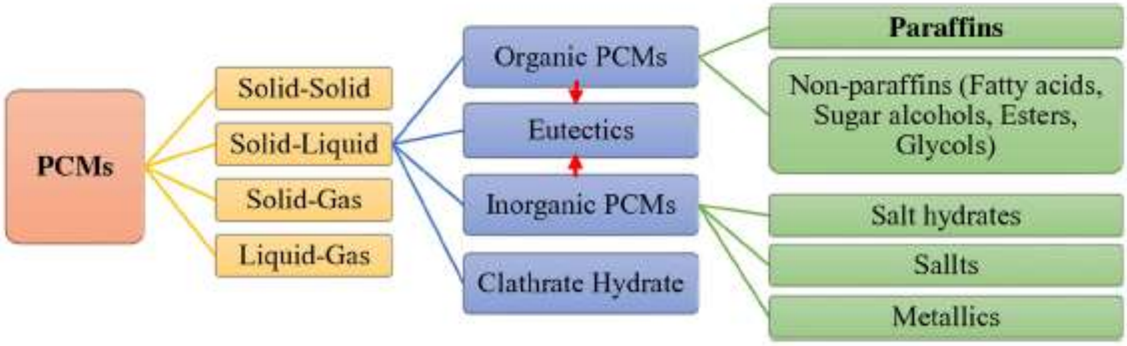

Figure 2.11 Classification of PCM (Al-Yasiri and Szabó, 2021).

2.4.2 Selection Criteria of PCM

In order to select the phase change material for a given application the following criteria should be considered properly.

- The melting point should be in the desired temperature range
- High latent heat of fusion per unit volume to store more energy in a given volume
- High thermal conductivity to assist charging and discharging of energy
- Low change in volume during phase change
- Non-flammable and non-toxic
- Cheap and could be easily available.
- Low cost and good environmental performance.

Few researches have been conducted on vapour absorption refrigeration systems integrated with phase change materials. Christopher *et al*., (2021) studied the optimization of solar collectors integrated with thermal energy storage tank vapour absorption refrigeration system using TRNSYS. The system consists solar collector with a serpentine tube arrangement, sensible heat storage (SHS) tank, pump, expansion valve, ammonia-water vapour absorption system, auxiliary heater, and two thermal insulated tanks in addition to other common vapour absorption refrigeration system components. The optimization was done by performance analysis of solar collector area, storage tank volume and height, the mass flow rate of operating fluids, absorber plate thickness, tube spacing, absorber tube diameter, glass thickness, and insulation thickness. After the physical model and simulation studies of the major components of the solar water heater and refrigeration system were developed, the obtained result was compared with reported data for validation. The result indicated that 24 m^2 flat plate collector area and 60 L/m^2 storage tank volume to collector area system could meet 65% of the annual thermal energy requirement for refrigeration units.

Raut *et al*., (2021) designed a solar-powered vapour absorption refrigeration system using $LiBr$-H_2O solution coupled with latent heat storage theoretically for a cooling capacity of 1kW. The system consists of an evacuated tube collector, vapour absorption refrigeration system, and latent heat storage as major components, and others are sized by adopting the heat exchanger design approach. It was sized for a cooling capacity of 1kW using an evacuated tube collector of 100 LPD capacity. The required heat provided to run the vapour absorption refrigeration system is 1.412kW, 1.46kW, and 0.96kW of the absorber, generator, and absorber respectively. Latent heat energy storage of 2.25kW is coupled with the system used for charging and discharging for 3 hours. Finally, the system design gives a COP of 0.68.

For this study, paraffin wax is selected as phase change material depending on the inlet temperature into generator and the temperature at which refrigerant is evaporated from the solution of absorbent refrigerant.

2.5 Literature Summary

As reviewed from the literature, solar refrigeration is studied based on its performance, source of power, type of solar collector, refrigerant type, and using phase change material or not.

Table 2.3 Literature Summary

Authors	**Source of power**	**Type of solar collector**	**Refrigerant**	**With PCM**	**Without PCM**
Christopher *et al.*, (2021)	Solar	Flat plate	NH_3-H_2O	√	
Raut *et al.*, (2021)	Solar	Evacuated tube	LiBr-H_2O	√	
Bose *et al.*, (2020)	Solar	Flat plate	LiBr-H_2O		√
Hashim and Kassim (2021)	Solar	Parabolic trough	LiCl-H_2O		√
Horuz and Callander (2004)	Hot gases	-	Aqua-ammonia		√
Tetemke *et al.*, (2021)	Geotherm al energy	-	NH_3-H_2O		√
Ghyadh *et al.*, (2020)	Solar	Parabolic trough	Water-methanol		√
Yadav and Saikhedkar (2017)	Solar	Parabolic disc and evacuated tube	NH_3-H_2O		√
Natnale (2019)	Solar	Evacuated tube collectors	LiBr-H_2O	√	

As shown in the table above, various researchers have studied the vapour absorption refrigeration system for a variety of applications, most of which use solar energy as a source of power because it is free energy radiated from the sun in the form of heat and light. Other types of energy are not as sufficient and abundant in all places like solar energy. The vapour absorption refrigeration system is classified into half effect, single effect, double effect, and triple effect based on performance and type of solar collector. From that single effect, the vapour absorption refrigeration system is that having a 0.6-0.8 coefficient of performance and used a non-concentrating solar collector in a major case. Also, it has only one generator while others have more than two generators to perform the system effectively. So, the single effect vapour absorption refrigeration system is simple and used for low cooling capacity.

As reviewed from the literature, the most common working fluids in the vapour absorption refrigeration systems are NH_3-H_2O and LiBr-H_2O. From those LiBr-H_2O absorbent refrigerants is mostly applicable if the required temperature is above 0°C. But the main problem of this system is the possibility of solid formation. Since the refrigerant turns to ice at 0°C, the pair cannot be used for low-temperature refrigeration. Whereas NH_3-H_2O refrigerant absorbent is mostly used in evaporators with low freezing points or temperatures below 10°C.Additionally, when volatility absorbent such as NH_3-H_2O is used, the system requires an extra component called "a rectifier", which will purify the refrigerant before entering the condenser, because the absorbent used (water) is highly volatile, it will be evaporated together with ammonia (refrigerant).

From the above points, ammonia water refrigerant- absorbent is selected for this study by adding rectifier in the top of the generator, because of its availability and easily applicable for vaccine storage within the required temperature intervals.

2.6 Research Gap

From the reviewed works of literature, many researchers have been working on single-effect vapour absorption refrigeration systems using solar thermal power for different applications like air conditioning, water-cooling systems and vaccine storage. Also integrating phase change material with solar-powered vapour absorption refrigeration system to fulfil unavailability and fluctuation of solar energy was studied by few researchers which is very important especially for vaccine storage. But there is a gap on where the phase change material is stored in the system and the shape of material which carries phase change material that affect the rate of heat transfer between the fluid and phase change material also performance of the system.

By analysing the above gaps this thesis was studied the performance of single-effect vapour absorption refrigeration system by experimental methods using solar thermal energy source for vaccine storage in rural health centers by putting the phase change material in appropriate position. In this system phase change material was stored in the generator where the refrigerant for the system is evaporated or separated from the absorbent. It has advantage because the refrigerant has direct contact with the material which carries PCM that helps the system especially during solar unavailability and fluctuation. Also, the selected shape of material which carries PCM are zigzag in shape and it’s good to increase rate of heat transfer between the working fluids.

CHAPTER THREE

MATERIALS AND METHODOLOGY

3.1 Materials

The materials used for this thesis work includes, solar thermal collectors and vapour absorption refrigeration system components. These components are: solar collector with its tracking system, condenser coil, evaporator coil, generator, and absorber, and glass wool insulating materials to reduce heat transfer, thermocouple, hose, expansion valve, two mini-pumps, refrigerant, absorbent, cold box for vaccine storage and phase change materials.

3.2 Methodology

Theoretical and experimental approaches are used as a methodology in this study. The theoretical approach uses governing equations to size and designs the components in the system. Software like SOLID WORK and EXCEL are also used to draw and develop the system integrals. An excel program has been used to determine the cooling load at different temperatures depending on the source of power from solar radiation and performance analysis of the system with and without phase change materials in generator. The experimental approach means converting the theoretical analysis and design into experimental work to test the required temperature in the evaporator and performance enhancement due to phase change materials added in the generator. Finally, validation of both theoretical and experimental work was done.

The objective of this study was achieved by the following methodologies.

- Identify the problem
- Review the related works of literature to know more about the problems
- Setting out objectives in order to solve the problems
- Collect data required from specific areas of study likes a number of children below five years who take the vaccine and also ambient temperature for the selected area
- Determine the refrigerant capacity based on the collected data
- Study the solar potential analysis for the selected area
- Identify the type of solar collector based on the refrigeration capacity determined first and design the one selected.
- Design the components of vapour absorption refrigeration system using the determined cooling capacity

- Collect raw materials based on design and sized that are available on the local market
- Develop the prototype of both solar system and VAR system
- Assembly of both system
- Test the performance of the system
- Apply performance improvement using adding of PCM
- Analyse the performance change
- Draw conclusion and recommendations

3.3 Research Design

Related literature has been studied to gain an insight into the area of interest background and other influencing factors. The literal is obtained from academic, articles, websites, etc. Then prototype is developed after the components are selected and the design is completed. The study has been done based on hypothesis testing, qualitative and quantitative research design techniques.

3.4 Data Sources and Collection Techniques

Data is collected from both primary and secondary sources. The primary sources of data had been conducted from interviews especially, in order to determine the refrigeration capacity of Mukiye Haro rural health center. Direct measurements like measurement of temperature in evaporator, generator and PCM by using a thermocouple and meteorological data was also collected from the nearby metrological station are taken as primary sources. Secondary sources of data include reference books, literature, and the internet.

For this study, the collected data was used to determine the cooling capacity of refrigerator, number of vaccines required or transported to the Mukiye Haro rural health center. This data is collected based on the number of doses of vaccine transported to this village by considering the number of children and others whose take vaccine. The collected data showed that, different vaccines are transported to this village in the interval of three months which are stored at the same temperature (2-8℃).

Table 3.1 Data collected from Mukiye Haro rural health center

Vaccine	Annual number of doses	Number of supply intervals per year	Number of doses per supply interval	Number of doses in one vial	Packed vaccine volume per dose (cm^3)	Vaccine storage volume (cm^3)
DTP-HepB Hib-IPV	3240	4	810	10	3.2	2592
PCV13	2160	4	540	4	3.4	1836
Rotavirus vaccine	3240	4	810	5	2.1	1701
TT	1080	4	270	10	3.1	837
Total vaccine volume per supply interval(cm^3)						6966
Volume of 25% safety stock(cm^3)						1741.5
Cold chain capacity requirement(cm^3)						8707.5

The summation of all vaccines storage volume per supply interval including the safety stock which is 25% of total volume gives cold chain capacity requirement (World Health Organization, 2017).

For this design the vaccine storage volume was determined from 36cm length, 21cm width and 25cm height. This volume was estimated by considering the size of secondary carton which carries vaccine and its arrangement in the refrigerator. Also, the volume of refrigerator frame was calculated from the insulator thickness surrounded the refrigerator to minimize heat transfer between the environment and the refrigerated space. Glass wool insulation is the recommended insulation for refrigeration system because of its low heat conductivity ($k=0.023 W/m.°C$). In order to determine the insulation thickness, if the storage temperature of the material is between 4.5-10°C (ASHRAE Handbook—Refrigeration, 2006) the recommended insulation thickness is 3mm. The storage temperature of vaccine in the evaporator is 5°C, due to this 3mm glass wool is selected for this system.

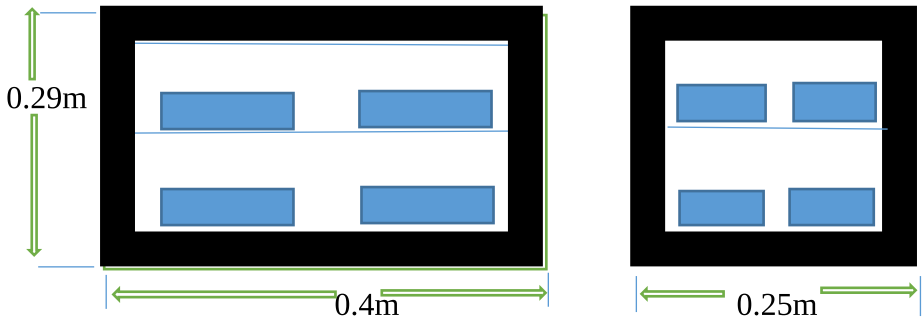

Figure 3.1 Arrangement of vaccine in refrigerator

Volume of refrigerator = vaccine storage volume + volume of refrigerator frame

Vaccine storage volume = 36× 21 ×25 cm^3 = 18900 cm^3 = 0.0189m^3

Volume of refrigerator = 40× 25× 29 cm^3 = 29000 cm^3= 0.029 m^3

Volume of refrigerator frame = 0.029- 0.0189 m^3 = 0.001 m^3

To calculate the cooling capacity of the refrigerant first heat transfer analysis was done by using the following parameters (ASHRAE Handbook—Refrigeration, 2006).

Thickness of galvanized steel (L_A) = 0.001m

Thickness of glass wool(L_B) = 0.03m

Thickness of aluminium plate(L_C) =0.0005m

Thermal conductivity of galvanized steel(k_A)= $48.5W/m.K$

Thermal conductivity of glass wool (k_B)= $0.023W/m.K$

Thermal conductivity of aluminium(k_C)= $229W/m.K$

In still air the value of inside heat transfer coefficient and outside heat transfer coefficient at low and medium wind speed are 20 and 30 $W/m^2.K$ respectively (ASHRAE Handbook—Refrigeration, 2006). For this design by considering the average wind speed of Adama the selected heat transfer coefficients are $hi = 9.08W/m^2.K$ and $ho = 25\ W/m^2.K$.

The vaccine storage is constructed from the galvanized steel plate, glass wool insulators and aluminium plate with their respective thickness and the heat transfer through this composite material are determined from: conduction heat transfer by assuming steady state heat conduction, convection heat transfer between the wall and surrounding and neglect radiation heat transfer because its value is minimum.

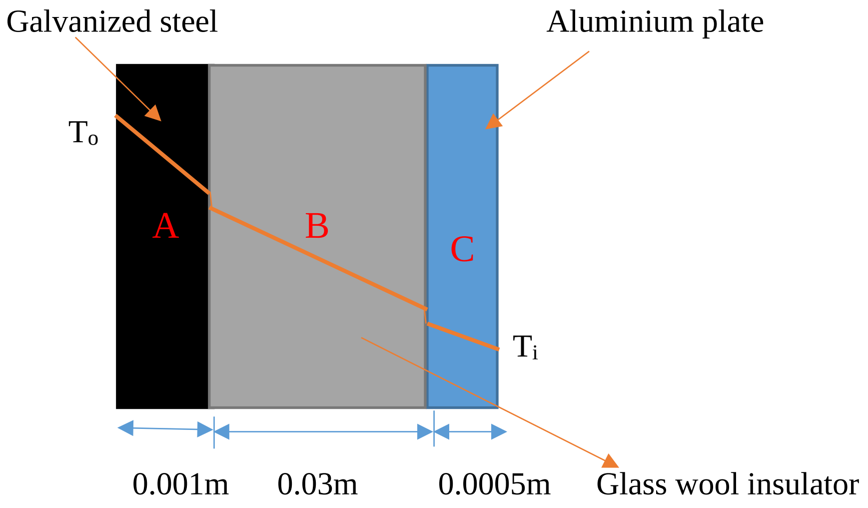

Figure 3.2 Heat transfer through the refrigerator wall

Estimation of convection and conduction heat transfer

Assuming steady state heat conduction through the wall and applying Fourier's law

$$Q=\frac{A\left(T_0-T_i\right)}{\frac{1}{h_0}+\frac{L_a}{k_A}+\frac{L_b}{k_B}+\frac{L_c}{k_C}+\frac{1}{h_i}} \tag{3.1}$$

Where Q= rate of heat transfer in (W)

A= outside area direction of heat transfer in (m^2)

To = outside air temperature in (°C)

Ti = inside temperature in refrigerated space (°C)

L= Thickness of the materials (m)

k = thermal conductivity of the materials (W/m. K)

$ho\ and\ hi$= outside and inside convective heat transfer coefficients ($W/m^2.K$)

A, Heat transfer through refrigerator door to inner chamber

In order to select the ambient temperature for a given cooling system greatest temperature difference between thermal load and ambient environment is recommended. This helps to maintain our system for every other situation (Praveen *et al.*, 2018).

$To\ =\ 30$°C (Assume maximum ambient temperature of Adama)

$Ti =\ 5$°C (Refrigerated space temperature)

The heat transfer from high temperature (ambient temp) to refrigerated space temperature can be found from

$$Q_d = \frac{A_d\left(T_0 - T_i\right)}{\frac{1}{h_0} + \frac{L_a}{k_A} + \frac{L_b}{k_B} + \frac{L_c}{k_C} + \frac{1}{h_i}} \tag{3.2}$$

Where Q_d= heat transfer through the refrigerator door into the vaccine storage

B, Heat transfer through the back of refrigerator into inner chamber

Surface area of back of refrigerator through which heat is transferred into inner chamber = surface area of the door which is

$$Q_{ba} = \frac{A_{ba}\left(T_0 - T_i\right)}{\frac{1}{h_0} + \frac{L_a}{k_A} + \frac{L_b}{k_B} + \frac{L_c}{k_C} + \frac{1}{h_i}} \tag{3.3}$$

Where Q_{ba}= heat transfer through back of refrigerator into the vaccine storage

The heat transfer from in front and back of refrigerator to the inner chamber is 1.55W each because of equal area which is $0.09m^2$.

C, Heat transfer through top of refrigerator into the inner chamber

$$Q_t = \frac{A_t\left(T_0 - T_i\right)}{\frac{1}{h_0} + \frac{L_a}{k_A} + \frac{L_b}{k_B} + \frac{L_c}{k_C} + \frac{1}{h_i}} \tag{3.4}$$

Where Q_t= heat transfer through top of refrigerator into the vaccine storage

D, Heat transfer through the bottom to the inner chamber is similar to the top

$$Q_{bo} = Q_t \tag{3.5}$$

Where Q_{bo} = heat transfer through bottom of refrigerator into the vaccine storage

The rate of heat transfer from top and bottom of refrigerator to the inner chamber is 1.22 W each because of equal area which is 0.0756m^2.

E, Heat transfer through the right-side wall can be calculated from

$$Q_{rs} = \frac{A_{rs}\left(T_0 - T_i\right)}{\frac{1}{h_0} + \frac{L_a}{k_A} + \frac{L_b}{k_B} + \frac{L_c}{k_C} + \frac{1}{h_i}} \tag{3.6}$$

Where Q_{rs} = heat transfer through right side of refrigerator into the vaccine storage

F, Heat transfer through the left side wall is similar with the right side.

$$Q_{ls} = Q_{rs} \tag{3.7}$$

Where Q_{ls} = heat transfer through left side of refrigerator into the vaccine storage

The rate of heat transfer from right and left side of refrigerator to the inner chamber is 0.9W each because of equal area which is 0.0525m^2.

Total heat transfer from the surrounding of refrigerator to the inner chamber became the summation of all side in Equation (3.8) and its result is 7.34 W

$$Q_T = Q_d + Q_{ba} + Q_t + Q_{bo} + Q_{rs} + Q_{ls} \tag{3.8}$$

G, Heat transfer in cooling chamber (Siddharth *et al.*, 2018)

$$Q = mC_p \Delta T \tag{3.9}$$

Where m= Mass of vaccines (kg)

Cp = Specific heat capacity (kJ/kgK)

ΔT = Change in temperature (K)

$$Q = \rho v C_p \Delta T \tag{3.10}$$

v = vaccine storage volume (m^3)

ρ= density (kg/m^3)

In order to calculate cooling capacity, the properties of water are used in place of vaccine, where the properties of water are $(\rho = 1000kg/m^3, c_p = 4.18kj/kg.K)$

$$\text{Overall heat load of the cooler } (Q_e) = Q_T + Q \tag{3.11}$$

From the Equation 3.11, the cooling capacity (Q_e) of the system was 0.26 kW

This is the amount of heat removed from refrigerated space to cool and maintain the required temperature in the refrigerator.

3.5 Solar Radiation Estimation

Solar energy is the most and abundant evenly distributed energy resource on earth. The sun discharges continuously an enormous amount of energy, where an average of 1376W/m^2 reach the outside of the terrestrial atmosphere which is called solar constant. Estimation of solar radiation is the most important parameter for the design and development of varies solar energy systems.

The amount of solar radiation falling on a surface on earth is estimated using several correlations that relate the radiation outside of the earth's atmosphere (extra-terrestrial radiation) with the radiation inside the earth's atmosphere (terrestrial radiation). In order to perform solar radiation analysis, the geometric relationship between a plane located on earth and the incoming solar radiation, that is the position of the sun relative to that plane, should be first determined. This relationship can be determined using several angles (Duffie and Beckman, 2013).

3.5.1 Fundamental Sun-Earth Angles

The major angles that describe the geometric relationship between the earth and the incoming solar radiation from the sun are,

1. Latitude (ϕ): the angular location north or south of the equator, north positive; $-90° \le \phi \le 90°$. The latitude of Adama is 8.54° north of the equator.

2. Declination (δ): the angular position of the sun at solar noon with respect to the plane of the equator, north positive; $-23.45° \le \delta \le 23.45°$.

$$\delta = 23.45 \times \sin\left(\frac{360}{365} \times (284 + n)\right) \tag{3.12}$$

Where, n is the day of the year (counted from January 1).

3. Slope or tilt angle (β): the angle between the inclined plane surface under consideration and the horizontal; $-180° \le \beta \le 180°$.

4. Solar Time: Time based on the apparent angular motion of the sun across the sky with solar noon the time the sun crosses the meridian of the observer. Solar time is the time used in all of the sun-angle relationships. So, it is necessary to convert standard time to solar time

by applying the equation of time which takes into account the perturbations in the earth's rate of rotation which affect the time, the sun crosses the observer's meridian (Duffie and Beckman, 2013).

$$\text{Solar time} - \text{standard time} = 4(Lst - Lloc) + E \tag{3.13}$$

Where: Lst -is the standard meridian for the local time zone

$Lloc$ -is the longitude of observers the location, and longitudes are in (°) West, that is, 0°< L < 360°.

The parameter E is the equation of time (min) and sited (Kalogirou, 2014).

$$E = 229.2(0.000075 + 0.001868\, cos\, 2B - 0.032077\, sin\, B - 0.014015\, cos\, 2B - 0.04089\, sin\, 2B) \tag{3.14}$$

Where: $B = 360\ 365\ (n - 1)$, in degree

n –is day of the year

5. Hour angle (ω): the angular displacement of the sun east or west of the local meridian due to the rotation of the earth on its axis at 15° per hour; positive in the afternoon and negative in the forenoon.

$$\omega = [\text{solar time} – 12{:}00]\ (\text{in hours}) \times 15° \tag{3.15}$$

6. Zenith angle (θz): the angle between the vertical and the line to the sun, that is, the angle of incidence of beam radiation on a horizontal surface.

$$cos\, \theta z = cos\, \delta\, cos\, \phi\, cos\, \omega + sin\, \phi\, sin\, \delta \tag{3.16}$$

Where, ϕ − angular location north or south of the equator; $-90 \leq \phi \leq +90$

δ − solar declination; $-23.45℃ \leq \delta \leq +23.45°$

7. Surface azimuth angle (γ): the deviation of the projection on a horizontal plane of the normal to the surface from local meridian. γ = 0 for surfaces facing south.

8. Sunrise and sunset times and day length: The sun is said to be rise and set when the solar altitude angle (α) is zero. So, the hour angle at sunset, ω_s, can be found by (Kalogirou, 2014).

$$\omega_s = \cos^{-1}\left(-\tan\delta \times \tan\phi\right) \tag{3.17}$$

Where, ω_s −is taken as positive for sunset

ϕ − latitude angle

δ − declination angle

The length of sun shine hour (Ns) is computed from (Kalogirou, 2014).

$$N_s = \frac{2}{15}\omega_s \tag{3.18}$$

9. Angle of incidence (θ): the angle between the sun's rays's incident on the plane surface and normal to that surface.

$$\cos\theta = (\cos\phi\cos\beta + \sin\phi\sin\beta\cos\gamma)\cos\delta\cos\omega + \cos\delta\sin\omega\sin\beta\sin\gamma + \sin\delta\,(\cos\beta\sin\phi + \cos\phi\sin\beta\cos\gamma) \tag{3.19}$$

3.5.2 Estimation of Daily Extra-Terrestrial Radiation on Horizontal Surface

The extra-terrestrial radiation on a surface normal to sun's rays kept at a distance of sun-earth (not the mean distance, but the actual distance on that day, that time), the I_{sc} will essentially be the solar constant, modified to take into account the varying distance between the sun and the earth extraterritorial radiation (Iext) is given by (Tiwari *et al.*, 2016):

$$I_{ext} = I_{SC}\left[1 + 0.033\cos\left(\frac{360}{365}n\right)\right] \tag{3.20}$$

Where: I_{sc} − solar constant = $1367 W/m^2$

n − day of the year, 1 for January 1st

Extra-terrestrial solar radiation that would fall on a horizontal surface at the location is given by:

$$I_0 = I_{ext}\cos\theta_z \tag{3.21}$$

Where θz is zenith angle

$$I_0 = I_{sc}\left[1 + 0.33\cos\left(\frac{360}{365}n\right)\right]\left[\cos\delta\cos\phi\cos\omega + \sin\phi\sin\delta\right] \tag{3.22}$$

By integrating Equation above from sunrise to sunset we can obtain the daily extra-terrestrial solar radiation on a horizontal surface as:

$$H_0 = \frac{24 \times 3600}{\pi} I_{sc} \left[1 + 0.033 \cos\left(\frac{360}{365} n \right) \right] \left(\cos\phi \cos\delta \sin\omega_s + \frac{\pi\omega_s}{180} \sin\phi \sin\delta \right) \text{........} \quad (3.23)$$

Where, H_0 - monthly average radiation at extra-terrestrial radiation of the same location

ω_s- is the sunset hour angle in degree

3.5.3 Estimation of Monthly Average Daily Global Radiations on Horizontal Surface

Radiation data are the best source of information for estimating average incident radiation. In Ethiopia sunshine data based solar energy estimation has been used frequently in different researches for solar radiation energy estimation and for designing purpose of solar system. Bekele *et al.,* (2013) estimated solar radiation by using sunshine data of the different sites based on well-known Angstrom model. Surface solar radiation on a ground level was suggested by Angstrom, who relate it with the amount of sunshine hour in the day, using some empirical constant obtained by regression analysis (Tiwari *et al*., 2016). Also (Venkatachalam and Solomon, 2019) estimated solar radiation based on sunshine hour for five years recorded from Adama metrology agency. In this study average daily global radiation in horizontal and tilt surface for diffuse, beam and global radiation are calculated. Also, hourly global and diffuse radiation are calculated.

$$H_G = H_0 \left(a + b \left(\frac{\bar{ns}}{Ns}\right)\right) \quad (3.24)$$

Where, a and b are regression constant given by:

$$a = -0.11 + 0.23 \cos\phi + 0.323 \frac{\bar{ns}}{Ns} \quad (3.25a)$$

$$b = 1.449 - 0.533 \cos\phi - 0.694 \frac{\bar{ns}}{Ns} \quad (3.25b)$$

Where, H_G is global daily solar radiation on a horizontal surface,

$\bar{ns}$ is the daily hours of bright sunshine hour and

Ns is the maximum possible daily hours of bright sunshine.

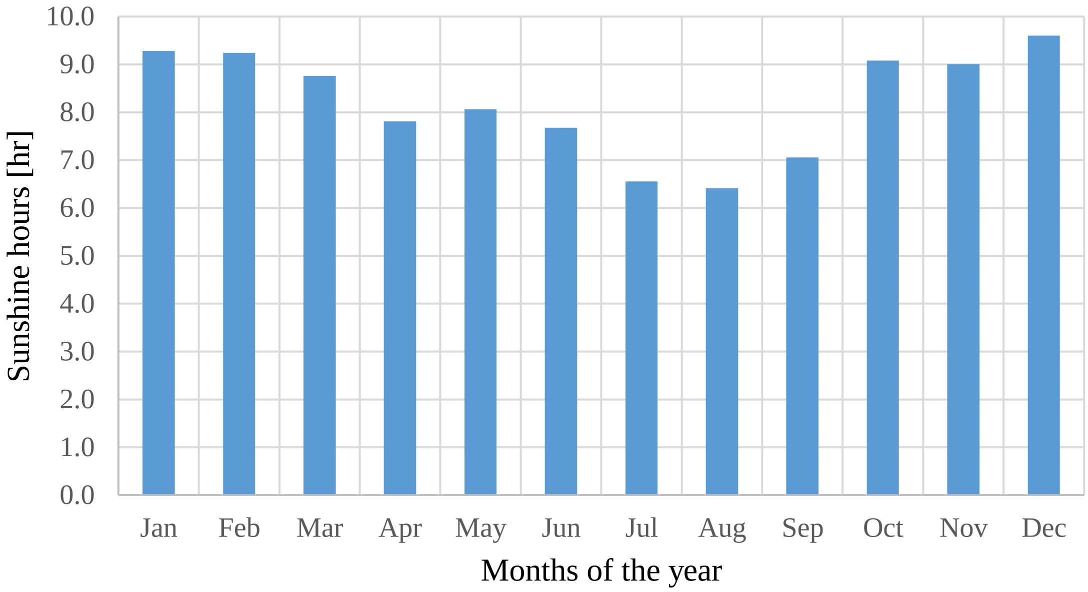

Figure 3.3 Sunshine hours of Adama for an average climatic condition for average of six years

3.5.4 Estimation of Monthly Average Daily Global and Diffuse Radiation on Horizontal Surface

The monthly average daily diffuse solar radiation on a horizontal surface can be determined from the monthly average daily global radiation and the number of bright sunshine hours (Tiwari *et al.*, 2016):

$$H_d = H_0\left(a + b(\frac{\bar{ns}}{Ns})\right) \tag{3.26}$$

The monthly average daily beam radiation on horizontal surface is calculated from the difference between monthly average daily global and diffuse radiations.

$$H_b = H_G - H_d \tag{3.27}$$

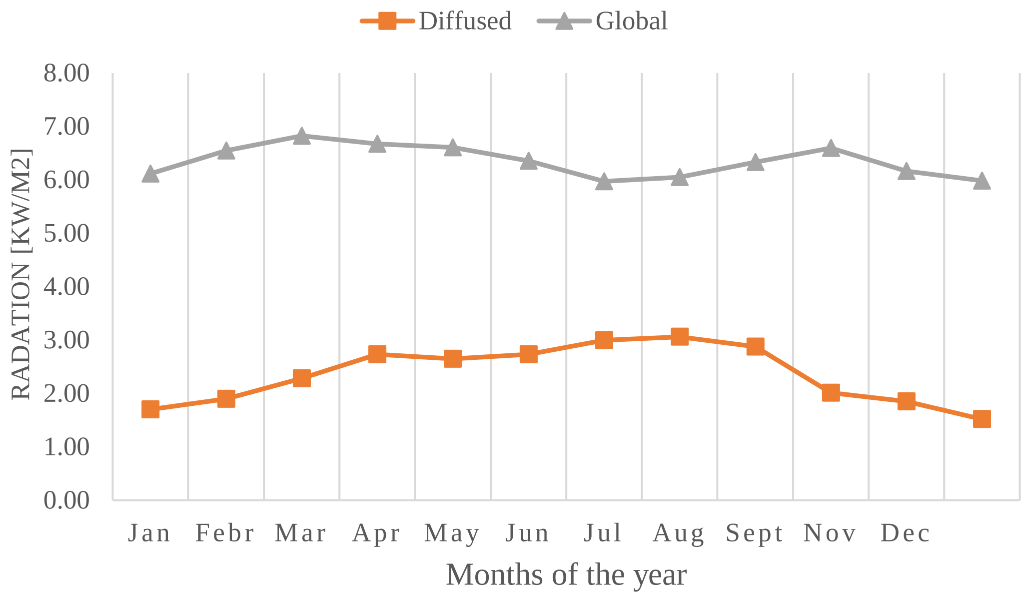

Figure 3.4 Monthly average daily global and diffuse radiation on horizontal surface

3.5.5 Estimation of Monthly Average Hourly Global Radiation on A Horizontal Surface

The monthly average hourly global radiation on a horizontal surface can be determined from the monthly average daily global radiation (Duffie and Beckman, 2013).

$$\frac{I_G}{H_G} = \frac{\pi}{24}(a + b\cos\omega)\frac{\cos\omega - \cos\omega s}{\sin\omega s - \frac{\pi}{180}\omega s * \cos\omega s} \tag{3.28}$$

Where $$a = 0.409 + 0.5016\sin(\omega_{sr} - 60) \tag{3.29}$$

$$b = 0.6609 - 0.4767\sin(\omega_{sr} - 60) \tag{3.30}$$

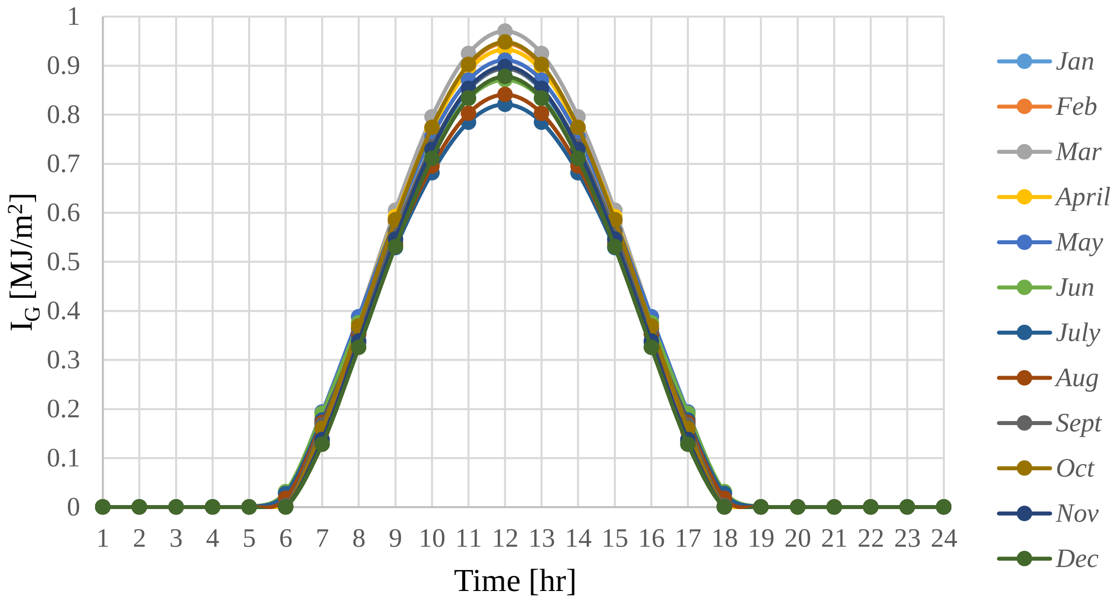

Figure 3.5 Monthly average hourly global radiation on horizontal surface

3.5.6 Estimation of Monthly Average Hourly Diffuse and Beam Radiation on Horizontal Surface

The monthly average hourly diffuse radiation on a horizontal surface can be determined from the monthly average daily diffuse radiation on a horizontal surface (Duffie and Beckman, 2013).

$$\frac{I_d}{H_d} = \frac{\pi}{24}\left(\frac{\cos\omega - \cos\omega_{sr}}{\sin\omega_{sr} - \frac{\pi}{180}\omega_{sr}\cos\omega_{sr}}\right) \tag{3.31}$$

The monthly average hourly beam radiation on a horizontal surface is the difference between the monthly average hourly global and diffuse radiations.

$$I_b = I_G - I_d \tag{3.32}$$

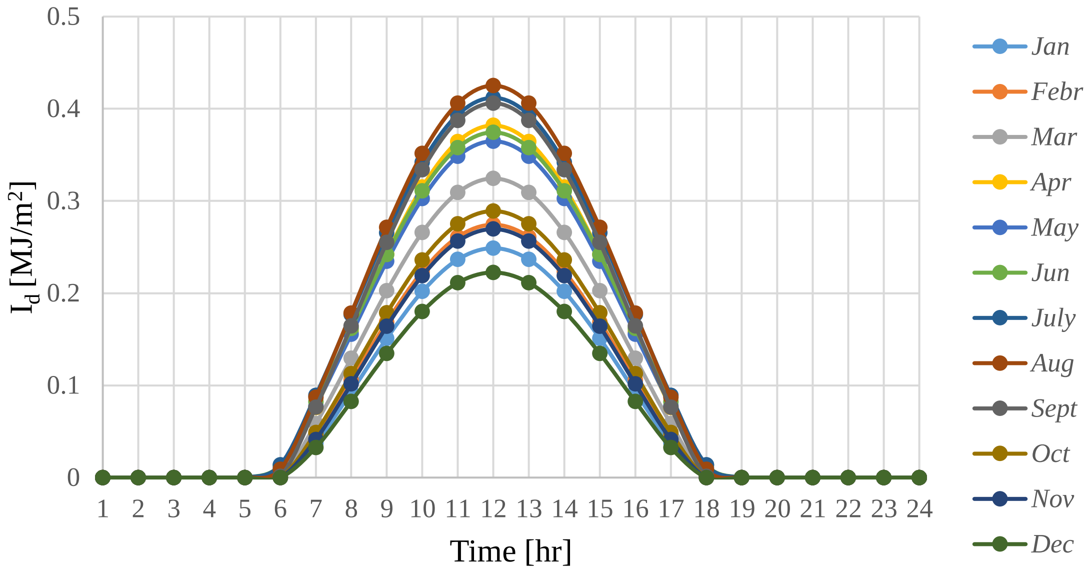

Figure 3.6 Monthly average hourly diffuse radiation on horizontal surface

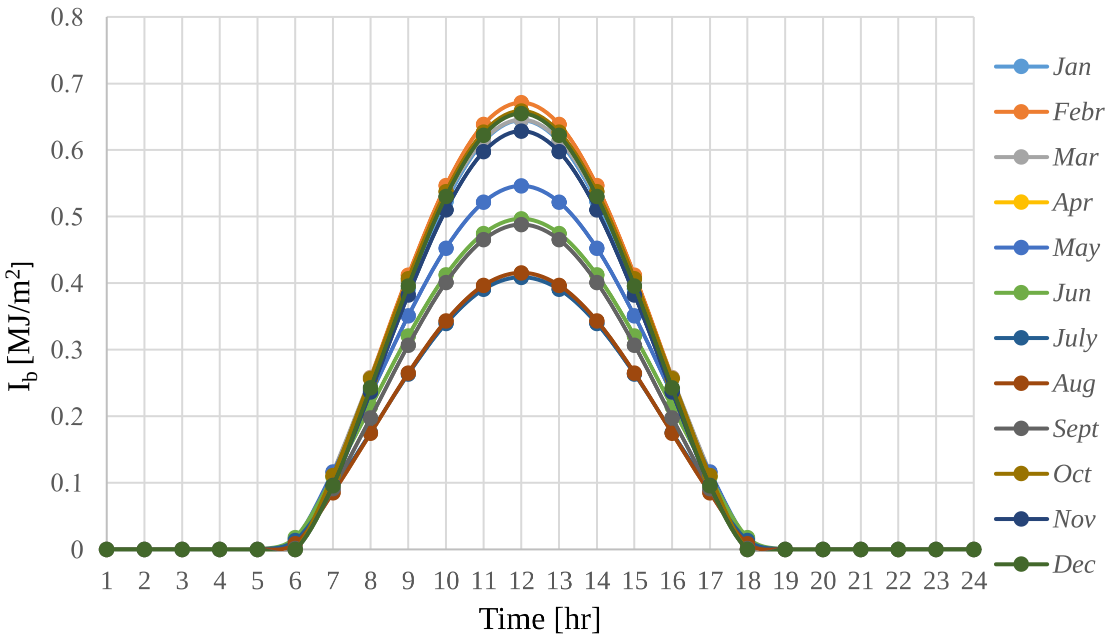

Figure 3.7 Monthly average hourly beam radiation on horizontal surface

3.5.7 Estimation of Hourly Variation of Atmospheric Temperature

There are many methods of calculating variation of daylight of ambient temperature. Among them the hourly variation of temperatures can be predicted from the daily maximum and daily minimum temperatures using the sine-exponential model (Dall'Amico and Hornsteiner,2006). This method was developed by (Parton and Logan, 1981) and it describes the diurnal cycle by a sine function during daytime and a decreasing exponential function during night time. The major assumption of the model is the maximum temperature will occur sometime during the daylight hours before sunset and the minimum temperature will occur during the early morning hours. The mathematical description for day and night time, respectively are expressed as (Parton and Logan, 1981):

For day light hours

$$T_i = (T_{\max} - T_{\min}) * \sin(\frac{\pi m}{y+2a}) + T_{\min} \tag{3.33}$$

For night hours

$$T_i = (T_{sunset} - T_{\min}) \exp(\frac{-bn}{Z}) + T_{\min} \tag{3.34}$$

Where, Ti is temperature at the i_{th}hour,

Y and Z are the length of the day and the night in hours respectively,

a - the lag coefficient for maximum temperature = 1.8 h

b - the night time temperature coefficient =2.2

m- the number of hours after the minimum temperature occurs until sunset and

n- the number of hours after sunset until the time of the minimum temperature

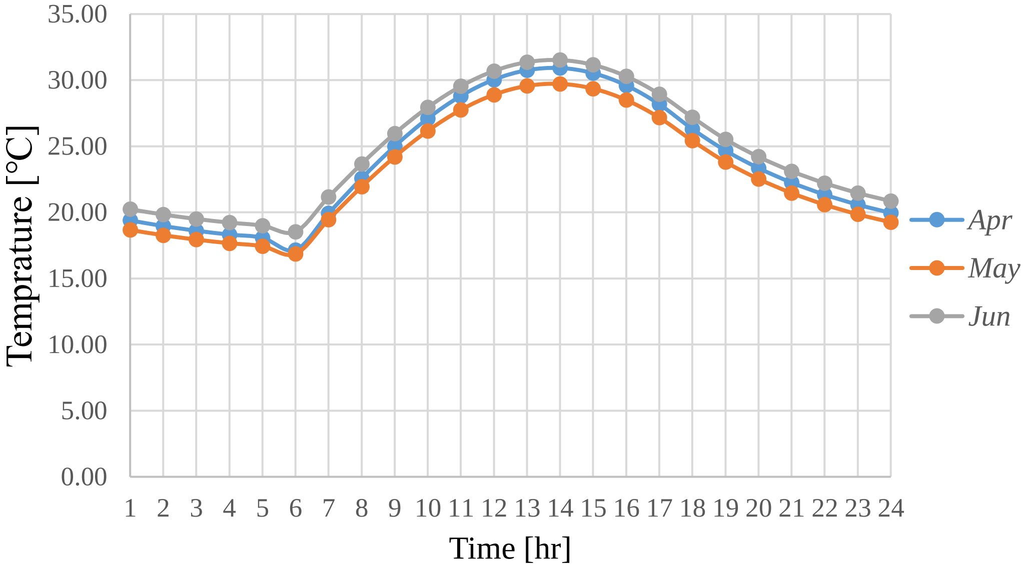

Figure 3.8 Average variation of ambient temperature of Adama

CHAPTER FOUR

DESIGN OF SYSTEM COMPONENTS

This chapter presents the design components of vapour absorption refrigeration system based on the calculated cooling capacity to maintains the required temperature of vaccine storage, design and size of solar collector required depends on the required temperature in the generator to separate the refrigerant from the absorbent and it also include selection and sizing of phase change materials.

4.1 Design of Single Effect Vapour Absorption Refrigeration System Components

Vapour absorption refrigeration system contains condenser, evaporator and expansion valve like vapour compression refrigeration system. But the compressor in the vapour compression refrigeration system is replaced by generator, absorber, pump and heat exchanger in order to cool a substance in the system. So, design of these components is discussed in these sub topics depending on the cooling capacity, temperature required for vaccine storage and temperature required to separate ammonia from water in the generators or the temperature at which ammonia-water refrigerant solution are evaporated by considering heat losses.

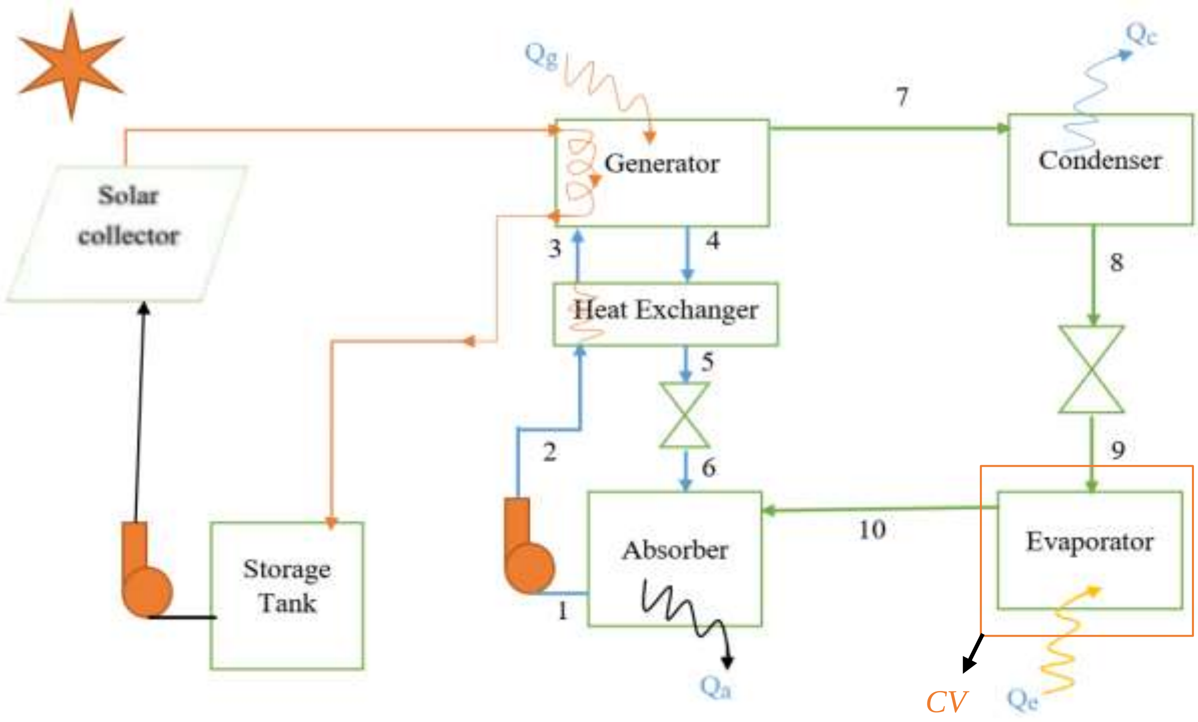

Figure 4.1 Solar powered vapour absorption refrigeration system components

In order to design the various components of single-effect ammonia- water absorption system i.e., condenser, evaporator, absorber, solution heat exchanger and generator following assumptions must be considered. Those assumption was taken from the worked literatures by (Raghuvanshi and Maheshwari, 2011; Bhowmick and Kundu, 2021; Huirem and Sahoo, 2020; Mohanty and Padhiary, 2015; Kurem and Horuz, 2001).

The assumptions are

- Generator and condenser as well as evaporator and absorber are under same pressure.
- There are no pressure changes except through the flow restrictors and the pump.
- The system is divided into two pressure limits, one is high pressure limit and other is low pressure limit. High pressure is corresponding to generator temperature (T_7) and low pressure is corresponding to evaporator temperature (T_{10}).
  - $P_1 = P_6 = P_9 = P_{10}$ = Low pressure
  - $P_2 = P_3 = P_4 = P_5 = P_7 = P_8$ = High pressure
- At points 1, 4 and 8 there is only saturated liquid and sub cooled liquid at 2, 3 and 5.
- At point 10, there is only saturated vapour. At points 7 and 9, the state is in superheated vapour and liquid-vapour refrigerant, respectively.
- Assume strong solution contain more percentage of refrigerant and less percentage of absorbent and weak solution contain more percentage of absorbent and less percentage of refrigerant.
- Percentage of strong solution at state 1, 2 and 3 and Percentage of weak solution at state 4, 5 and 6 will remain same.
- The two flow restrictors are adiabatic
- No liquid carryover from evaporator
- The refrigerant is pure through connecting line of 7, 8, 9, and 10.
- Pump is isentropic
- No jacket heat loss
- The LMTD expression adequately estimate the latent changes

In this design the initial temperature of generator, condenser and absorber are identified based on the required temperature in the cooling effect (evaporator) and type of refrigerant absorbent the system used. For this study the refrigerant absorbent solution is NH_3-H_2O which its boiling point is 37.7℃ (Yadav and Sharma, 2016). By taking the worked literature on solar powered vapour absorption refrigeration system using ammonia water absorbent refrigerant solution as a reference, the system components are designed and its performance was analysed. Shukla *et al*., (2015) and Oni (2018) are worked on this area where the parameter they used are listed in Table 4.1.

In this study, the evaporator temperature is determined based on the temperature required for vaccine storage (Shukla *et al*., 2015) and types of material needed (thermal conductivity) for transport refrigerant in the system. Depending on this, the temperature of ammonia vapour flow in the evaporator coil is -2℃ to maintain the evaporator temperature at 5℃ and the condenser temperature was taken from (Shukla *et al*., 2015 and Oni ,2018) work which is 30℃. But for generator and absorber temperature, analyses were done by taking different temperature based on the reviewed literature in Table 4.1.

Table 4.1 The most favourable working temperatures of solar powered refrigeration system used ammonia-water refrigerant absorbent

Parameters	Shukla *et al.*, (2015)		Oni (2018)		Present study
	Range of inlet temperature (℃)	Inlet temperature used (℃)	Range of inlet temperature (℃)	Inlet temperature used (℃)	Inlet temperature used (℃)
Generator	60- 99	64	70-115	82	75
Condenser	28- 60	30	30-40	30	30
Absorber	16- 32	20	30-40	30	25
Evaporator	2.5- 10	4	- 6-10	6	-2

Description: The above parameters are selected mainly based on the refrigerant absorbent in the solution**.** Since ammonia water are refrigerant absorbent where ammonia is as a refrigerant and water as absorbent for this system, in order to separate the refrigerant from the absorbent in the generator, the optimum temperature from the solar collector is needed. This is because of, if the inlet temperature from the collector is high the more heat is transferred in to the generator that vapour water in addition ammonia refrigerant that reduce the system performance and also, low inlet temperature affects the system performance. Additionally, the evaporator temperature is selected based on the range of vaccine to be stored at required temperature (2-8℃).

Analysis for the selected generator and absorber temperature for constant condenser and evaporator temperature.

Evaporator

$$m_9 = m_{10} = m \tag{4.1}$$

$$Q_e = m\left(h_{10} - h_9\right), kJ/s \tag{4.2}$$

Where

$h_{10} = h_g$ @ evaporator temperature (-2°C) = 1466.92 kJ/kg from (Appendix D)

$h_9 = h_f$ @ condenser temperature (30°C) = 341.81kJ/kg from (Appendix D)

Mass flow rate of ammonia was calculated from Equation 4.2 and it is $2.3 * 10^{-4}\ kg/s$.

In order to determine the concentration of weak and strong solution, we have high pressure and low pressure in the system from (Appendix D).

Low pressure = saturation pressure at evaporator temperature (-2°C)

= $P\ sat@$ -2°C = 3.9 bar

High pressure = saturation pressure at condenser temperature (30°C)

= $Psat@$30°C= 11.6 bar

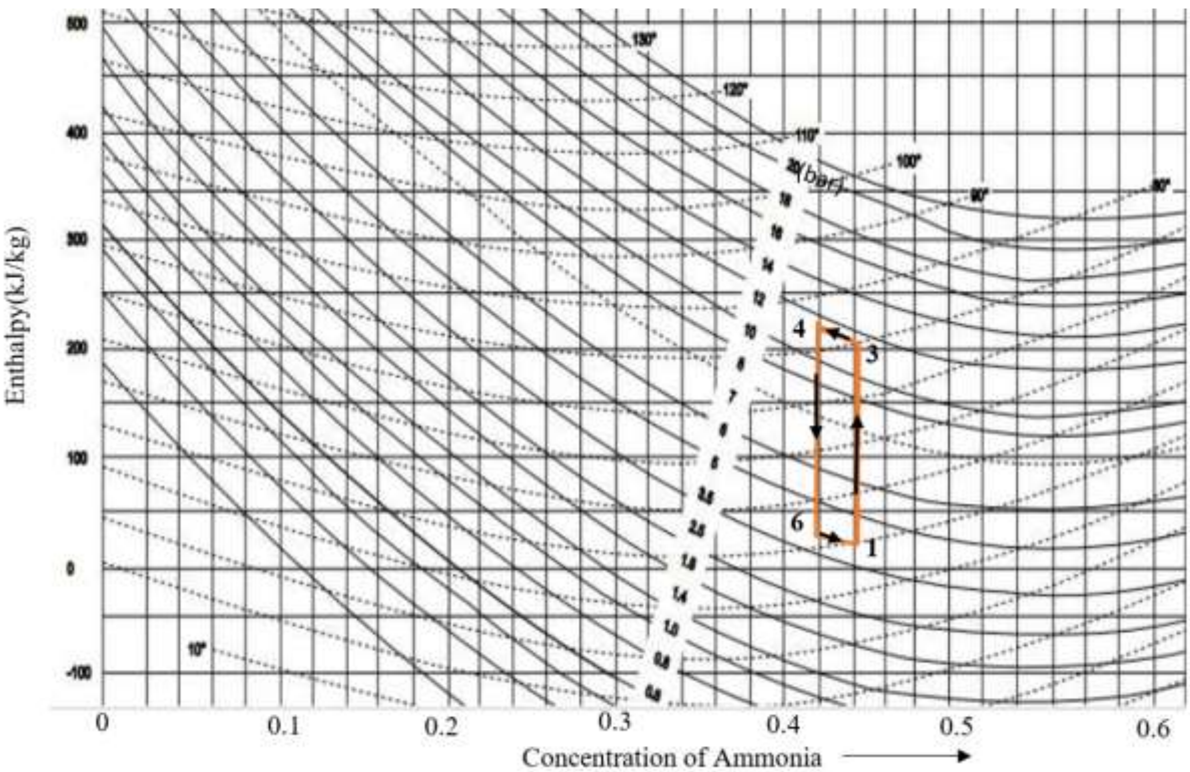

Figure 4.2 Enthalpy Composition Diagram for NH_3-H_2O System (Appendix F)

For absorber temperature of 25°C and generator temperature of 75°C

Table 4.2 Solution concentration

Temperature (°C)	Pressure(bar)	Concentration
25	3.9	0.43
75	11.6	0.42

Now, Circulation ratio,

$$\lambda = \frac{\xi_{ws}}{\left(\xi_{ss} - \xi_{ws}\right)} \tag{4.3}$$

$$\lambda = 0.42/\,(0.43 - 0.42) \; = \; 42$$

From total Mass balance

$$m + m_{ss} = m_{ws} \tag{4.4}$$

$$m_{ss} = \lambda \times \dot{m} \tag{4.5}$$

$$m_{ws} = \left(1 + \lambda\right) \times \dot{m} \tag{4.6}$$

From Equation 4.5 and 4.6, the mass flowrate of strong and weak solution is $9.74 \times 10^{-3}\ kg/s$ and $9.97 \times 10^{-3}\ kg/s$ respectively.

Table 4.3 Enthalpy and Concentration at various state point

State point	P (bar)	T (°C)	Concentration (Kg of NH_3 /Kg of solution)	Enthalpy, (kJ/kg)
1	3.9	25	0.43	7
2	11.6	25	0.43	7
3	11.6	40	0.43	223
4	11.6	75	0.42	220
5	11.6	28	0.42	10
6	3.9	28	0.42	10
7	11.6	75	0.98	1620
8	11.6	30	0.98	341.8
9	3.9	-2	0.98	341.8
10	3.9	-2	0.98	1459.5

Description: The above table was filled based on the number given on schematic diagram on Figure 4.1. Some of them are read from enthalpy composition diagram for NH_3-H_2O system (Appendix F) by using either concentration and pressure to get temperature and enthalpy or using pressure and temperature to get enthalpy. Also, others were read from saturation table of ammonia at a given temperature or pressure to get enthalpy (Appendix E).

In order to calculate the coefficient of performance of the system, thermodynamic system (first law) is the basic equation to analyse the mass and energy in the system.

Energy Analysis

Energy analyses is performed based on the first law of thermodynamics to evaluate energy efficiency by using energy balance equation. This balance is employed to determine and reduce heat losses. The general mass and energy conservation equations for the steady flow open system can be expressed as (Cengel and Boles, 2010)

Mass balance $$\sum \dot{m}_i = \sum \dot{m}_o \tag{4.7}$$

Energy balance $$\dot{Q} - \dot{W} = \sum \dot{m}_o h_o - \sum \dot{m}_i h_i \tag{4.8}$$

Where, $\dot{Q}$ and $\dot{W}$ are heat and work transfer rates, respectively in (W),

$\dot{m}_o$ and $\dot{m}_i$ are outlet and inlet mass flow rates of refrigerant in (kg/s), respectively,

$\dot{h}_o$ and $\dot{h}_i$ are outlet and inlet enthalpies of refrigerant in (kJ//kg), respectively,

By using equation 4.7 and 4.8 the vapour absorption refrigeration system components are analysed to determine the coefficient of performance and design of the system components. To do this, by using the schematic diagram of the system shown in figure 4.1 the control volume (CV) for each component is taken as shown in figure 4.1 for evaporator or vaccine storage. So, the mass and energy balance for each system are discussed as follows.

For Solution heat exchanger

Mass balance $$m_1 = m_2 = m_3 = m_{ss} \tag{4.9}$$

$$m_4 = m_5 = m_6 = m_{ws} \tag{4.10}$$

Energy balance $$Q_{HX} = m_{ss}\left(h_3 - h_2\right) = m_{ws}\left(h_4 - h_5\right) kJ/S \tag{4.11}$$

From the mass and energy balance $$m_2 h_2 + m_4 h_4 = m_3 h_3 + m_5 h_5 \tag{4.12}$$

$$h_3 = \frac{m_2 h_2 + m_4 \left(h_4 - h_5\right)}{m_3} \tag{4.13}$$

Condenser

Mass balance $$m_7 = m_8 = m \tag{4.14}$$

Energy balance $$Q_c = m\left(h_7 - h_8\right) \text{ kJ/s} \tag{4.15}$$

Expansion Valve

Mass balance $$m_8 = m_9 = m \tag{4.16}$$

Energy balance $$h_8 = h_9 \text{ because it is isenthalpic process.} \tag{4.17}$$

Generator

Mass balance $$m_3 = m_4 + m_7 \tag{4.18}$$

Energy balance $$Q_g = mh_7 + m_{ws}h_4 - m_{ss}h_3 \text{ , } kJ/s \tag{4.19}$$

Absorber

Mass balance $$m_{10} + m_6 = m_1 \tag{4.20}$$

Energy balance $$Q_a = mh_{10} + m_{ws}h_6 - m_{ss}h_1 \tag{4.21}$$

The amount of energy absorbed or released in the system component was analysed depending on the energy equation of each component where the enthalpy values are listed in Table 4.3 and mass flow rate are first calculated. Coefficient of performance for this system is defined as the ratio of amount of heat released from the system from evaporator to maintain the system at required temperatures to the input energy to the generator and for the pump to circulate the refrigerant and water for solar collector. However, the work of pump is negligible when compared with the input energy to the generator. So, the coefficient of performance was calculated from equation 4.22.

$$COP = \frac{Q_e}{Q_g + W_p} \tag{4.22}$$

The coefficient of performance of the system was obtained from the ratio of required cooling capacity of 0.26 kW in the system to the energy required in the generator to maintain the system at the required temperature wich is 0.396 kW from equation 4.19. The coefficient of performance of 0.66 was obtained by neglected work of pump.

Analysis the effect of generator temperature and absorber temperature on system performance

This analyse was done by varying absorber temperatures (25, 28, 30 and 32°C) and generator temperatures (75,80 and 85°C) for constant condenser and evaporator temperature where the condenser temperature was taken from literatures (Shukla *et al.*, 2015 and Oni, 2018) which is 30°C and the evaporator temperatures is the temperature at which vaccine to be maintained in refrigerator.

The analyses were done depending on the cooling capacity of vaccine storage and refrigerant absorbent solution which is ammonia water solution.

Table 4.4 Effect of generator temperature (75℃) for different absorber temperatures

Generator temperature (75°C)				
Absorber temperature (°C)	$Qc(kW)$	$Qa(kW)$	$Qg(kW)$	COP
25	0.29	0.358	0.395	**0.66**
28	-	-	-	**-**
30	-	-	-	**-**
32	-	-	-	-

Note: dash line (-) represent where the circulation ratio (λ) is undefined or negative.

Table 4.5 Effect of generator temperature (80℃) for different absorber temperatures

Generator temperature (80°C)				
Absorber temperature (°C)	$Qc(kW)$	$Qa(kW)$	$Qg(kW)$	COP
25	0.299	0.348	0.43	0.6
28	0.299	0.398	0.438	0.59
30	0.299	0.389	0.422	0.62
32	-	-	-	-

Table 4.6 Effect of generator temperature (85 ℃) for different absorber temperatures

Generator temperature (**85**℃)				
Absorber temperature (℃)	$Qc(kW)$	$Qa(kW)$	$Qg(kW)$	COP
25	0.302	0.386	0.428	0.6
28	0.302	0.406	0.431	0.6
30	0.302	0.375	0.424	0.61
32	0.302	0.375	0.434	0.59

The above table shows, the analysis of vapour absorption refrigeration system component for vaccine storage at required temperature in refrigerator. Different analysis was done by changing the generator temperature and absorber temperature for constant condenser and evaporator temperature. From this analysis the maximum coefficient of performance is obtained at 75℃ of generator temperature and 25℃ absorber temperature, where the condenser temperature is constant (30℃) and the evaporator temperature is -2 ℃. So, for our design this generator and absorber temperature are selected.

Depending on the coefficient of performance, amount of energy gained and loosed from the system the VAR system components are designed as follows.

4.1.1 Generator Design

Generator is a component of vapour absorption refrigeration system where refrigerant is separated from the absorbent by using external source of energy. In this study the external source is harvested from solar energy depending on the required temperature in the generator. Phase change material is also added in the generator to maintain the required temperature during the fluctuation of solar energy and at the time of sunset because the solar energy is intermittent type of energy.

In order to design the generator, the temperature inlet and outlet is first assigned.

Hot water inlet to the generator is 5℃ higher than the required temperature in the generator.

Hot water exits the generator after drop 6℃ from its temperature.

$$H_{wi} = T_g + 5℃$$

$$H_{we} = H_{wi} - 6℃$$

To determine the temperature of strong solution inlet to the generator, the heat exchanger absorption refrigeration system is used. A minimum temperature allowed in heat exchanger of absorption refrigeration system is 13.8 ℃ (Thulukkanam,2000) by assuming the heat exchanger effectiveness.

Assume 70% heat exchanger effectiveness in this design to determine the strong solution temperature inlet to the generator by using:

$$\varepsilon = \frac{T_{ss} - T_g}{T_a - T_g} \tag{4.23}$$

Where T_{ss} = Temperature of strong solution inlet to the generator

T_g = Generator temperature

T_a = Absorber temperature

ϵ = Heat exchanger effectiveness

Using equation 4.23, the temperature of strong solution was T_{ss} = 40 (it is safe because of the temperature difference is greater than 13.8℃)

The following assumption are used to analysis heat exchanger, which are closely approximated in practice.

- Steady flow
- Kinetic and potential energy changes are negligible
- The specific heat of the fluid is constant
- Axial heat conduction along the tube is negligible
- The outer surface of the heat exchanger is perfectly insulated

Heat transfer analysis in the generator

The external heat transfer area of the generator (A_g) required is calculated as:

$$Q_g = U_o \times A_g \times LMTD \tag{4.24}$$

Where Q_g = Heat input to the Generator

U_o = Overall Heat transfer coefficient.

$LMTD$ = Logarithmic mean temperature difference

In order to calculate the heat transfer analysis, the following data are used

Q_g = 0.395kW

T_g = 75℃

$T_{hi} = T_{wi}$ = 80°C

$T_{ho} = T_{hwe}$ = 74°C

$T_{ci} = T_{ss}$ = 40°C

$T_{co} = T_{av}$ = 75°C

Shell and tube heat exchanger were selected for this design because the strong solution exit from the heat exchanger flow over the coil in the generator which carries hot water in order to separate the refrigerant from the absorbent in the generator.

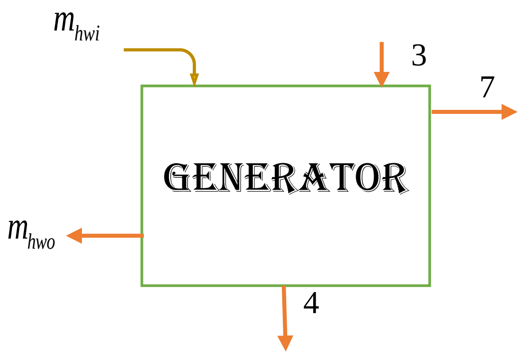

Figure 4.3 Generator

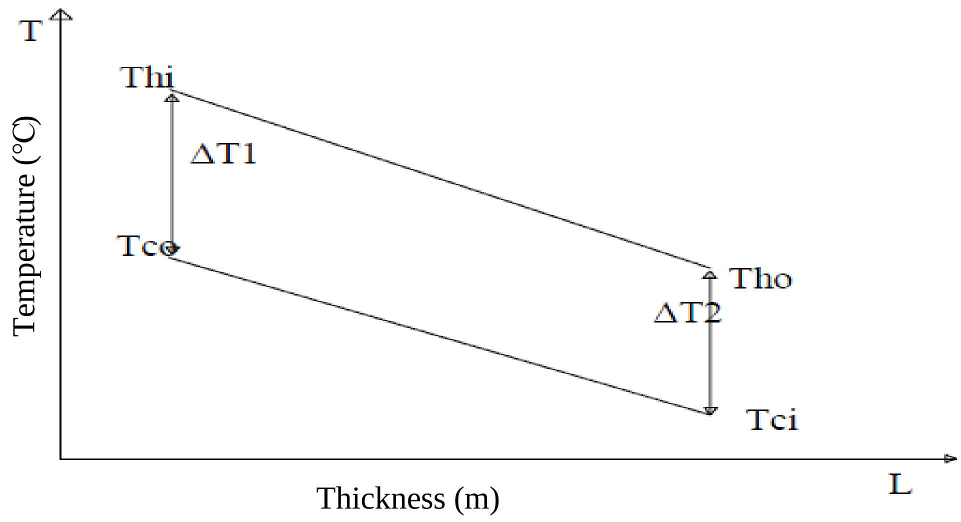

Figure 4.4 Temperature difference in generator

Logarithmic mean temperature difference (LMTD) is calculated as:

$$[LMTD] \; or \; \theta_m = \frac{\theta_1 - \theta_2}{\ln\left(\frac{\theta_1}{\theta_2}\right)} \tag{4.25}$$

Where $\theta_1 = T_{hi} - T_{co}$

$\theta_2 = T_{ho} - T_{ci}$

From Equation 4.25 the logarithmic mean temperature difference is 15.13 ℃.

In order to find the inside heat transfer coefficient, first calculate the mass flow rate of hot water inside the tube by using the thermo-physical property of water at mean temperature.

Property of water at mean temperature (80+74)/2 that means at 77 ℃ is taken from (Shah and Sekulic,2003).

The mass flow rate of hot water inside tubes

$$\dot{m}_{hw} = \frac{Q_g}{C_{pw} \times \Delta T_w} \tag{4.26}$$

Steel pipe of inside and outside diameter 11.42 and 12.7 mm respectively was selected from Table 4.7 for hot flow in the generator because other nonferrous materials like copper and brass are attacked by ammonia.

The velocity of hot water flow inside the steel tube can be determined from:

$$V_{hw} = \frac{\dot{m}_{hw}}{\rho \times \pi \times \left(\frac{d_i^{\,2}}{4}\right)} \tag{4.27}$$

The Reynold number can be calculated by

$$R_e = \frac{\rho \times V_t \times d_i}{\pi} \tag{4.28}$$

$$= \frac{4 \times \dot{m}_{hw}}{\pi \times \mu_{hw} \times d_i} \tag{4.29}$$

Assuming fully developed flow, the flow can be laminar or turbulent, one can use the general derived equation for laminar or Dittus-Boelter equation if it is turbulent flow (Kakac *et al.*, 2002).

If $Re < 2300$, laminar

$$N_u = \frac{h_i d_i}{k} = 3.66 \tag{4.30}$$

Else, turbulent

$$N_u = \frac{h_i d_i}{k} = 0.023 \times Re^{0.8} Pr^{0.4} \tag{4.31}$$

Where R_e = Reynold number

P_r = Prandtl number and

N_u = Nusselt number

From Equation 4.29, the Reynolds number is 4852 which is > 2300 (turbulent) and by using Equation 4.31, the internal heat transfer coefficient in the generator is $1687.9\ W/m^2.K$. For heat exchangers or generators, mild steel with an outer shell diameter of 250mm and a height of 350mm is specified (Gandhi and Arakerimath, 2016).

In order to calculate the external heat transfer coefficient in the generator, the properties of ammonia water at the mean temperature (57.5℃) and strong ammonia concentration were read from (Appendix C).

Using the above parameters, the outside transfer coefficient (ho) in the generator, the shell side heat transfer coefficient was calculated from the kern methods (Cao, 2010) formula by using the following assumptions.

Baffle spacing (β) = 1/5 × internal shell diameter

Tube pitch (P_t)= 0.0254m, Clearance (c)= 0.0084m, Thickness of shell(t) = 3mm

In order to calculate the heat transfer coefficient in the shell side(ho):

$$R_e = \frac{D_e \times G_s}{\mu} \tag{4.32}$$

where D_e = equivalent diameter of the shell

μ = dynamic viscosity of the fluid

G_s = mass velocity

$$D_e = \frac{4\times(\frac{1}{2}p_t\times0.86\times p_t-\frac{1}{2}\times\frac{\pi}{4}\times {d_o}^2)}{\frac{1}{2}\times\pi\times d_o} \tag{4.33}$$

$$G_s = \frac{\dot{m}_{ss}}{a_s} \tag{4.34}$$

where $\dot{m}_{ss}$ = mass flow rate of strong solution

$a_s =$ shell side cross flow

$$a_s = \frac{D_s \times c \times \beta}{P_t} \tag{4.35}$$

where D_s = shell internal diameter

By inserting the values

$$a_s = 0.0043m^2,\ G_s = 0.054\frac{kg}{m^2.s},\ D_e = 0.043\text{m},\ \text{Re} = 7.06$$

Using the above result

$$\frac{h_0 \times D_e}{k} = 0.36 \times \text{Re}^{0.55} \times P_r^{\ 0.33}\left(\frac{\mu}{\mu_w}\right)^{0.14} \tag{4.36}$$

Overall heat transfer coefficient can be calculated from

$$\frac{1}{U_0} = \left(\frac{d_0}{d_i \times h_i} + \frac{d_0 \times \ln\left(\frac{d_0}{d_i}\right)}{2k} + \frac{1}{h_0} \right) \tag{4.37}$$

The length of generator coil was calculated from

$$Q_g = U_0 \times A_g \times F \times LMTD \tag{4.38}$$

Assume correction factor value is = 0.7.

$$A_{gc} = \frac{Q_g}{U_0 \times F \times LMTD} \tag{4.39}$$

where A_{gc} = area of generator coil

To calculate the length of generator coil:

$$A_{gc} = \pi \times d_0 \times l \tag{4.40}$$

$$l_{gc} = \frac{A_{gc}}{\pi \times d_0} \tag{4.41}$$

By using equation 4.36, the external heat transfer coefficient(ho) and using equation 4.37, the overall heat transfer coefficient (U_0) were calculated which are 17.6 $W/m^2.K$ and 15.77 $W/m^2.K$ respectively. Also, the length of the generator coil is calculated from equation 4.41 and it's 3 meters.

4.1.2 Condenser Design

Condenser is a component of vapour absorption refrigeration system where the refrigerant vapour is changed into saturated liquid by rejecting heat using air cooled or water-cooled system. Air cooled condenser is as the name implies, air is the external fluid and the refrigerant reject heat to air flowing over the condenser. In this study natural air-cooled condenser is selected because it is simple and naturally circulate without any need of extra components. The material used for condenser pipe is usually copper and aluminium with the tube diameter and thickness is listed below in Table 4.7. Even though the thermal conductivity of copper is high but for refrigeration system which uses ammonia water refrigerant solution where ammonia is refrigerant it is not recommended because it is not compatible with ammonia. So, steel tube having 5.64 and 6.35mm inner and outer diameter respectively are selected based on the available in the market and reviewed literature (Yadav and Sharma,2016).

Table 4.7 Standard pipe size for evaporator and condenser (Cao,2010).

Tube size(in)	Outside diameter(mm)	BWG	Wall thickness(mm)
1/4	6.350	22	0.711
		24	0.559
3/8	9.525	18	1.245
		20	0.889
		22	0.711
1/2	12.700	18	1.245
		20	0.889
5/8	15.875	16	1.651
		18	1.245
		20	0.889

Heat transfer analysis in the condenser

Condenser is a heat exchanger where the ammonia refrigerant vapour from the generator and surrounding air interchanges heat to give the saturated liquid ammonia at the exit. The heat transfer in the condenser can be from:

Conduction $$Q_{cond} = \frac{kA}{t}(T_c - T_s) \quad (4.42)$$

Convection $$Q_{conv} = hA(T_c - T_s) \quad (4.43)$$

Radiation $$Q_{rad} = \epsilon\sigma A({T_c}^4 - {T_s}^4) \quad (4.44)$$

In the condenser, there are two regions where in the initial region refrigerant condenses from superheated vapour to saturated vapour, whereas the second region where it goes from saturated vapour to saturated liquid. In order to analyses the heat transfer in this region, the length of condenser ammonia vapour refrigerant from the generator inter and saturated liquid ammonia live the condenser due to heat exchanges between two fluids. Due to this the length of condenser can be calculated from the two different flow regimes superheated vapour and two-phase mixture. In order to calculate this by assuming the flow is cross flow and the heat transfer in the condenser and length of the condenser can be calculated from:

$$Q_c = Q_{sup} + Q_{two\ phase} = U_0 \times A_c \times F \times LMTD \quad (4.45)$$

Where Q_c = heat transfer rate in condenser

Q_{sup}= heat transfer rate in superheated region

$Q_{two\ phase}$ = heat transfer rate in the two regions

Uo = overall heat transfer in the condenser

A_c = Surface area of condenser

LMTD = Logarithmic mean temperature difference

Logarithmic mean temperature difference in this system is calculated as:

The inlet temperature of ammonia vapour into the condenser (T_7) = 75℃

The outlet temperature of saturated liquid ammonia exits the condenser (T_8) = 30℃

The inlet temperature of ambient air into the condenser (T_i) =28℃

Air outlet from the condenser (T_e) = 31℃(Assumption)

$$LMTD = \frac{\Delta T_1 - \Delta T_2}{\ln\left(\frac{\Delta T_1}{\Delta T_2}\right)} \quad (4.46)$$

Where $\Delta T_1 = T_7 - T_e$

$\Delta T_2 = T_8 - T_i$

Using Equation 4.46, the logarithmic mean temperature difference is 286.6 K

To calculate the length of condenser, the length of superheated region and two-phase region must be calculated separately.

1, Length of condenser for super-heated regions

$$\dot{Q}_{sup} = h7 - h_{g@30℃} \tag{4.47}$$

$Where\ h_{g@30℃} = 1486.1\ kJ/kg$ From (Appendix D)

$$\dot{Q}_{sup} = 133.9\ kJ/kg$$

$$Q_{sup} = \dot{m} \times Q_{sup} \tag{4.48}$$

2, Length of condenser for two phase regions

In order to calculate the length of condenser in this region first determine the overall heat transfer between the refrigerant flow in condenser coil and ambient air.

Heat transfer inside the tube of steel pipe having inside and outside diameter 5.64 and 6.35mm respectively, can be calculated by using ammonia gas properties at T_C= 30℃ from (Appendix B).

Using the above parameters

$$R_e = \frac{4\dot{m}}{\pi d_i \mu} \tag{4.49}$$

$$= 415.8 \text{ which is} < 2300 \text{ (turbulent flow)}$$

So, the Nusselt number (N_u) = 3.66 according to Dittus-Boelter equation

$$h_i = \frac{N_u \times k}{d_i} \tag{4.50}$$

In order to find external heat transfer coefficient (ho), the properties of air at average temperature (28+31)/2 = 29.5℃ was read from (Appendix A).

From $$R_e = \frac{V \times d_0}{\nu} \tag{4.51}$$

Where V = free stream velocity at Adama take 0.5m/s for design (Kumar *et al*.,2015)

do = outer diameter of the condenser (m)

υ = kinematic viscosity (m^2/s)

The correlation suggested by Zukauskas for circular cylinder in cross flow is (Bergman *et al.,2011*).

$$N_u = C \times R_e^{\,m} \times P_r^{\,n} \left(\frac{P_r}{P_{rs}} \right)^{\frac{1}{4}} \tag{4.52}$$

For $0.7 \le \Pr \le 500$

$1 \le \mathrm{Re} \le 10^6$

Also, if $\Pr \le 10$, n= 0.37 and if $\Pr \ge 10$, n= 0.36

The value of C and m are given in the table below based on the Reynold numbers.

Table 4.8 C and m selection for different Reynold number (Bergman *et al*.,2011).

Re_D	C	m
0.4–4	0.989	0.330
4–40	0.911	0.385
40–4000	0.683	0.466
4000–40,000	0.193	0.618
40,000–400,000	0.027	0.805

So, it is possible to use the above formula because the

$$R_e = 407.26 \text{ and } P_r = 0.706$$

The value of constant C and m are 0.684 and 0.466 respectively, also n= 0.37 and Reynold number was calculated from Equation 4.51 and its value is 10.26.

From the Nusselt number:

$$h_0 = \frac{(N_u \times k)}{d_0} \tag{4.53}$$

The overall heat transfer coefficient can be calculated from:

$$\frac{1}{U_0} = \left(\frac{d_0}{d_i \times h_i} + \frac{d_0 \times \ln\left(\frac{d_0}{d_i}\right)}{2k} + \frac{1}{h_0} \right) \tag{4.54}$$

The length of condenser in the superheated region can be calculated from

$$Q_{\sup} = U_0 \times A_c \times F \times LMTD \tag{4.55}$$

where F= correction factor and its value = 1 for condenser and boiler (Shah,2014).

$$A_{\sup c} = \frac{Q_{\sup}}{U_0 \times F \times LMTD} \tag{4.56}$$

where A_{supc} = area of superheated condenser coil

To calculate the length of condenser in superheat regions

$$A_{\sup c} = \pi \times d_0 \times l \qquad (4.57)$$

$$l_{\sup} = \frac{A_c}{\pi \times d_0} \qquad (4.58)$$

The length of super-heated condenser is calculated by using the rate of heat transfer in the condenser of superheated part, which is calculated from equation 4.48. Also, the internal and external heat transfer coefficient was calculated from equation 4.50 and 4.53, whose values are 27.7 $W/m^2.K$ and 21.12 $W/m^2.K$ respectively. The overall heat transfer coefficient (U_0) of the system was calculated from equation 4.54, which is 11.37 $W/m^2.K$. By using the above results, the length of superheated condenser coil is calculated using equation 4.58 and its length was 0.47 meter.

The length of condenser in the two-phase region can be calculated from (Appendix D)

$$Q_{tp} = \dot{m} \times (h_{g@30°C} - h_{f@30°C}) \qquad (4.59)$$

In order to calculate the length of condenser in two phase regions

$$Q_{tp} = U_0 \times A_c \times F \times LMTD \qquad (4.60)$$

$$A_{tpc} = \frac{Q_{tp}}{U_0 \times F \times LMTD} \qquad (4.61)$$

where A_{tpc} = area of two-phase condenser coil

From area of two-phase condenser coil, the length of two-phase region can be calculated as:

$$l_{tp} = \frac{A_{tpc}}{\pi \times d_0} \qquad (4.62)$$

Similar to the length of the superheated region of the condenser, the two-phase region condenser length was calculated by using the rate of heat transfer in the two-phase region of the condenser length in equation 4.59 and its value was 0.26 kW. Based on the rate of heat transfer to give the required temperature in the evaporator, the length of the two-phase region condenser was calculated by using equation 4.62 and its value was 4.03 meters. The total length of the condenser was the summation of the two-phase region and the superheated region, which is 4.5 meters.

4.1.3 Evaporator Design

Evaporator is an important device used in the low-pressure side of refrigeration where the refrigerant vaporizes to generate the desired refrigeration system. In this system the boiling point of refrigerant must always less than the temperature of the medium which is to be cooled. In order to design the evaporator, the capacity or amount of heat absorbed by evaporator to cool the substance was first determined.

The heat absorbed or heat transfer capacity of evaporator is given by:

$$Q_e = U \times A \times \left(T_2 - T_1\right) \tag{4.63}$$

Where U= Overall heat transfer coefficient $(W/m^2.K)$

A= Area of evaporator surface in m^2

T_2 = Temperature of medium to be cooled (temperature outside the evaporator) in ℃

T_1 = Temperature inside the evaporator in ℃

Heat transfer in the evaporator through:

Conduction $$Q_{cond} = \frac{kA}{t}(T_s - T_e) \tag{4.64}$$

Convection $$Q_{conv} = hA(T_s - T_e) \tag{4.65}$$

Radiation $$Q_{rad} = \epsilon\sigma A(T_s^4 - T_e^4) \tag{4.66}$$

From different type of evaporator, natural convection bare tube coil evaporator is selected because of its simple construction, easy to clean and defrost. In this design, evaporator temperature, refrigerant properties, refrigeration effect, tube diameter selection are very important to determine the length of evaporator and its area.

To determine the length of the evaporator:

$$Q_e = U_0 \times A_e \times F \times LMTD \tag{4.67}$$

where Q_e = heat transfer rate in evaporator

Uo = over all heat transfer in the evaporator

A_e = Surface area of evaporator

LMTD = Logarithmic mean temperature difference

.

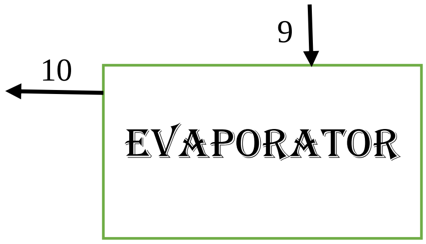

Figure 4.5 Evaporator

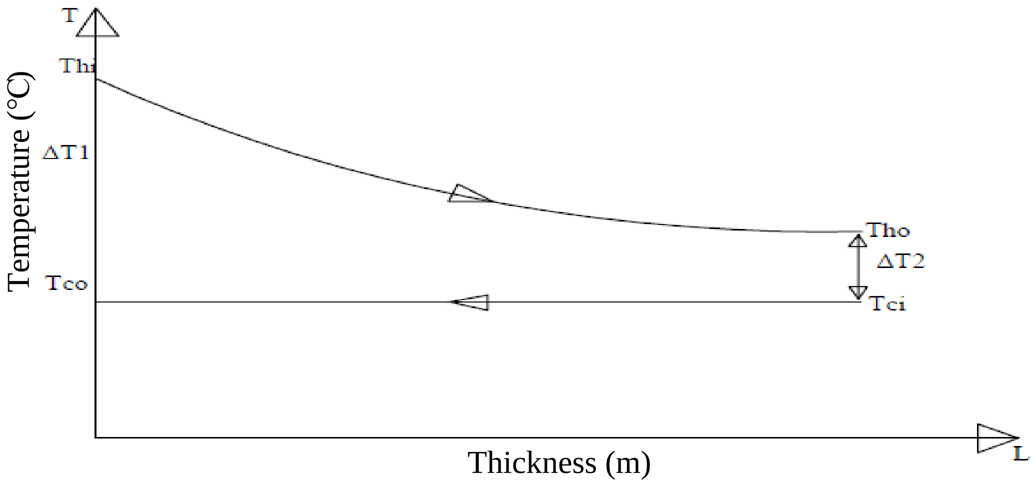

Figure 4.6 Heat transfer profile in the evaporator.

Where T_{hi} = inlet temperature of ambient air in to the evaporator = 28℃

T_{ho} = the required temperature in the evaporator for vaccine storage= 5℃

$T_{co} = T_{ci}$ = inlet and outlet temperature of refrigerant in evaporator coil = -2℃

From equation 4.68 Logarithmic mean temperature difference can be calculated from the temperature difference in this system

$$LMTD = \frac{\Delta T_1 - \Delta T_2}{\ln\left(\frac{\Delta T_1}{\Delta T_2}\right)} \tag{4.68}$$

where $\Delta T_1 = T_{hi} - T_{co}$

$\Delta T_2 = T_{ho} - T_{ci}$

From Table 4.7 the selected diameter of evaporator coil is steel tube having 5.64 and 6.35mm inner and outer diameter similar with the condenser.

To calculate the length of evaporator, the heat transfer was first analysed based on the cooling effect and the required temperature in the evaporator. Inside transfer coefficient in evaporator coil (hi) can be calculated from Equation 4.50 by identifying the fluid flow quality. The quality of fluid flow in the tube can be determined from

$$\chi = \frac{h_{f@30℃} - h_{f@-2℃}}{h_{g@-2℃} - h_{f@-2℃}} = 0.12 \tag{4.69}$$

$$\mu = \mu_l + \chi\left(\mu_v - \mu_l\right) \tag{4.70}$$

$$C_p = C_{pl} + \chi\left(C_{pv} - C_{pl}\right) \tag{4.71}$$

$$k = k_l + \chi\left(k_v - k_l\right) \tag{4.72}$$

By using the properties of ammonia refrigerant at evaporator temperature at -2℃ read from (Appendix B) and ṁ = $2.32 \times 10^{-4}\ kg/s$ length of evaporator is determined.

Using the above parameters

$$R_e = \frac{4\dot{m}}{\pi d_i \mu} \tag{4.73}$$

$= 318.3$ which is < 2300 (laminar flow)

So, the Nusselt number (N_u) = 3.66 according to Dittus-Boelter equation

$$h_i = \frac{N_u \times k}{d_i} \tag{4.74}$$

In order to find external heat transfer coefficient (h_0), properties of air at average temperature (28+5)/2 = 16.5℃ is read from (Appendix A).

From $$R_e = \frac{V \times d_0}{\nu} \tag{4.75}$$

Where V = free stream velocity at Adama take 0.5m/s for design (Kumar *et al.*,2015)

do = outer diameter of the evaporator coil (m)

υ = kinematic viscosity (m^2/s)

The correlation suggested by Zhukauskas for circular cylinder in cross flow is (Bergman *et al.*,2011)

$$N_u = C \times R_e^{\ m} \times P_r^{\ n} \left(\frac{P_r}{P_{rs}} \right)^{\frac{1}{4}} \tag{4.76}$$

For $0.7 \leq \mathrm{Pr} \leq 500$

$1 \leq \mathrm{Re} \leq 10^6$

Also, if $Pr \ \leq 10$, n= 0.37 and if Pr≥10, n= 0.36, C and m value is taken from Table 4.8 based on Reynold numbers.

The value of constant C and m are 0.684 and 0.466 respectively also n= 0.37 based on the Reynold number. The Nusselt number is calculated from equation 4.76 based on the Reynold number and constant value read from the table and its value was 22.5.

From the Nusselt number:

$$h_0 = \frac{\left(N_u \times k\right)}{d_0} \tag{4.77}$$

The overall heat transfer coefficient can be calculated from:

$$\frac{1}{U_0} = \left(\frac{d_0}{d_i \times h_i} + \frac{d_0 \times \ln\left(\frac{d_0}{d_i}\right)}{2k} + \frac{1}{h_0} \right) \tag{4.78}$$

The length of evaporator coil can be calculated from

$$Q_e = U_0 \times A_e \times F \times LMTD \tag{4.79}$$

Assume the correction factor = 0.7,

$$A_e = \frac{Q_e}{U_0 \times F \times LMTD} \tag{4.80}$$

To calculate the length of evaporator coil

$$A_e = \pi \times d_0 \times l \tag{4.81}$$

$$l_e = \frac{A_e}{\pi \times d_0} \tag{4.82}$$

The evaporator length was calculated by using the rate of heat transfer in the evaporator (cooling capacity), the internal and external heat transfer coefficient from equation 4.74 and 4.77, whose values are 323.8 $W/m^2.K$ and 90 $W/m^2.K$ respectively. The overall heat transfer coefficient (U_0) of the system was calculated from equation 4.78, whose value is

68.5 $W/m^2.K$. By using the above results, the length of the evaporator was calculated using Equation 4.82, and its length was 4 meters.

4.1.4 Absorber Design

Absorber is a components of vapour absorption refrigeration system where refrigerant and absorbent mixed each other to form solution. The solution is formed from ammonia vapour(refrigerant) and water (absorbent) which has a capacity to absorb more ammonia gas that leave the evaporator. From different type of absorber, direct contact heat exchanger is selected and the weak solution from the generator and ammonia vapour from the evaporator are mixed directly then strong ammonia solution are formed.

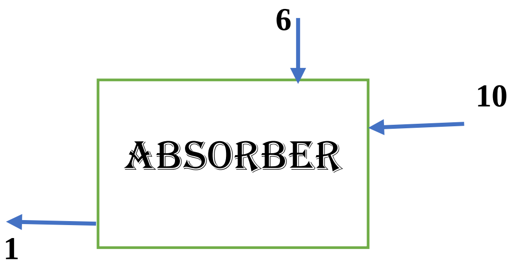

Figure 4.7 Absorber

As showed from the figure above, the weak solution from the generator passed the heat exchanger are mixed with the ammonia vapour from the evaporator. The diameter of absorber which carries the solution can be determined from the heat transfer between the weak solution, vapour ammonia and average ambient air that used to cool the system.

The total volume flow rate into the absorber is the volume flow rate of weak solution and volume flow rate of ammonia vapour.

= $\dot{m}ws$ ×specific volume of weak solution + $\dot{m}$ × specific volume of ammonia vapour

= $9.97 \times 10^{-3}\ kg/s \times 1.168 \times 10^{-3}\ m^3/kg + 2.3 \times 10^{-4}\ kg/s \times 0.31 m^3/kg$

= $0.829 \times 10^{-4}\ m^3/s$

The properties of ammonia are listed in the Appendix C that are used to determine properties of ammonia solutions. In addition to the above properties of ammonia: it was toxin, flammable, irritating and food destroying. Also, it attacks nonferrous metal in the present of water therefore copper and brass are never used with ammonia refrigeration system.

In order to identify the size of absorber first identify the proportion of ammonia water mixed with each other. To find mass of water in the mixture the following formula are used from (Manojprabhakar *et al.,* 2014). Mass of water in the solution from the given ammonia mass can be calculated from:

Mass of the solution = density $\times$ volume of solution (4.83)

Take properties of ammonia solution (ρ =0.851 $\frac{g}{ml}$, 2.5L volume and 42% concentration of ammonia in water by mass).

From mass of the solution 42% was mass of ammonia which is 892.5g and the rest is mass of water 1232.5g.

By considering the mass of the solution, the size of the absorber is 100mm diameter and 300mm length cylinder made up of mild steel material (Gandhi and Arakerimath,2016). The outlet of the absorber is connected to the pump and it lifts the solution from absorber to the generator. The absorber is fully closed without any leakage.

4.1.5 Heat Exchanger Design

In this heat exchanger heat transfer takes place between strong solution of ammonia water leaving the evaporator and weak ammonia solution from the generator. The tube and shell heat exchanger having 200mm diameter and 250mm height of shell with 11.42 and 12.7mm inner and outer diameter of tube respectively are selected for this system.

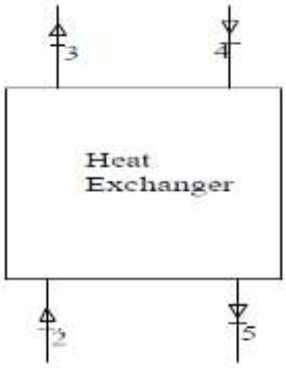

Figure 4.8 Heat exchanger

The heat transfer in heat exchanger is between generator living temperature (75℃) and the strong solution living the absorber at (25℃).

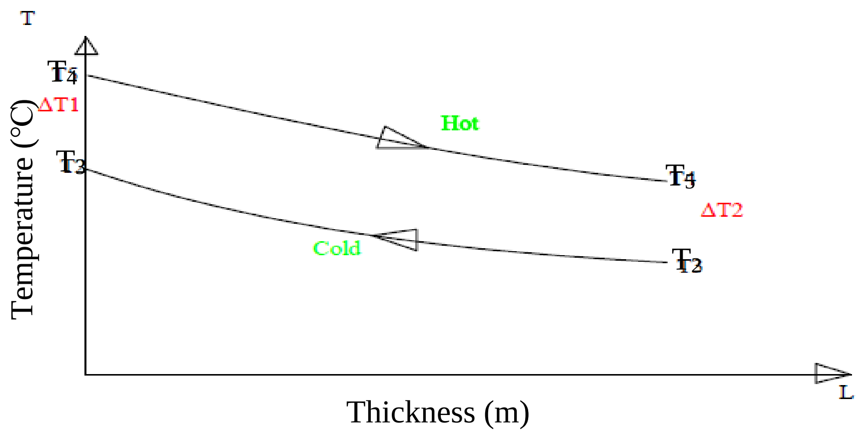

Figure 4.9 Design of heat exchanger

Where $T4$ = exit temperature from the generator = 75°C

$T5$ = inlet temperature to the absorber = 28°C

$T3$ = inlet temperature of strong solution to generator = 40°C

$T2$ = exit temperature from the absorber = 25°C

From equation 4.18 assume cross flow in heat exchanger, the logarithmic temperature difference was calculated from:

$$LMTD = \frac{\Delta T_1 - \Delta T_2}{\ln\left(\frac{\Delta T_1}{\Delta T_2}\right)} \tag{4.84}$$

Where $\Delta T_1 = T_4 - T_3$

$\Delta T_2 = T_5 - T_2$

The heat transfer between the hot fluid (weak solution) and cold fluid (strong solution) can be calculated as follows:

The internal heat transfer coefficient(hi) is calculated using data, from strong solution at mean temperature (33°C) and ammonia concentration from (Appendix C)

Using the above parameters

$$R_e = \frac{4\dot{m}_{ss}}{\pi d_i \mu} \tag{4.85}$$

$= 1971.8$ which is < 2300 (laminar flow)

So, the Nusselt number (N_u) = 3.66 according to Dittus-Boelter equation

$$h_i = \frac{N_u \times k}{d_i} \tag{4.86}$$

Also, for the strong solution flow in the shell from generator the external heat transfer coefficient (h_0) is calculated by using the property of strong solution at mean temperature (52℃) and weak ammonia solution from (Appendix C)

From

$$\mathrm{R}_e = \frac{\rho \times v \times d_0}{\mu} \tag{4.87}$$

Where v = Velocity of strong solution in the shell (assume 1m/s)

do = outer diameter of the heat exchanger coil (m)

μ = dynamic viscosity (kg/m. s)

Using McAdam's equation

$$\mathrm{Nu} = 0.023\, R_e^{\,0.8} \times P_r^{\,0.3} \tag{4.88}$$

From the Nusselt number: $$h_0 = \frac{(N_u \times k)}{d_0} \tag{4.89}$$

The overall heat transfer coefficient can be calculated from:

$$\frac{1}{U_0} = \left(\frac{d_0}{d_i \times h_i} + \frac{d_0 \times \ln\left(\frac{d_0}{d_i}\right)}{2k} + \frac{1}{h_0} \right) \tag{4.90}$$

The length of heat exchanger coil can be calculated from

$$Q_{HE} = U_0 \times A_{HE_c} \times F \times LMTD \tag{4.91}$$

Assume the correction factor = 0.7,

$$A_{HE_c} = \frac{Q_{HE}}{U_0 \times F \times LMTD} \tag{4.92}$$

Where A_{HEc} = area of heat exchanger coil

To calculate the length of condenser in superheat regions

$$A_{HE_c} = \pi \times d_0 \times l \tag{4.93}$$

$$l_{HE_c} = \frac{A_{HE}}{\pi \times d_0} \tag{4.94}$$

The length of heat exchanger was calculated by using the rate of heat transfer in equation 4.14, the internal and external heat transfer coefficient from equation 4.86 and 4.89 which their value is 171.46 $W/m^2.K$ and 5170.4 $W/m^2.K$ respectively. The overall heat transfer coefficient (U_0) of the system was calculated from Equation 4.90 which its value is 149.5 $W/m^2.K$. By using the above results, the length of heat exchanger was calculated using equation 4.94 and its length is 1.8 meters.

4.1.6 Expansion Valve Selection

Every refrigerating unit requires a pressure-reducing device to meter the flow of refrigerant from the high-pressure side to the low-pressure side of the refrigerating system according to load demand. The capillary tube is a well-known expansion device in small refrigeration systems, such as household refrigerators and freezers. It is used to decrease the refrigerant pressure and temperature from the condenser to the evaporator (Pirompugd and Wongwises, 2016). When the refrigerant leaves the condenser and enters the capillary tube, its pressure drops down suddenly due to the very small diameter of the capillary. In the capillary, the fall in pressure of the refrigerant takes place due to the small opening of the capillary. A capillary tube is 1–6 m long with an inside diameter generally from 0.5–2.28 mm. In this study 2.5m length and available diameter that already uses in vapour compression refrigeration system capillary tube is used. The selected length is based on the pressure drop in the system, which means as capillary tube length increase the pressure drop in the system also increase. For this system the pressure drop is up to 3.4 bar and the selected length is enough to reduce in to the required pressure (Tetemke *et al.*, 2021).

The advantages of using the capillary tube in the refrigeration systems was a very simple that can be manufactured easily and it is not much costly, has no moving parts and it is compact in size. Due to this it doesn’t need more maintenance.

4.2 Phase Change Material

It is a thermal capacitor that helps to mitigate the imbalance energy of supply and demand by storing energy when it is available and releasing it when it reduces or unavailable. This energy storage can be in the form of latent energy or sensible energy. Latent energy storage is the one that store more energy per volume than sensible heat and have ability to charge and discharge large amount of heat from small mass at constant temperature. It works when the available energy increases the chemical bond of the materials break down and the material changed from solid to liquid to absorb heat. Similarly, when the energy available is less than the melting point of phase change materials it transfers stored heat to the fluid.

4.2.1 Selection of Phase Change Material

The criteria of selecting phase change materials for a given applications are: melting point, working temperature range, chemical stability with same container material, Heat capacity, latent heat, thermal conductivity and cost of phase change materials (Gomez,2011). Depending on the temperature required to separate the ammonia from the ammonia water solution in the generator the selected phase change material in this study was paraffin wax having melting point of 58-60℃. This is due to ammonia refrigerant can vaporise from ammonia water solution at temperature above 37℃ . Also, the paraffin wax selection was based on the availability and melting point temperature by considering the operating temperature of the system (Lingayat and Suple, 2013). The selected phase change material is shown in table 4.9.

Table 4.9 The selected phase change material properties (Raut *et al*.,2021)

Paraffin wax	Melting point (℃)	Density (kg/m^3)	Heat of fusion (kJ/kg)	Latent specific heat capacity($kJ/kg.K$)	Sensible specific heat capacity ($kJ/kg.K$)
6035	58-60	780	189	2.88	2.93

4.2.2 Sizing of Phase Change Materials

It is the method of determining the amount of phase change material required in this system. In order to do this, first identify where the phase change material is to be stored. In this system, the PCM was stored in the generator where the heat transfer between hot fluid from the solar collector and ammonia water solution from the absorber occurs. So, these phase change materials receive heat from the generator coil and ammonia water solution, which is heated by external energy from the solar collector. Additionally, the shape of phase change material storage also affects the performance of the system if heat is not properly transferred between the phase change material and the solution. By considering this, the developed shape for this system was:

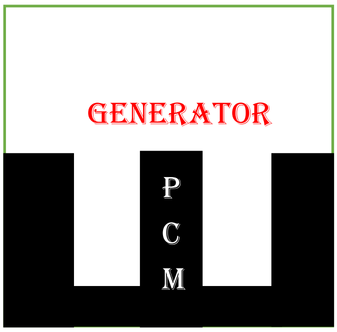

Figure 4.10 PCM in the generator

The required volume of phase change material can be determined from the following steps: The quantity of heat needed to be stored in latent heat thermal energy storage can be estimated first from

$$Qs = \dot{m}_f \times cp_f \times t \times 1.5(T_f - T_i) \tag{4.95}$$

Where, Q_s = capacity of stored heat in kJ, $\dot{m}_f$ = mass flow rate of fluid (kg/s), cp_f = specific heat transfer of fluid (kJ/kg. K), t = storage time(s), T_f = final temperature of the storing medium (℃), T_i = initial temperature of the storing medium (℃). Also, the mass of PCM can be calculated from:

Amount of latent heat thermal energy storage PCM needed to sore Qs was determined as (Niyas *et al.*, 2017):

$$Q_s = m[cp_s(T_m - T_i) + f\Delta H + cp_l(T_f - T_i) \tag{4.96}$$

Where, m= mass of phase change material in kg, T_m = melting point of the storing medium (℃), f= melt fraction, cp_s =sensible specific heat capacity, cp_l = latent specific heat capacity, ΔH =latent heat of fusion in kJ/kg

The volume of phase change material can also determine from:

$$V_{pf} = \frac{mpf}{\rho pf} \tag{4.97}$$

From the above equations (4.91,4.92 and 4.93) by assuming 1-hour storage time, the capacity of stored heat (Qs) = 11290.6kJ, mass of phase change material = 14kg and volume of phase change material = 0.03m^3

Charging time: - It is the total time taken to convert the solid state PCM into a liquid state completely. The phase change material is said to be fully charged when the entire part is melted (i.e., when the melt fraction reaches a value of unity).

Discharging time: - It is the opposite of the charging time or temperature decrease in PCM. It is said to be fully discharged when the entire part is solidified and the melt fraction reaches a value of zero.

4.3 Design of Parabolic Trough Solar Collector

Model or design of parabolic trough solar collector consists of optical analysis for concentrator (reflector surface) and thermal analysis for receiver surface.

4.3.1 Optical Analysis of Parabolic Trough Solar Collector

In order to design the collector, predict the heat flux distribution around the receiver and overall efficiency the optical analysis is very important.

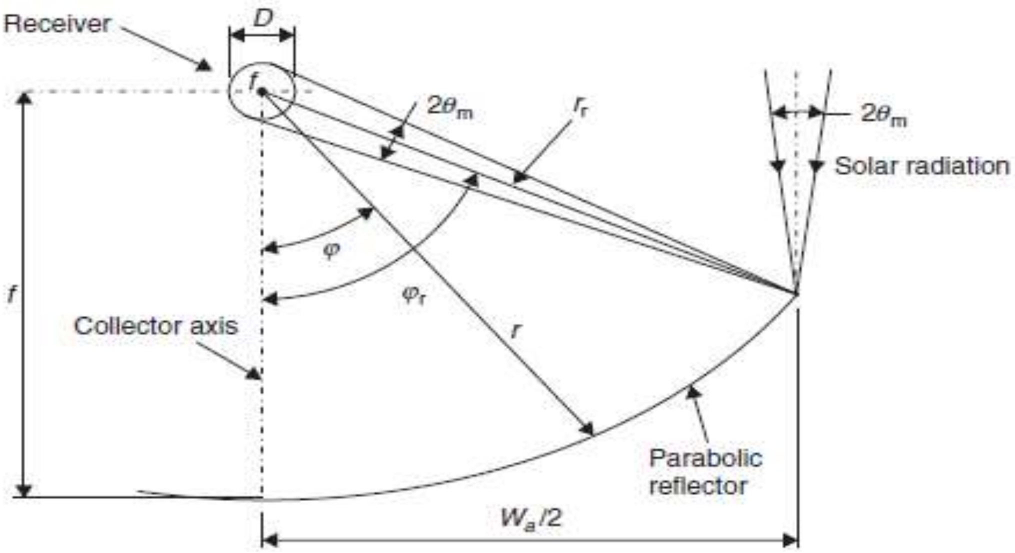

Figure 4.11 Parabolic trough geometry in x-y plane (Kalogirou, 2013)

The parabolic trough geometrical relations to analyse the optical performance is determined from the following relations.

$$y = \frac{x^2}{4f} \tag{4.98}$$

Where, f is the focal length or the distance from point A to point F in Figure 4.10.

The focal length was determined from (Kalogirou, 2013)

$$f = \frac{W_a}{4\tan\left(\frac{\varphi_r}{2}\right)} \tag{4.99}$$

Where, W_a= collector aperture width and φ_r= rim angle which is given by (Duffie *et al.*,1985).

$$\varphi_r = tan^{-1}\frac{8\times\left(\frac{f}{W_a}\right)}{16\times\left(\frac{f}{W_a}\right)^2-1} = sin^{-1}\frac{W_a}{2r_r} \qquad (4.100)$$

$$r_r = \frac{2f}{1+\cos\varphi_r} \qquad (4.101)$$

Where, r_r is the rim radius which is the maximum radius at the maximum rim angle $\varphi = \varphi r$. The local mirror radius (r) can be obtained at any point on the collector by (Duffie *et al.*,1985).

$$r = \frac{2f}{1+\cos\varphi} \qquad (4.102)$$

Where, φ is the angle between the collector axis and reflected beam at the focus.

For specular reflectors of perfect alignment, the size of the receiver required to intercept all the solar image can be obtained from trigonometry

$$D = 2r_r \times \sin\theta_m \qquad (4.103)$$

Where, θ_m half acceptance angle (degree)

For tabular receiver the concentration ratio is given by

$$C = \frac{W_a}{\pi D} \qquad (4.104)$$

By substituting equation 1 and 2 in equation 3

$$C = \frac{\sin\varphi_r}{\pi\sin\theta_m} \qquad (4.105)$$

Finally, length of parabolic surface (S) can be:

$$S = \frac{H_p}{2}\left\{\sec(\frac{\varphi_r}{2}) \times \tan\left(\frac{\varphi_r}{2}\right) + \ln\left[\sec(\frac{\varphi_r}{2}) + \tan(\frac{\varphi_r}{2})\right]\right\} \qquad (4.106)$$

Where H_p lactus rectum of the parabola.

Optical efficiency analysis

Optical efficiency is the ratio of the energy absorbed by the receiver to the energy incident on the parabolic trough collector's aperture. If all the incident solar radiation on the collector aperture is absorbed by the receiver, then there are no optical losses, but, in reality, there are not. The optical efficiency depends on the optical properties of materials like the geometry of the collector, imperfections arising from the construction of the collector and the properties of materials. In equation form:

$$\eta_0 = \rho\tau\alpha\gamma\left[\left(1 - A_f\tan(\theta)\right)\cos(\theta)\right] \qquad \textbf{(}4.107\textbf{)}$$

Where, ρ =reflectance of the mirror, τ = transmittance of the glass cover, α = absorptance of the receiver, γ = intercept factor, A_f = geometric factor and θ = angle of incident

These are not the only factors that influence optical efficiency; other factors such as shadowing effect, increase in end loss, and incident angle modifier also affect optical efficiency as the incident angle changes. End effect is also caused by abnormal parabolic trough operation, when the ray reflected from the near end of the concentrator is unable to reach the receiver. Amount of aperture area lost was given by (Kalogirou, 2013).

$$A_e = fW_a\tan(\theta)\left[1 + \frac{(W_a)^2}{48f^2}\right] \qquad (4.108)$$

Additionally, on this type of collector, shading and blockage of part are happened sometimes this also cause reduce the effect of aperture area. It is also expressed by:

$$A_b = \frac{2}{3}W_a h_p \tan\theta \qquad (4.109)$$

Where, h_p = height of parabola in (m)

From equation 4.104 and 4.105 the total loss of aperture area (A_l) can be:

$$A_l = \frac{2}{3}W_a h_p + fW_a\left[1 + \frac{(W_a)^2}{48f^2}\right] \qquad (4.110)$$

So, the geometric factor (A_f) is the ratio of the lost area to aperture area.

$$A_f = \frac{A_l}{A_a} \qquad (4.111)$$

4.3.2 Thermal Analysis of Parabolic Trough Solar Collector

The thermal efficiency of a parabolic trough collector is the ratio of heat gain by the absorber in the receiver pipe and heat transfer to the fluid in the pipe. Thermal analysis of a parabolic trough solar collector is used to determine the energy that is absorbed by the heat transfer fluid and heat loss in the receiver due to three modes of heat transfer: conduction, convection and radiation. The thermal performance and heat loss in a parabolic trough collector were analysed based on the energy balance between the working fluid and the surrounding.

The incident solar radiation that hit the reflector surface reflected to the absorber tube and the majority of energy absorbed by absorber coating is first transferred into absorber by conduction, next transfer into HTF by convection and the rest transfer into the atmosphere by radiation.

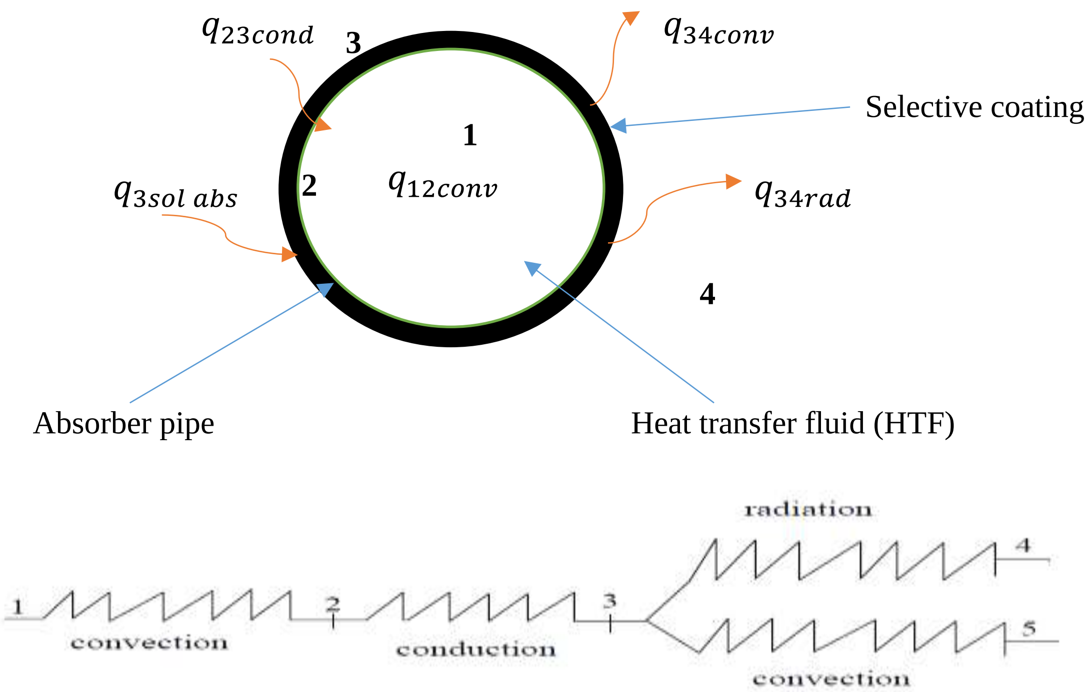

Figure 4.12 Energy balance and thermal resistance model in receiver of parabolic trough solar collector

where 1) heat transfer fluid, 2) absorber inner surface, 3) absorber outer surfaces, 4) sky, 5) radiation

A, Convection heat transfer between HTF and absorber

The heat transfer between the absorber and high temperature fluid is expressed by newton's low cooling as:

$$q_{12conv} = h_1 D_2 \pi \left(T_2 - T_1\right) \tag{4.112}$$

$$h_1 = N_{uD_2} \frac{k_1}{D_2} \tag{4.113}$$

Where h_1 = hot temperature fluid heat transfer coefficient at T_1(W/$m^2.K$), D_2 = inside diameter of the absorber pipe(m), T_1 = mean temperature of hot transfer fluid (°C), T_2 =

inside surface temperature of absorber pipe (°C), $N_{u_{D_2}}$ = Nusselt number based on D_2, k_1= thermal conductivity of high temperature fluid at $T_1 (W/m.K)$

The Nusselt number can be laminar or turbulent depends on the Reynold numbers.

For turbulent flow (Forristall, 2003)

$$N_{uD_2} = \frac{\frac{f_2}{8}(R_{eD_2} - 1000)P_{r1}}{(1 + 12.7\sqrt{\frac{f_2}{8}} \times P_{r1}^{\frac{2}{3}} - 1)}(\frac{P_{r1}}{P_{r2}})^{0.11} \tag{4.114}$$

$$f_2 = (1.82log_{10}(R_{eD_2}) - 1.64)^{-2} \tag{4.115}$$

Where, f_2 = Friction factor for the inner surface of the absorber pipe

P_{r1} = Prandtl number evaluated at the HTF temperature, T_1

P_{r2} = Prandtl number evaluated at the absorber inner surface temperature, T_2

For laminar flow, that means if the ($R_e < 2300$) the Nusselt number is constant and its value is 4.36 for the flow in the pipe (Kalogirou, 2013).

B, Conduction heat transfer through absorber wall

According to the Fourier's law of conduction the heat transfer between absorber pipe and selective coating can be expressed as follows:

$$q_{23cond} = \frac{2\pi k_{23}(T_2 - T_3)}{\ln\left(\frac{D_3}{D_2}\right)} \tag{4.116}$$

Where, q_{23cond} = Conduction trough absorber, k_{23} = thermal conductivity of absorber at mean temperature $(\frac{T_2+T_3}{2})(\frac{kW}{m}.K)$, D_3= Absorber outside diameter(m), D_2= Absorber inside diameter(m), T_3 = Absorber outside surface temperature (K).

The thermal conductivity is constant (i.e., for steel $k_{23} = (0.013)T_{23} + 15.2$) (ASM Handbook Committee, 1978).

C, Convection heat transfer between the surrounding and outside diameter of absorber.

Convection heat transfer between the outside diameter of absorber tube and atmosphere can be:

$$q_{34conv} = h_{34} D_3 \pi \left(T_3 - T_4\right) \tag{4.117}$$

$$h_{34} = \frac{k_{34}}{D_3} N_{uD_3} \tag{4.118}$$

Where, $T_4 =$ Ambient temperature (°C), $h_{34} =$ Convection heat transfer of the ambient air at $(\frac{T_3 - T_4}{2})$(kW/m^2.K), $k_{34} =$ thermal conductivity of air at $(\frac{T_3-T_4}{2})(kW/m.K)$, $N_{u_{D_3}} =$ average Nusselt number.

Nusselt number can be defined in two ways depending on the condition of heat transfer between the absorber and the atmosphere.

1, No wind case

If there is no wind, the convection heat transfer from the absorber to the environment will be by natural convection. The developed Nusselt number correlation by (Bergman *et al.*, 2011) in this case:

$$N_{uD_3} = 0.6 + \frac{0.387 R_{eD_3}^{\frac{1}{6}}}{\left[1 + \left(\frac{0.559}{P_{r34}}\right)^{\frac{9}{16}}\right]^{\frac{8}{27}}} \tag{4.119}$$

$$R_{eD_3} = \frac{\rho\beta\left(T_3 - T_4\right) D_3^{\ 3}}{\alpha_{34} v_{34}} \tag{4.120}$$

$$\beta = \frac{1}{T_{34}} \quad , \qquad P_{r34} = \frac{v_{34}}{\alpha_{34}}$$

Where, $R_{e_{D_3}} =$ Rayleigh number for air-based absorber outside diameter, D_3, g = gravitational constant, $\alpha_{34} =$ thermal diffusivity of air at $T_{34}(m^2/s)$, $\beta =$ volumetric thermal expansion(1/k), $v_{34} =$ kinematic viscosity for air at $T_{34}(m^2/s)$, $T_{34} =$ film temperature $(\frac{T_3+T_4}{2})$.

This correlation works at film temperature and the Nusselt number was in the interval of $10^5 < R_{e_{D_o}} < 10^{12}$.

2, **Wind case**

Wind affects the heat transfer between the substance and the atmosphere. For such case the Nusselt number was estimated by Zhukauskas' correlation for external forced convection was:

$$N_{uD_3} = CR_{eD_3}{}^{m} P_{r34}{}^{n} \left(\frac{P_{r3}}{P_{r4}} \right)^{\frac{1}{4}} \tag{4.121}$$

Where, m and C are read from the table 4.8 depending on the Reynold number. whereas the n value can be: $n = 0.37, for\ Pr \leq 10$

$n = 0.36, for\ Pr > 10$

All fluid properties are evaluated at atmospheric temperature and the correlations is valid at $0.7 < P_{r3} < 500$ and $1 \leq R_{e_{D_3}} < 10^6$

D, Radiation heat transfer

It is heat transfer due to temperature difference between the sky and the outside absorber diameter. The radiation heat transfer between the outside absorber and the sky can be expressed by (Bergman *et al*., 2011).

$$q_{34rad} = \sigma D_3 \pi \varepsilon_3 \left(T_3{}^4 - T_4{}^4 \right) \tag{4.122}$$

Where, $\sigma =$ Stefan-Boltzmann constant $(5.67 \times 10^{-8}) \frac{W}{m^2}.K^4$, $\varepsilon_3 =$ emissivity of absorber at outer surface, $T_4 =$ effective sky temperature.

E, Solar irradiance absorption in the absorber

$$q_{3sol_{abs}} = q_{si} \eta_{abs} \alpha_{abs} \tag{4.123}$$

Where, q_{si} =solar irradiation per receiver length(W/m)

$\eta_{abs} =$ effective optical efficiency at absorber

α_{abs}= absorbance of absorber

F, Collector heat removal factor

The heat removal factor is the ratio of the actual useful energy gain that would result if the collector-absorbing surface had been at the local fluid temperature. This heat removal factor can be given by (Kalogirou, 2013).

$$F_R = \frac{\dot{m}C_p}{A_r U_L}\left[1 - \exp\left(\frac{-A_r U_L F'}{\dot{m}C_p}\right)\right] \quad (4.124)$$

$$F' = \frac{\frac{1}{U_L}}{\frac{1}{U_L} + \frac{D_{ro}}{h_{fi}D_{ri}}\ln\left(\frac{D_{ro}}{D_{ri}}\right)} \quad (4.125)$$

$$U_L = \left[\frac{A_r}{h_{34conv} + h_{34rad}} + \frac{1}{h_i}\right]^{-1} \text{ (W/}m^2.K) \quad (4.126)$$

Where, $F' =$ the collector efficiency factor, $A_r =$ receiver area (m^2), $k_f =$ thermal conductivity of the working fluid ($W/m.K$), $D_{ro} =$ receiver tube outer diameter(m), $D_{ri} =$ receiver tube inner diameter(m), $h_{fi} =$ convective heat transfer coefficient inside the receiver tube (W/$m^2.K$). $U_L =$ thermal loss coefficient (W/$m^2.K$), $h_{34conv} =$ convective heat transfer coefficient between outer absorber diameter and ambient air, $h_1 =$ convective heat transfer between hot transfer fluid and inside absorber diameter.

The useful energy delivered (Q_u) from parabolic trough collector can be calculated from:

$$Q_u = \dot{m}C_p\left(T_{fout} - T_{fin}\right) \quad (4.127)$$

$$T_{fout} = T_{fin} + \frac{\eta_0 A_a I_b}{\dot{m}C_p} \quad (4.128)$$

$$Q_u = F_R A_a\left(\eta_0 I_b - U_L\left(\frac{T_{fin} - T_{amb}}{C}\right)\right) \quad (4.129)$$

Where, $Q_u =$ Useful energy delivered (W/m^2), $A_a =$ Aperture area (m^2), $I_b =$ Direct beam solar radiation(J/m^2), $T_{fin} =$ Temperature of fluid inlet (°C).

The available solar irradiation on the collector aperture (Q_s) is the product of unshaded aperture area (A_a) and direct beam solar irradiation (I_b).

$$Q_s = A_a \times I_b \quad (4.130)$$

$$A_a = A_r \times C \tag{4.131}$$

Where, A_a = Aperture area(m^2), A_r = receiver area(m^2), C = concentration ratio

The instantaneous thermal efficiency (η_{th}) of a solar concentrator was calculated from an energy balance on the receiver (Vijayan and Kumar, 2017) and the efficiency of the collector can be calculated from (Çağlar, 2016).

$$\eta_{th} = \frac{Q_u}{Q_s} = \frac{\dot{m} C_p \Delta T}{I_b A_a} \tag{4.132}$$

Where, $\dot{m}$ = mass flow rate of water (kg/s),

c_p =specific heat of water ($kJ/kg.K$

ΔT = temperature difference (K),

A_a = collector aperture area (m^2)

I_b = solar beam radiation (W/m^2)

Some specifications in design and size of parabolic trough solar collector

- Room temperature and inlet temperature of fluid is 25℃,
- Water is the working fluid for this system where its properties are determined at 25 ℃ (Specific heat: 4.18 $kJ/kg.K$; Density: 997 kg/m^3; Kinematic viscosity: $10^{-6} m^2/s$; Dynamic Viscosity:10^{-3} $kg/s.m$; Thermal Conductivity: 0.58 $W/m.k$; Thermal Diffusivity: $1.39 \times 10^{-7} m^2/s$)
- Galvanized steel covered with glass is used as reflective material.
- The air velocity around the tube is assumed 2.5m/s and there is no glass cover around the receiver tube.
- Mass flow rate of water in the tube = 0.003kg/s (Tabassum et al., 2019**),** (Arunkumar and Ramesh ,2022)

Table 4.10 Specification of parabolic trough solar collector

Parameter	**Value**
Aperture width (W_a)	1.3m
Collector length (L)	2m
Rim angle (φ_r)	90°
Focal length (f)	0.33m
Receiver diameter (r_{di})	23mm
Receiver diameter (r_{do})	25mm
Aperture area (A_a)	1.956m^2
Concentration ratio(C)	12.46

4.3.3 Sizing of Storage Tank

A storage tank is an important aspect of a solar water heating system which is used to store water. This stored water was circulated in the system by receiving heat from solar radiation with the help of a solar collector. The choice of storage tank material has an acute effect on system performance due to heat loss from the system. The shape of the storage also affects the rate of heat transfer. Cylindrical and rectangular shapes are the two major types of storage tank design, where the cylindrical one has more heat transfer rate (Gautam *et al.,* 2017). For this system, cylinder-shaped stainless steel is selected because the rate of heat transfer is low compared with other materials like aluminium and plastic. The sizing of the storage tank depends on the amount of water circulated in the system (solar collector) to operate the system effectively. For this study, the mass flow rate of water in the parabolic trough collector was 0.003kg/s and it was used for sizing the storage tank. By assuming the storage tank stored water for 60 minutes to circulate the system, and from this, the storage tank size was 10L. Also, in order to find the diameter and length of the storage tank, assume $\frac{H}{d_{st}} = 2.5$ (Uwah, 2020).

$$V_{st} = \frac{\pi d_{st}^{\,2}}{4} H \tag{4.133}$$

Where, V_{st} = Volume of storage tank

H = height and

d_{st} = diameter of storage tank.

By using the above formula, the diameter and height of the storage tank are 0.17 and 0.44m respectively.

4.3.4 Pumping Power

It is the power needed to circulate the fluid in a given system in order to perform the system effectively. In this system, it is used to circulate hot water generated in the solar collector from the storage tank to the parabolic trough collector receiver. Also, the other pump, which is used to circulate the strong solution from the absorber to the generator in the refrigeration parts.

The power delivered by the pump to the fluid is called hydraulic power. It is the energy required per hour to supply a volume of water at total dynamic head (Almarshoud,2016).

$$E_h = \frac{\rho \times g \times \mathbb{Q} \times H}{3.6 \times \eta_m \times \eta_p} \tag{4.134}$$

Where, E_h is the hydraulic power delivered by the pump to water (W), ρ is supply water density (kg/m^3), g is the increase of velocity due to gravity (m/s^2), H is the total pumping head in (m), Q is discharge rate required per hour (m^3/h), η_m and η_p are motor and pump efficiency respectively.

Using the above formulas, the pumping power for both hot water fluid and strong solution refrigerant absorbent is calculated. But for experimental testing, the available pump on the market is used. However, if there is an unavailability of electricity, this pump power can be harvested from the sun by using a photovoltaic panel.

The total power generated by solar PV array for water pump is given as:

$$P_{pv} = \frac{E_h}{(G_t \times \mathrm{P}_e \times F)} \tag{4.135}$$

Where, G_t—average daily solar irradiation $kWh/m^2/day$ incident on the array, F—array mismatch factor which value range between 0.85 and 0.90, p_e everyday subsystem effectiveness which has typical significance in between 0.2 to 0.6 (Raghuwanshi and Khare, 2018).

Power of solar PV are mainly depending on incident global solar radiation on the tilted surface of PV array and it is defined as (Almarshoud,2016).:

$$P_{pv} = A_{pv} \times G_t \times \eta_{pv} \times (1-\lambda_m) \times (1-\lambda_e) \qquad (4.136)$$

Where, A_{pv} is area of PV array, η_{pv} is efficiency of solar PV array, λ_m and λ_c are miscellaneous and power conditioning loss respectively.

From the above equations the size of PV array used for water pumping system can be:

$$A_{pv} = \frac{\rho \times g \times Q \times H}{3.6 \times G_t \times \eta_{pv} \times \eta_m \times \eta_p \times \eta_{inv} \times (1-\lambda_m) \times (1-\lambda_c)} \qquad (4.137)$$

Where, η_{inv} is efficiency of inverter.

The input efficiency of PV array (%) is given by

$$\eta_{pv} = \frac{P_{pv}(W)}{G_t(W/m^2) \times A_c(m^2)} \times 100 \qquad (4.138)$$

Where, P_{pv} - the amount of power generated by solar PV array, G_t - average daily solar irradiation ($kWh/m^2/day$) incident on the array, A_c - surface area of the solar cell (m^2).

The overall solar water-pump system efficiency is obtained using

$$\eta_{total} = \eta_{pv} \times \eta_{mp} \qquad (4.139)$$

were, η_{pv} - efficiency of PV array, η_{mp} - the efficiency of the motor pump system.

CHAPTER 5

EXPRIMENTAL SET-UP PREPARATIONS

This chapter contains a detailed fabrication process of each component of both solar collector part and refrigeration system, the setup used for the experiment, test procedure and final assembly supported with photographs is presented.

5.1 Fabrication of Vapour Absorption Refrigeration System

A vapor absorption refrigeration system contains a generator, absorber, evaporator (vaccine storage), condenser, heat exchanger, pump, and expansion valve in order to cool the vaccine in the vaccine storage. The fabrication process of these components is based on design and materials available in the local market by considering their costs.

5.1.1 Fabrication of Generator and Thermal Energy Storage Part

In this system, the phase change material is placed in the generator in order to store heat when there is an unavailability and fluctuation of solar radiation. The generator is made of galvanized steel having 250mm outer shell diameter, 1mm thickness and 350mm height. It has also a 3m steel pipe generator coil of 11.42 and 12.72 mm, inner and outer diameter respectively, which is used to transfer heat from the solar collector to the strong solution as shown in Figure 5.1(a). Figure 5.1(b) shows a rectifier attached to the top of the generator to rectify water vapour.

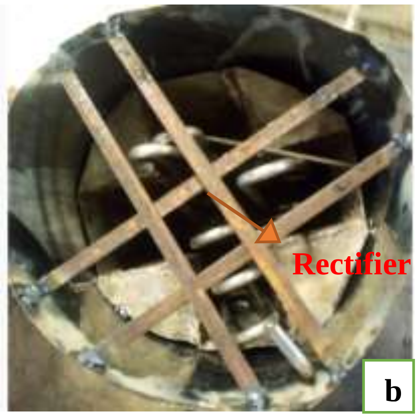

Figure 5.1 a) Generator coil in the generator b) Generator with Rectifier

The phase change material (paraffin wax) is stored at the bottom of the generator, which has a 0.03m^3 volume, and the size for both the generator and phase change material becomes 250mm in diameter and 500mm in height. The preparation process of PCM is first to minimize the size of solid PCM that is used to melt easily, melt and final filling to the bottom and side of the generator as shown in Figure 5.2.

Figure 5.2 Preparation of phase change materials a) sizing the PCM, b) melting, c) filling

5.1.2 Fabrication of Vaccine Storage

The vaccine storage is constructed from 0.4m length,0.25m width and 0.29m height of rectangular in shape based on the required size to store vaccine according to gathered data. It is covered by 0.001m thick galvanized steel in both inside and outside, 0.005m thick glass wool of 0.023W/m^2 thermal conductivity in between inside and outside surface in order to store vaccine in appropriate temperature. The steel pipe evaporator coil having 6.35 mm diameter and 4m length are arranged in this vaccine storage by dividing the storage into upper and lower compartments. Also, the condenser coil having same diameter with evaporator coil and 4.5m length are arranged on the back side of the vaccine storage that is used for condensing the ammonia vapour to liquid. All these components are connected to each other by gas welding as shown in Figure 5.3(c).

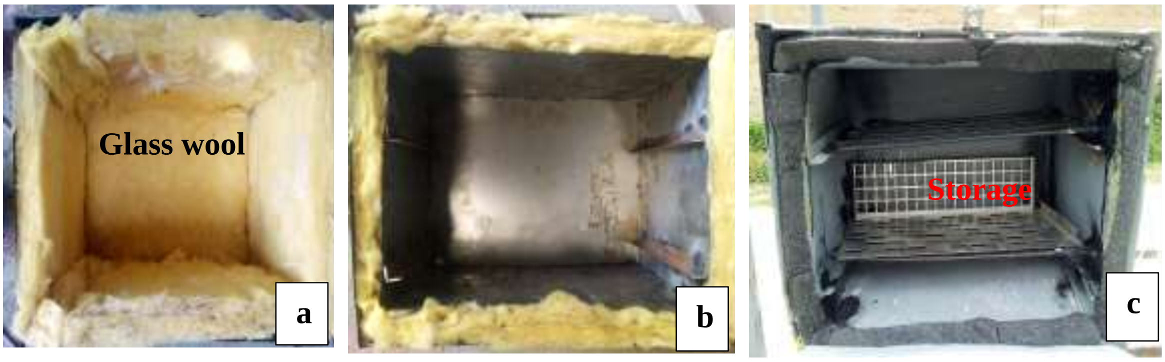

Figure 5.3 Preparation of vaccine storage. a and b) Covering by glass wool insulator, c) Assembly

In addition to phase change material, generator and vaccine storage, absorber having 100mm diameter and 300mm length cylinder made up of mild steel material where absorbent and refrigerant are mixed together, shell and tube heat exchanger having 200mm diameter and 300mm length of shell with 11.42 and 12.7mm inner and outer diameter of steel pipe tube of 1.8m length, expansion valve that used to control the pressure in the system and 0.5hp pump that is used to pump strong solution to the refrigerant are components of vapour absorption refrigeration fabricated and selected for this system. It was assembled each other with generator, vaccine storage and other components as shown below in Figure 5.4.

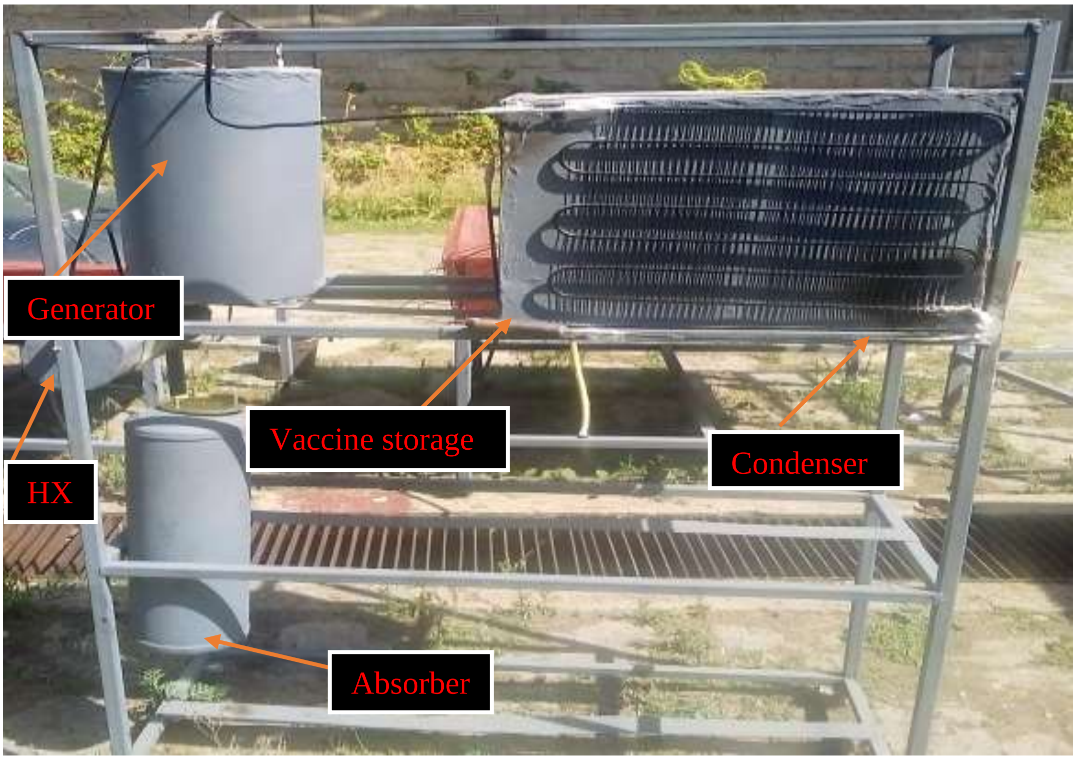

Figure 5.4 Assembly of vapour absorption refrigeration system components

5.2 Fabrication of Parabolic Trough Solar Collector

Parabolic trough solar system consists of galvanized steel covered by glass collector having 1.3m aperture width and 2m length, 0.025m outer diameter and 2m length stainless steel receiver tube, north-south solar tracking system with its base, 0.3m diameter and 0.45m height water storage tank was fabricated in this study based on the design and material available. It has also manual tracking system that used to rotate parabolic trough solar collector based on the direction of sun.

Figure 5.5 Preparation of parabolic trough solar collector a) without glass cover, b) with glass cover and tracking system

5.3 Assembly of Parabolic Trough Solar Collector and Single effect Vapour Absorption Refrigeration System

The solar powered vapour absorption refrigeration system integrated with phase change material is fabricated in this study and the photographic view of solar powered vapour absorption refrigeration system integrated with phase change materials for vaccine storage are showed in Figure 5.6 below. It contains parabolic trough solar collector of 2m length,1.3m aperture width galvanized steel covered with glass and 25mm receiver diameter. Also the vapour absorption refrigeration system components includes:- vaccine storage, evaporator coil that submerged in the vaccine storage and separate it into two compartment, Filter-drier that set up before the capillary tube to absorb any moisture that may be present within the refrigerant circuit so that the refrigerant condensed inside the condenser flows via the filter- drier right into a capillary tube, air cooled condenser that attached on the back side of vaccine storage, generator that have stainless steel coil inside to transfer heat from the solar collector to both ammonia solution and phase change materials, heat exchanger, absorber that store ammonia solution, two pumps that are used to pump ammonia solution and water in the collector. These two systems are assembled by hose and each component are connected by tube. Six calibrated temperature sensors (thermocouples) are mounted at the generator outlet, phase change materials, absorber inlet, evaporator (vaccine storage), inlet and outlet of parabolic trough solar collector. The fabrication prosses has been done based on the available material in the market by considering the costs and design. The data are recorded from the thermocouples by using digital thermocouple.

Figure 5.6 Assemble of parabolic trough solar collector and single effect vapour absorption refrigeration system components

5.4 Measuring Instruments

The instrument used while doing the experiment are thermocouple for measuring temperature and weight load to measure the PCM weight.

Thermocouples: The temperature during the experiments was measured by the thermocouples which are located along the length of the collector. K-type thermocouples are used in the setup. A data reader is used to read the temperature sensed by thermocouples and the values are recorded manually. The thermocouples can read values between -200 to 1250 °C. The detailed calibration process is presented in Appendix I

CHAPTER 6

RESULTS AND DISCUSSIONS

This chapter includes the effect of generator and absorber temperature change on system performance, the obtained result from both parabolic trough solar collector performance and single effect vapour absorption refrigeration system powered by solar energy used for vaccine storage from numerical and experimental result. It also includes the effect of phase change material on the overall system performance.

6.1 Effect of Various Generator and Absorber Temperature on Solar Powered VAR System Performance

The effect of generator and absorber temperature on system performance was analysed by taking the condenser temperature constant from the literature and the evaporator temperature based on the required temperature in the system (vaccine storage) by considering heat loss between the refrigerant flow in the tube and the space where vaccine is stored. This effect was analysed by taking different absorber temperatures (25,28,30 and 32℃) and generator temperatures (75,80 and 85℃) starting from the concentration ratio is valid for this system. The analysis has been done by taking various absorber temperature on each generator temperature to identify the effect on system performance as shown in Figure 6.2 and 6.3. Also, the amount of heat input to the system and rejected from the system to cool the substance at the required temperature was analysed for each selected generator and absorber temperature.

The analysis result showed that, as the generator temperature increase the rate of heat rejected from the condenser is also increase. From the system performance analysed between different absorber and generator temperature, the maximum coefficient of performance is obtained at 75℃ and 25℃ generator and absorber temperature respectively for constant condenser temperature (30℃) and evaporator temperature (-2℃) which is 0.66.

This coefficient of performance was also calculated from the experimental result by using the energy balance of the system in figure 4.1. It was calculated by using the average generator, absorber, evaporator and condenser temperature obtained from the experimental, those are 70, 27, 2 and 28℃ respectively. Mass flow rate, enthalpy of each system components and pressure in the system is also determined based on the data taken from the experiment and it's shown in Appendix G. The coefficient of both experimental and theoretical is shown in Figure 6.5.

This result was compared with the work of (Raut *et al.*,2021) that worked on vapour absorption refrigeration system powered by solar collector by using LiBr-H_2O refrigerant absorbent for the system and its coefficient of performance was 0.68. Also (Shukla *et al.*, 2015) worked vapour absorption refrigeration system with NH_3-H_2O absorbent refrigerant and the coefficient of performance obtained was 0.598 for refrigeration capacity of 3.788kW by using 64℃ generator temperature,30℃ condenser temperature, 20℃ absorber temperature and 4℃ evaporator temperatures. So, the coefficient of performance in this study was good compared with the above two literatures. The results are shown in Figure 6.5.

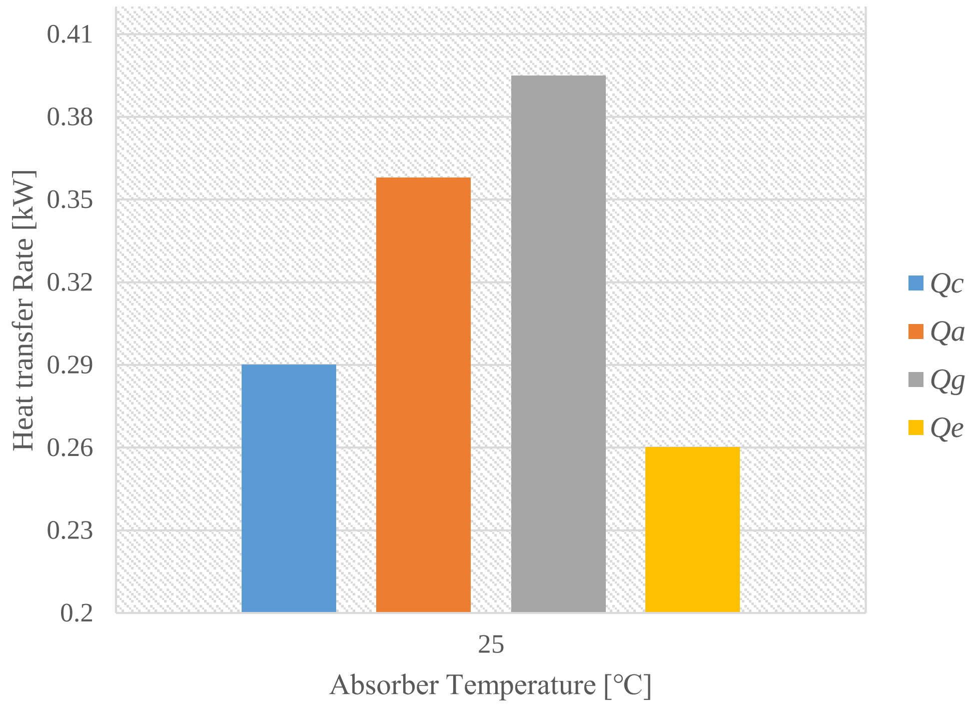

Figure 6.1 Effect of generator temperature (75 ℃) for different absorber temperature

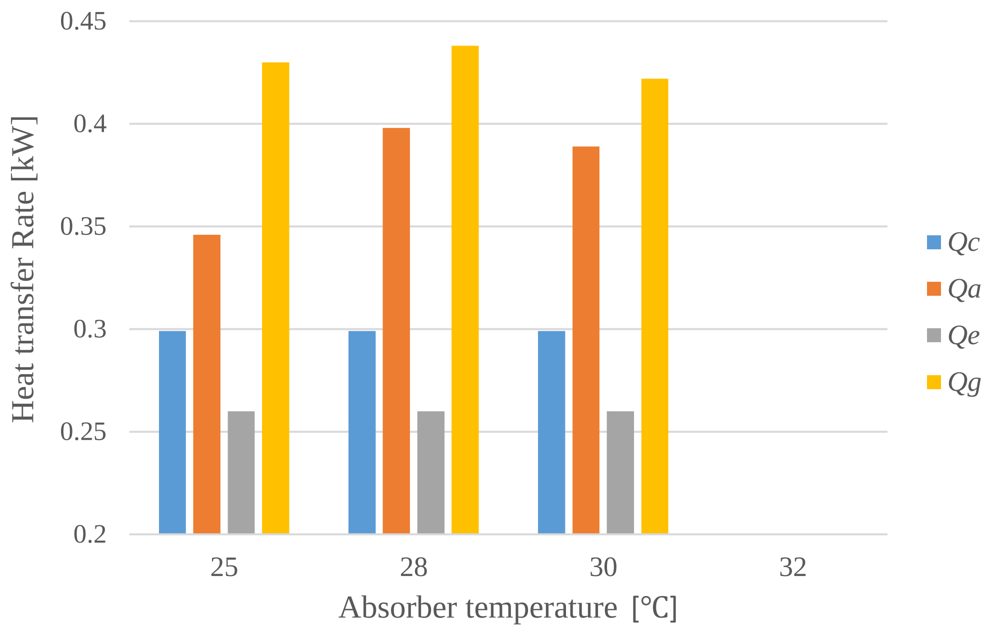

Figure 6.2 Effect of generator temperature (80 °C) for different absorber temperatures

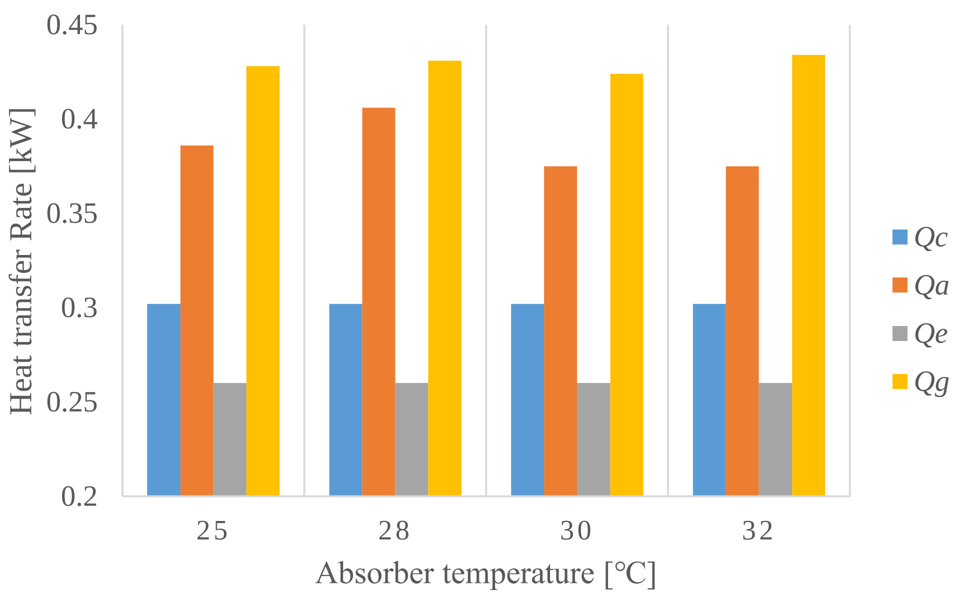

Figure 6.3 Effect of generator temperature (85 °C) for different absorber temperatures

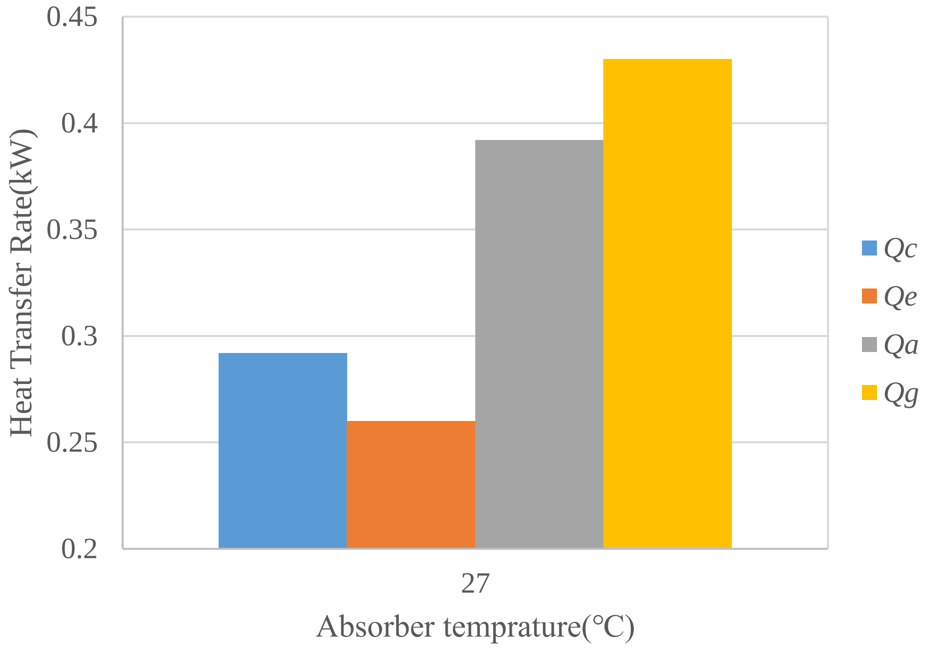

Figure 6.4 Rate of Heat Transfer in the System from Experimental Test for Average Temperature of System Components.

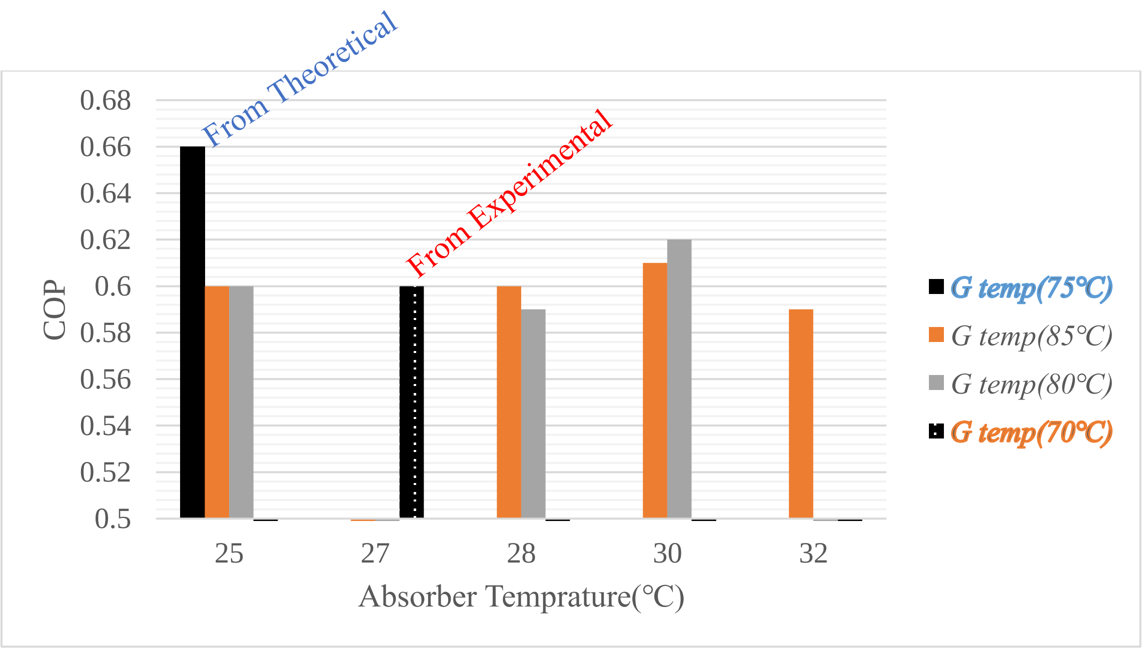

Figure 6.5 Coefficient of performance for different absorber and generator temperatures from experimental and theoretical.

6.2 Parabolic Trough Solar Collector Analysis Results

The parabolic trough solar collector is analysed based on sunshine hour data taken from the East Shewa metrological agency of Adama town for average of six years. The monthly average hourly beam radiation of each season is shown in the figure below. The figure shown below indicates maximum beam solar radiation is recorded in (February 16, October 15 and December 10) respectively and minimum beam solar radiation is in (July 17, August 16 and September 15) respectively.

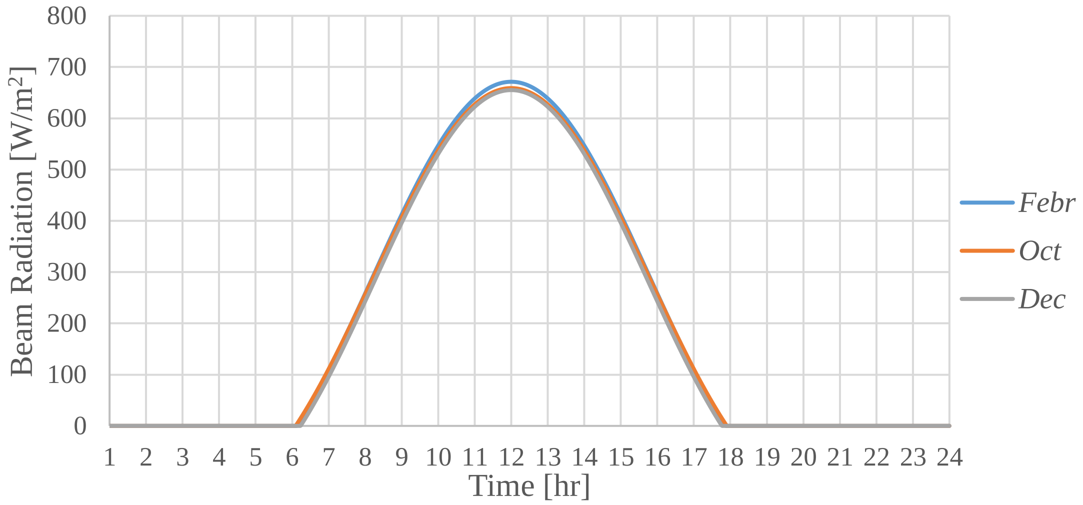

Figure 6.6 Hourly beam incident solar radiation on horizontal surface for three months which are high solar radiation

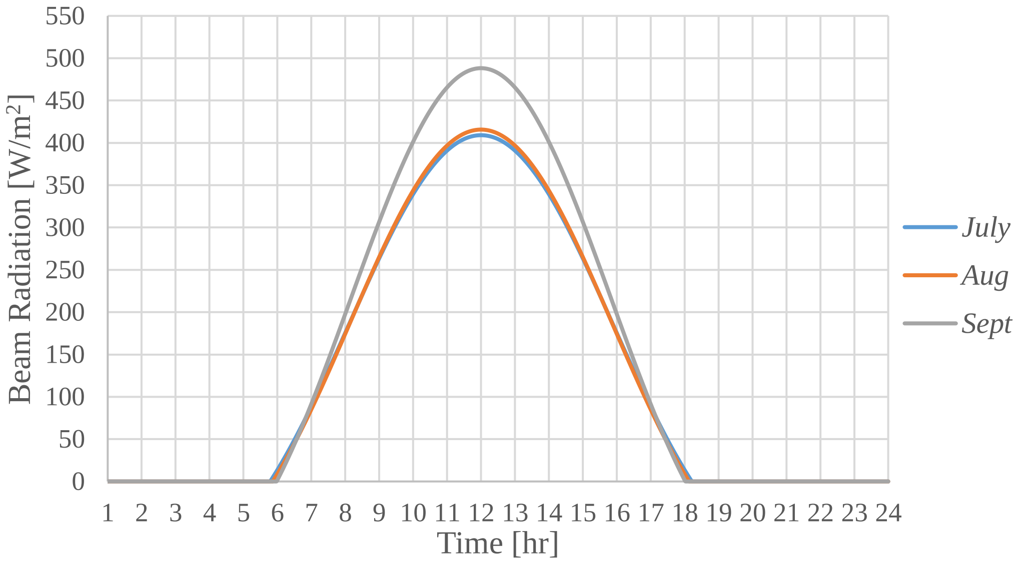

Figure 6.7 Hourly beam incident solar radiation on horizontal surface for three months which are low solar radiation.

6.2.1 Temperature Outlet of Parabolic Trough Solar Collector (PTSC)

The temperature outlet of PTSC that used as input energy for single-effect vapour absorption refrigeration system for vaccine storage is analysed as shown in figure below. This analysis was done based on the input energy required for generator (75℃) which has high coefficient of performance based on the analyses done in the chapter 4, the mass flow rate of the fluid is 0.003 $kg/\ s$ according to (Tabassum *et al.*, 2019; Arunkumar and Ramesh, 2022). The numerical analysis was done by changing the aperture length and collector length of the collector to get the required temperature (inlet generator temperature) where other parameter is depends on these two parameters for representative day of the month in the year. From the analysis result, using aperture width $(Wa) = 1.3m$, collector length=2m and other parameters listed in Table 4.10, the average outlet temperature of parabolic trough solar collector in representative day of month in the year is 78.4℃. It is greater than the required temperature in the generator and it have advantage because there's few lose in the connecting hose that connect the generator and collector. Also, it was valid when compared with the work of (Itabiyi *et al.*, 2021) which the maximum outlet temperature of parabolic trough solar collector constructed from 1.2m aperture length and 2.1m collector length was 70℃. The outlet temperature of the parabolic solar collector in the representative day of the year and its average temperature are listed in Figure 6.8,6.9 and 6.10 respectively.

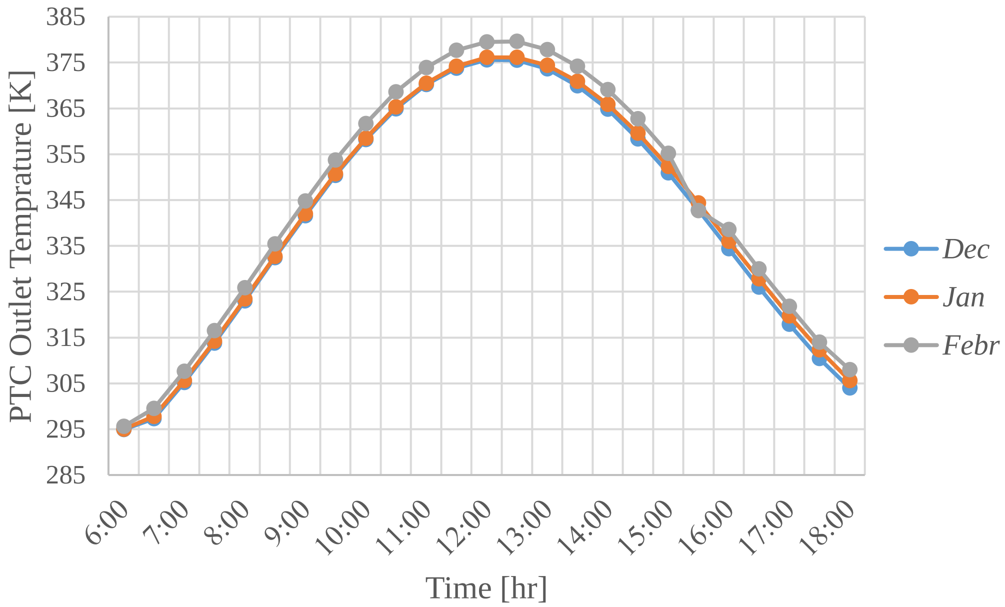

Figure 6.8 Hourly outlet temperature of parabolic trough solar collector in representative day of winter seasons.

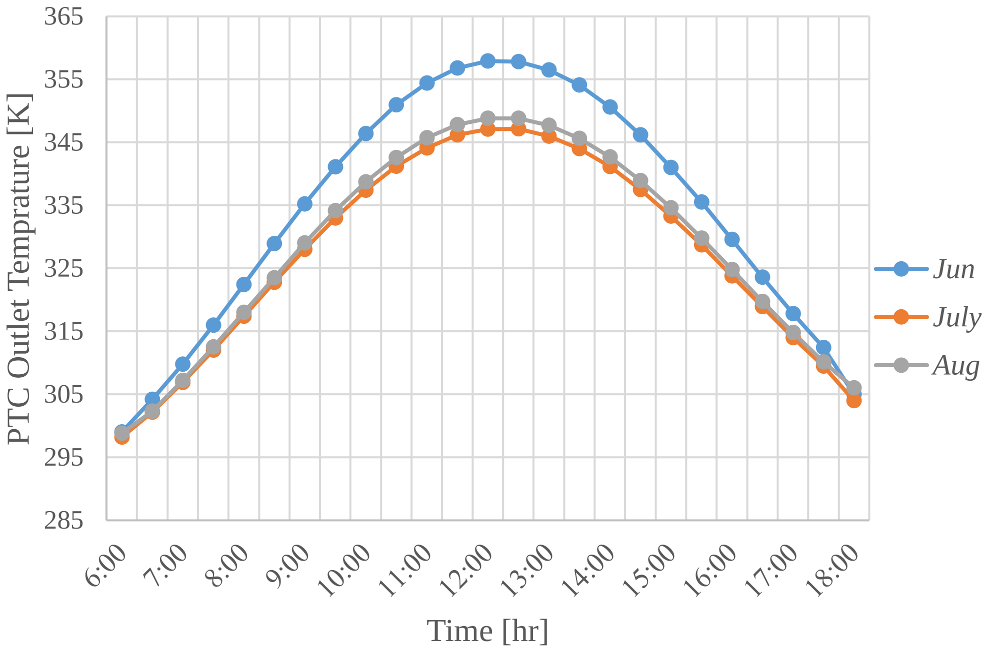

Figure 6.9 Hourly outlet temperature of parabolic trough solar collector in representative day of summer seasons.

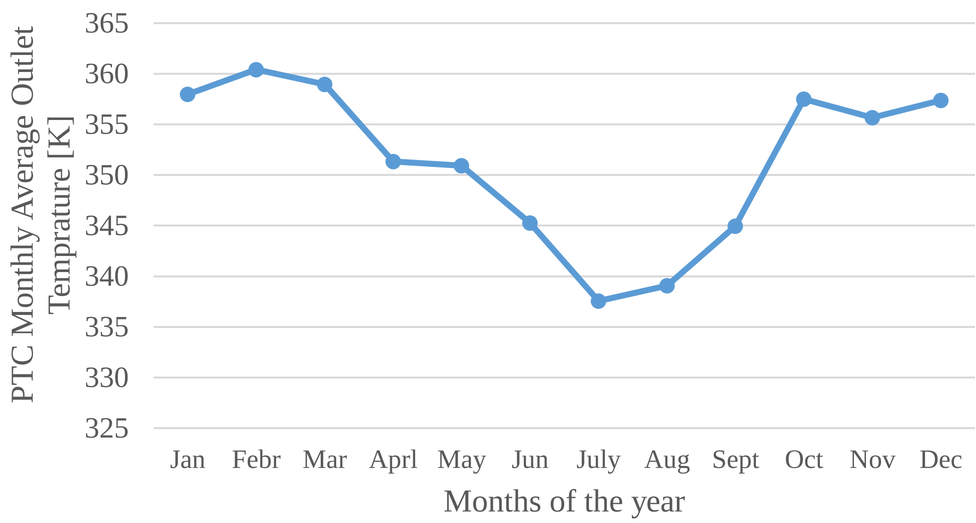

Figure 6.10 Monthly average outlet temperature of parabolic trough in representative day of each month.

6.2.2 Useful Energy Gain by Parabolic Trough Solar Collectors

The useful energy gain from parabolic trough solar collector is depends on the mass flow rate, the inlet water temperature and outlet water temperature of the fluid. It is determined based on the collected and analysed data from sun rise to sunset or sunshine hour. From the collected data the maximum energy collected is usually high at noon time. This useful energy is depending on the size of the solar collector or its width and length of the collector. In this system number of collectors is one which have a 1.3m aperture width and 2m collector length with 25mm absorber diameter. Also, the mass flow rate temperature affects the useful energy needed in the system. From the analyses the average useful energy gain from the parabolic trough solar collector in the representative day of the month in the year is 0.414kW, which is input energy for the generator in this system. From the vapour absorption refrigeration system, the energy required in the generator that used to evaporate ammonia from the strong solution is 0.395kW. So, the sized parabolic trough solar collector is safe to give the required cooling temperature in the system. The useful energy for representative day of the month and its average are drawn below:

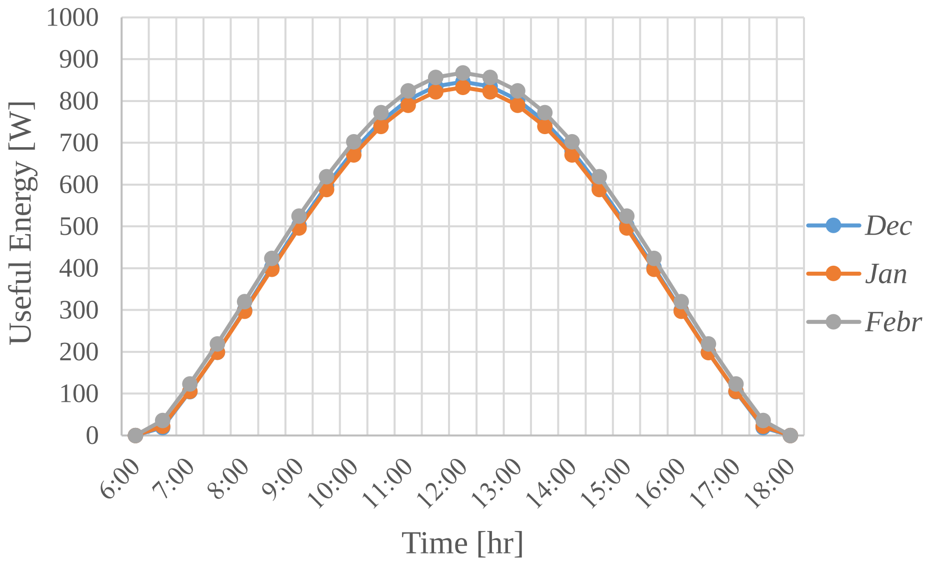

Figure 6.11 Hourly useful energy gain of parabolic trough solar collector in representative day of winter seasons

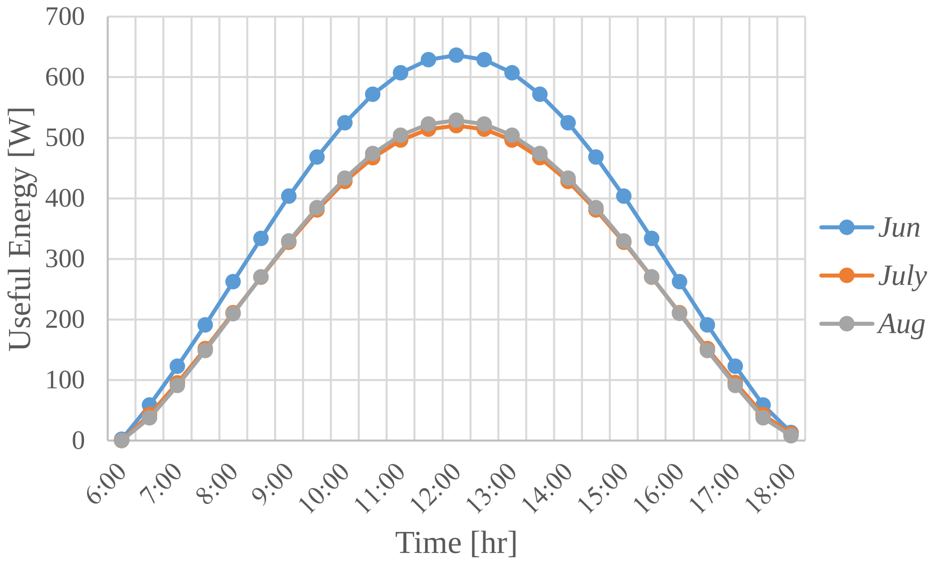

Figure 6.12 Hourly useful energy gain of parabolic trough solar collector in representative days of summer seasons

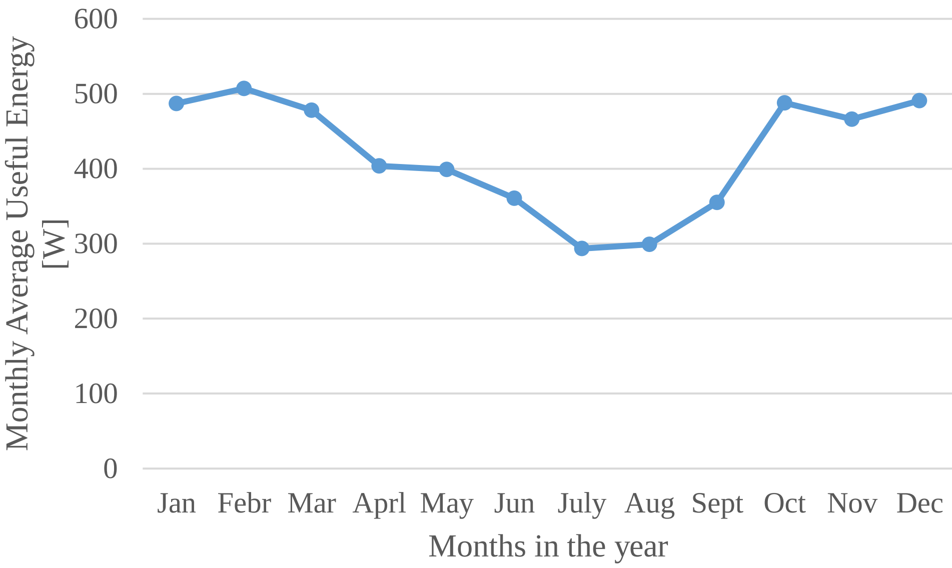

Figure 6.13 Monthly average useful energy gain from parabolic trough solar collector in representative days of each month.

6.2.3 Thermal Efficiency of Parabolic Trough Solar Collector

The efficiency of the collector is based on the heat transfer fluid in the collector, inlet and outlet fluid temperature, mass flow rate and solar radiation from sunrise to sunset. In this study the numerical analysis of parabolic trough solar collectors was done using data taken from metrological agency for average of six years solar radiations. The result shows that the maximum and minimum thermal efficiency are recorded in February 16 and July 17 respectively and also the average thermal efficiency of parabolic trough solar collector in representative day of the month in the year is 73%. The thermal efficiency of PTC in representative day of each month and its average are shown in Figure below.

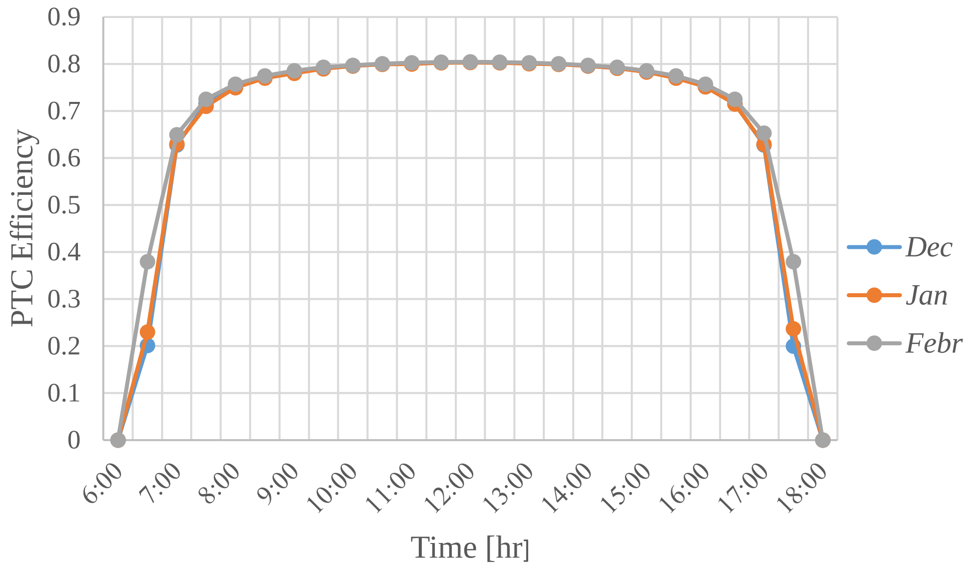

Figure 6.14 Thermal efficiency of parabolic trough solar collector in representative days of Winter seasons

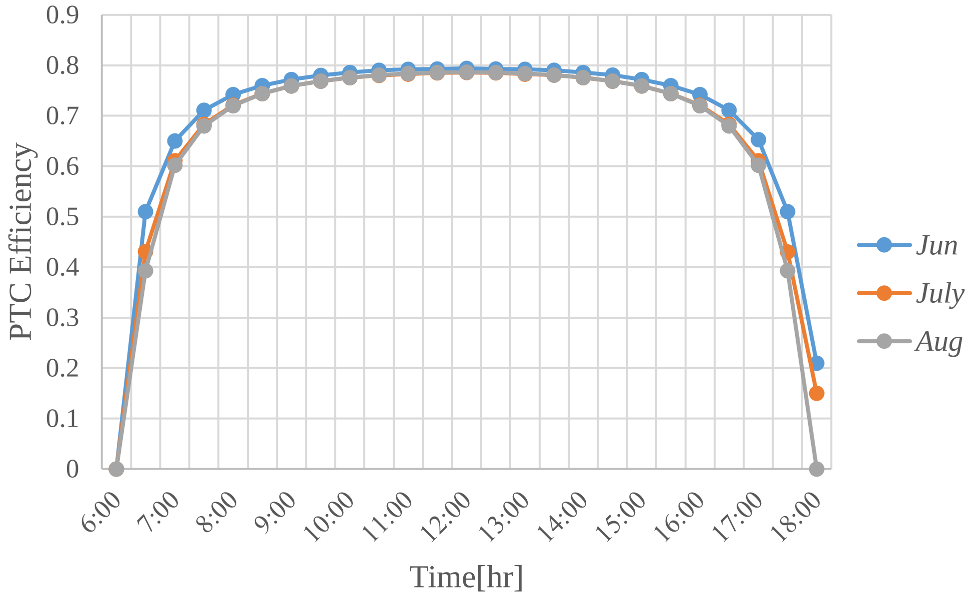

Figure 6.15 Thermal efficiency of parabolic trough solar collector in representative days of summer seasons

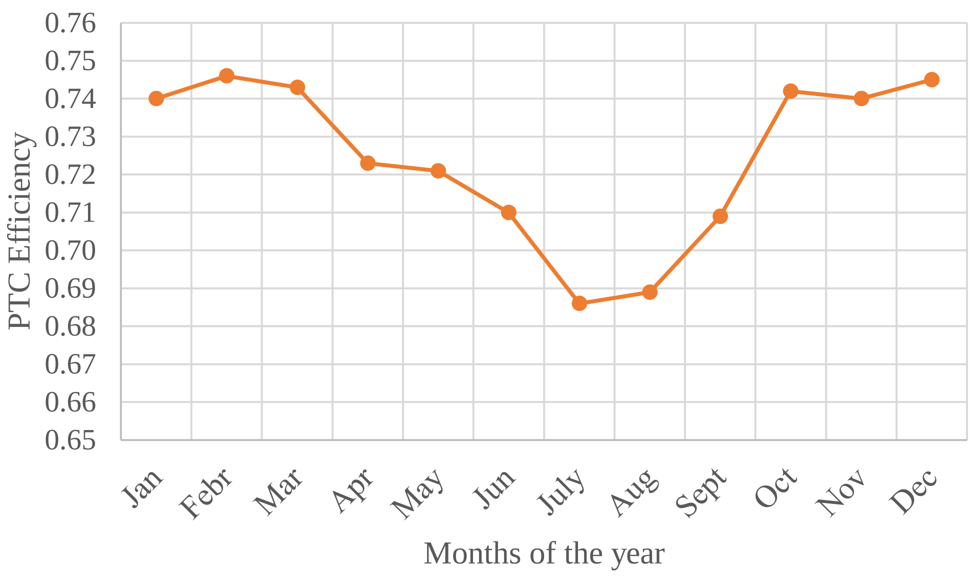

Figure 6.16 Monthly average thermal efficiency of parabolic trough solar collector in representative days of each month.

6.3 Experimental Result Analysis of Solar Powered Vapour Absorption Refrigration System Integrated with Phase Change Materials.

The solar powered vapour absorption refrigeration system integrated with phase change material was fabricated from available material depending on the design parameters and the experimental test was performed for five days from June 26 to 30 in Adama conditions. During the experiment, the inlet temperature of fluid (water), the outlet temperature from the collector, the generator temperature, and the temperature of phase change material were measured by using a digital thermometer and the effect of one parameter on the other was analysed. Also, in the vapour absorption refrigeration system, the absorber temperature and evaporator temperature are also measured. This test has been done by taking the water, which is initially equal to the ambient temperature, and pumping it to the parabolic trough solar collector, where it received more heat and entered to the generator. The system is also recirculated to give a maximum temperature for the system.

The experimental test was analysed in two ways; those are: with phase change material integrated and without. In without phase change material, the inlet temperature of the parabolic trough solar collector slowly increases as the solar radiation increases up to solar noon and also the outlet temperature increases in a similar way to the inlet temperature, as shown in Figure 6.17. The outlet temperature enters into the generator through the coil transfer heat to the generator or to ammonia solutions. As the outlet collector temperature rises, more heat is transferred to the generator and ammonia is vaporized from the ammonia solution to cool the vaccine in the evaporator. When the temperature of the inlet generator falls below the boiling point of ammonia solution, the system is shuts down until heat is added to the generator.

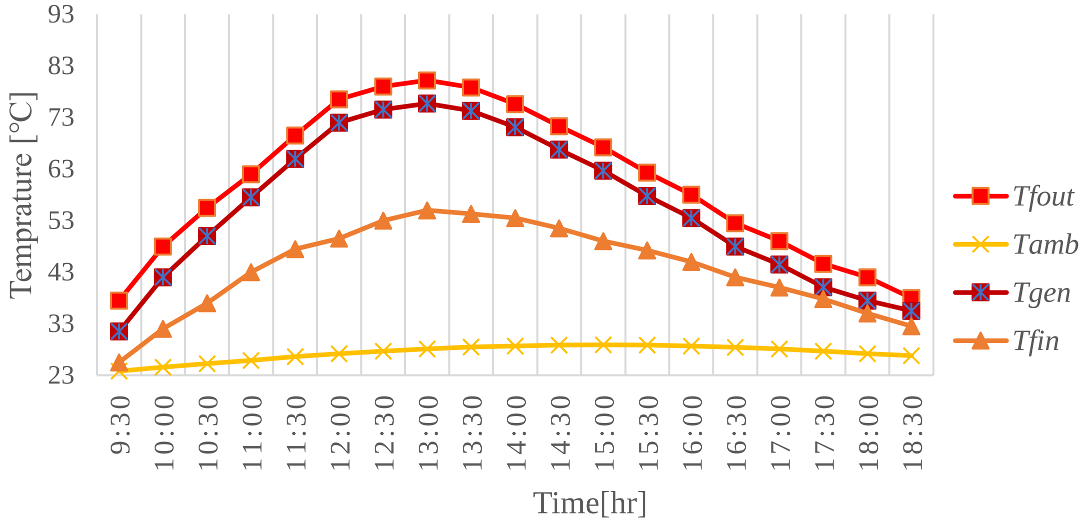

Figure 6.17 Variation of outlet solar collector and generator temprature without PCM with time.

To increase the system working time during low and unavailable solar radiations, integrating phase change material is the best solutions. The effect of adding phase change material on the VAR system is analysed by using outlet collector temperature and generator temperature parameters. As shown in the Figure 6.18, the inlet and outlet temprature of parabolic trough solar collector is slowly increase as the solar radiation increase up to the solar noon and the outlet temprature enters into generator coil transfer heat for both PCM and solution in the generator.

As the outlet temprature from the collector increase, the rate of heat transfer to the generator and phase change material is increase. When the generator inlet temprature or outlet temprature from the collector increase above the boiling temprature of the ammonia solution ,the ammonia is changed into vapour to make the refrigration system fuctional. Also as inlet temprature to the generator increase, the phase change material temprature became increase up to its melting point as shown in Figure 6.18. This is happened around the noon where maximum solar radiation was attained. The generator temprature is directily proportional with outlet solar collector up to the time of discharching of phase change material and once the collector outlet temprature is decreased below the melting temprature of the phase change materials, the PCM starts discharge the stored energy to the solution in the generator and the system became continousely work for some hours.

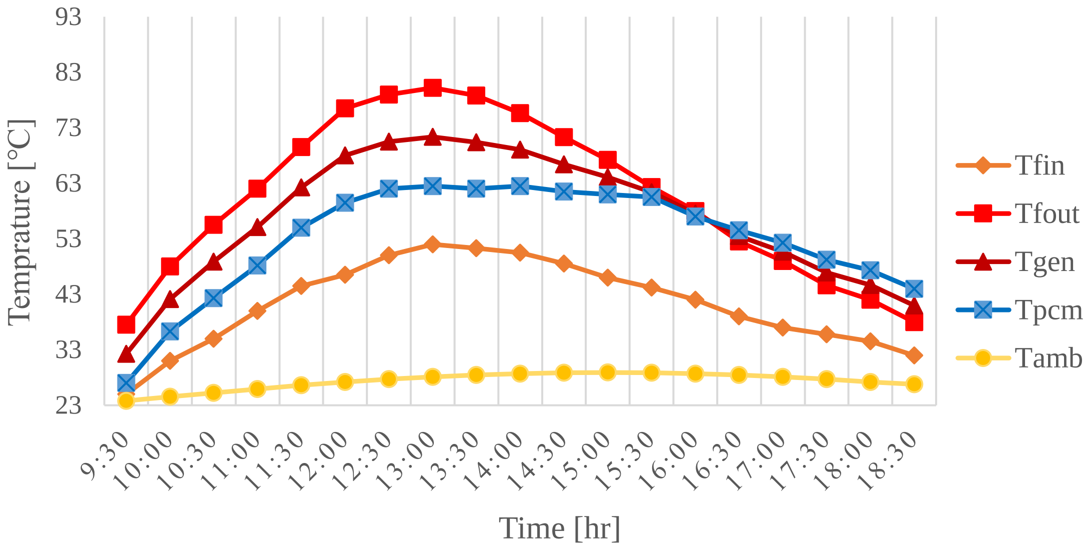

Figure 6.18 Effect of phase change material on generator temperature with time

6.3.1 Effect of Generator Temperature and Phase Change Materials on Evaporator Temperatures

The vaccine storage must be maintained in the required temperature which is average of 5℃. To do this the input energy to the generator or the outlet temperature from the solar collector is relatively high to vapor ammonia from the ammonia solutions. In these experimental studies, the evaporator temperature was analysed in two ways: those are with and without load. One carton of PCV vaccine which contains 500ml volume is used in this study to analyse the effect of load on the system performance. For the without load, the experimental result showed that the generator temperature is low or less than the boiling point of ammonia solution for few minutes starting from the experiment was started and during this time the evaporator temperature is equal with ambient temperature and it decrease rapidly when the generator temperature increases above the boiling point of the ammonia solution. As the generator temperature increase, ammonia is vapourised from ammonia solution and it circulate in the system and maintains the evaporator temperature at the required temperature after few minutes. It continuously stayed at required temperature until the inlet generator temperature is below the boiling temperature of the solutions or the heat transfer between the two are stable or the rate of heat transfer is low. The Figure 6.19 below shows the effect of generator temperature on the evaporator temperature for without load. Also Figure 6.20 shows the effect of evaporator temperature with load.

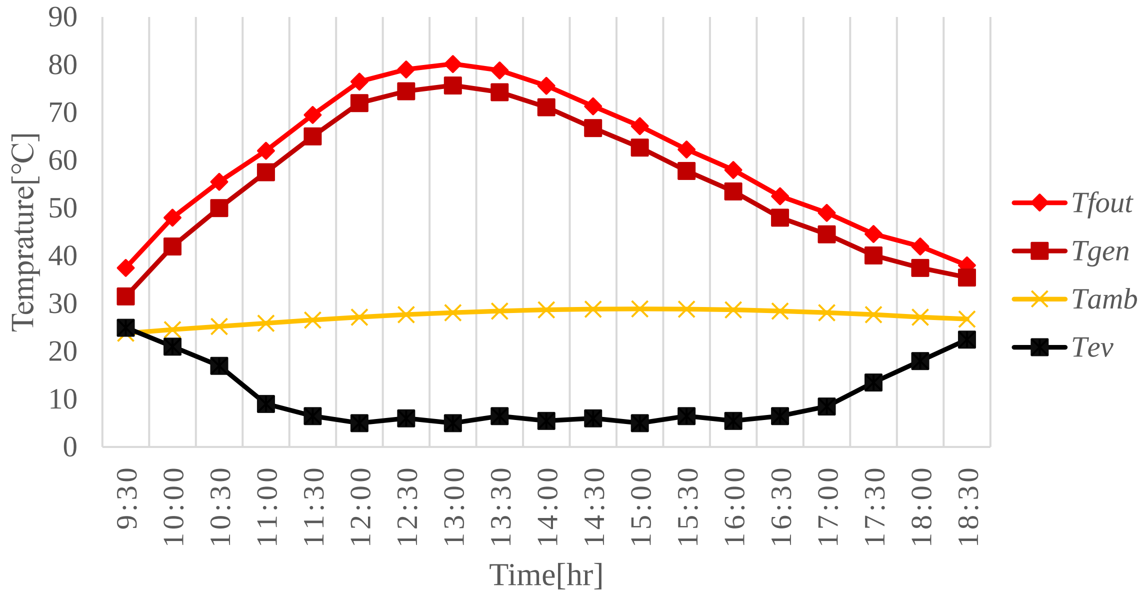

Figure 6.19 Variation of generator and evaporator temprature of without load and without PCM.

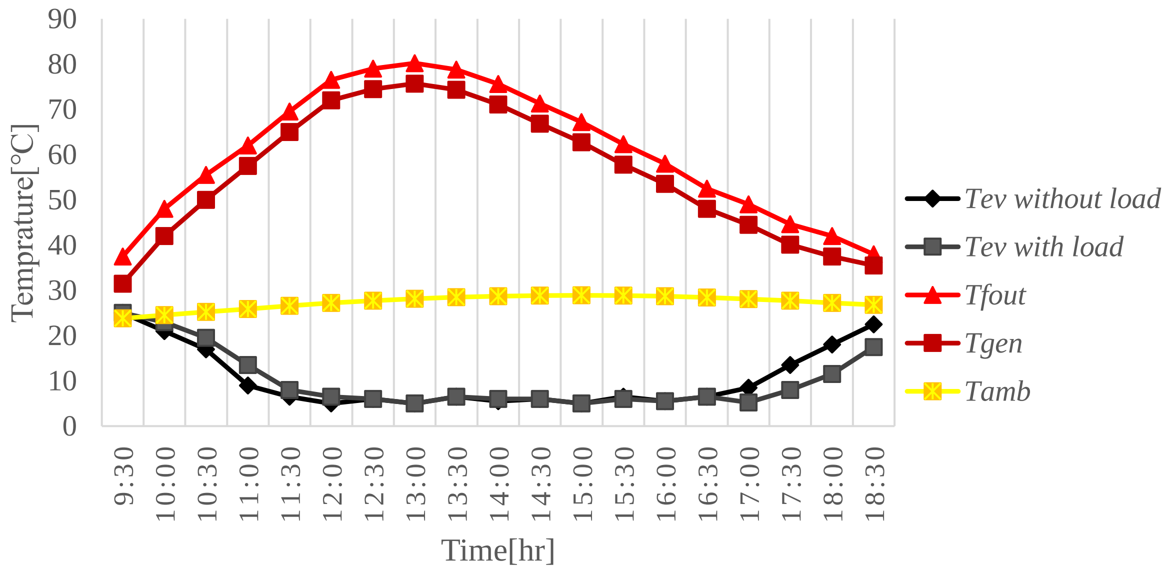

Figure 6.20 Variation of generator and evaporator temprature with load and without PCM.

The next is when phase change material is added into the generator. The phase change material stored in the generator transfer stored heat to the ammonia solution when the inlet temperature from the solar collector is become low. So, the evaporator temperature continuously maintained at required temperature until the phase change material stop releasing heat to the solutions. The effect of load in the evaporator is also proportional with the effect of phase change material on the system. Figure 6.21 below shows the effect of generator temperature on evaporator temperature.

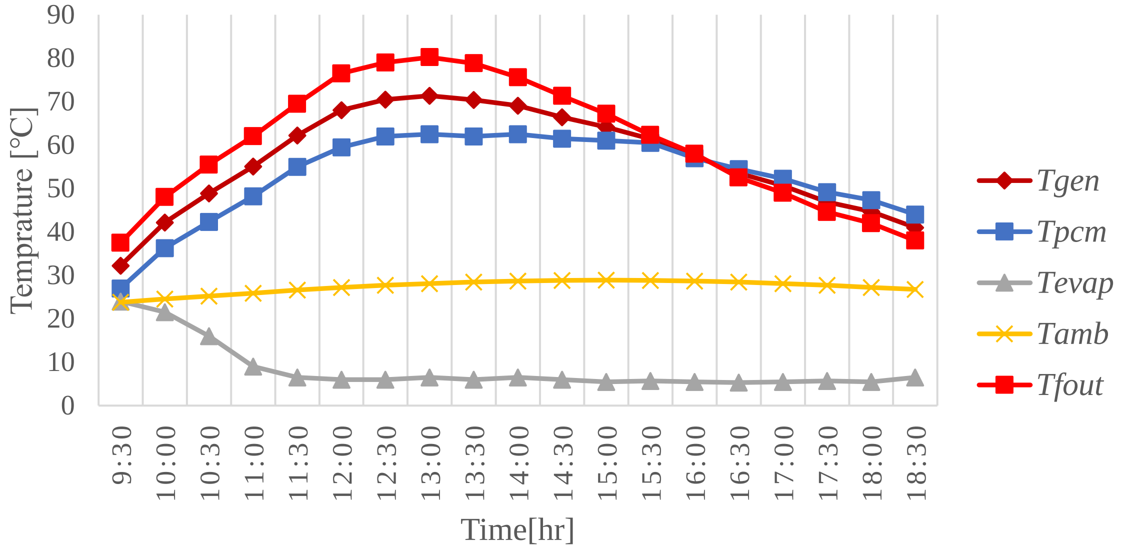

Figure 6.21 The effect of phase change material on generator and evaporator temperature without load with time.

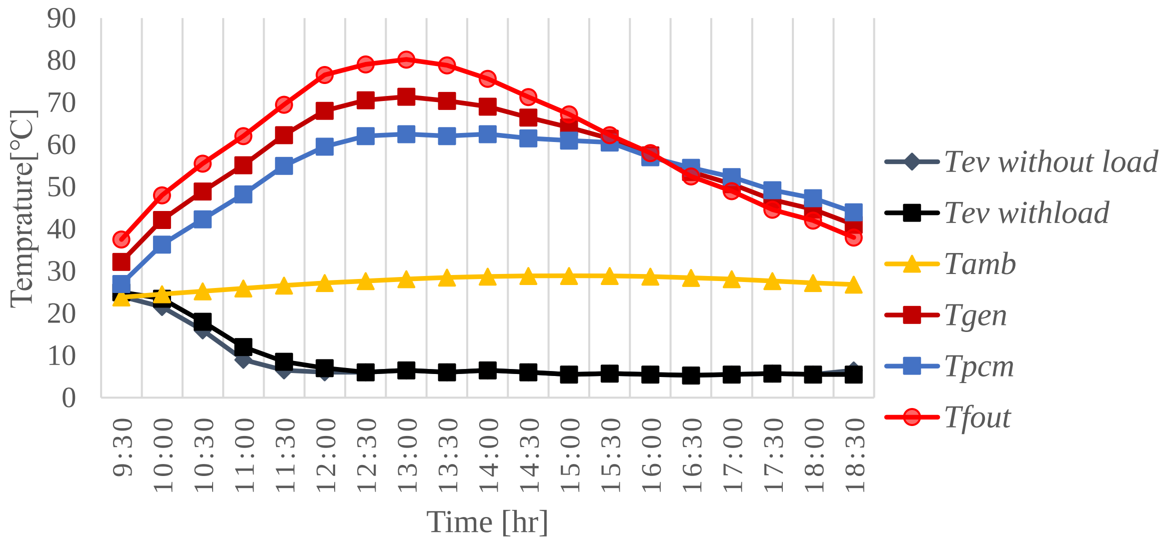

Figure 6.22 The effect of phase change material on generator and evaporator temperature with load with time.

6.3.2 Experimental Results of Thermal Energy Storage

Phase change material is the one that store energy from available source and discharge it when it is unavailable. In this study paraffin wax is used for phase change material which the melting temperature is 58-60°C. This phase change material is stored in the generator which is used to maintain the generator temperature at the required temperature when the solar energy is not available. The charging and discharging of this PCM was depends on the inlet temperature to the generator from the solar collector. Initially the temperature of phase change material is equal with the ambient temperature and it gradually increase as the inlet generator or outlet collector temperature increase. The charging time is a time it takes until the phase change material completely melt or store more energy. As shown in Figure 6.23 the charging time takes three hours and thirty minutes or up to the phase change material attain above melting temperature. Also, after few hours this stored energy starts discharging due to the input energy from the solar collector to the generator is lower than the melting temperature of the PCM. So, it releases heat to the ammonia solution in the generator that helps to continue vapour ammonia from ammonia solution until the heat released from the phase change material is stop or completely solidify. From the experimental result it takes almost equal time with charging time.

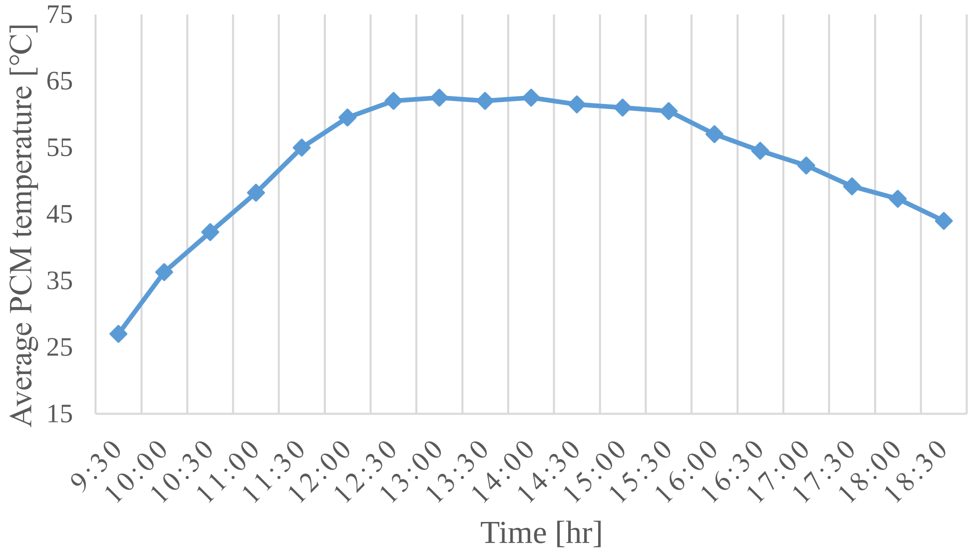

Figure 6.23 Average temperature variation of paraffin wax in generator.

From the Figure 6.23 above the phase change material (paraffin wax) was passed three steps. The first one is charging time from 9:30-13:00. In this step the outlet temperature from the solar collector is high and it transfer heat to the phase change material until it completely melts or store more energy. It contains more latent heat energy and few sensible energies. The second step is from 13:00-15:30, in this step also the outlet collector temperature is higher than the melting temperature of PCM. In this step there are only sensible heat and variation of PCM temperature is low. As the input energy to the generator is below the melting temperature of the phase change materials the stored energy during charging time is transfer to the low temperature (generator temperature) which is called discharging time and it's from 15:30-18:30. Generally, the phase change material stored in the generator continuous the system at required temperature for three hours after the solar radiation (collector outlet temperatures) is reduced below the required temperature in the system. From the above result it was valid with the work of (Raut et al,2021) works on solar powered vapour absorption refrigeration system coupled with latent heat energy storage which the charging and discharging time takes 3 hours. While it used LiBr-H_2O absorbent refrigerant rather than NH_3-H_2O in this study.

6.3.3 Overall Analysis of Integration Parameters in Solar Powered Vapour Absorption Refrigeration System.

In solar powered vapour absorption refrigeration system, the outlet temperature from the solar collector and phase change materials affects the system directly and indirectly. Figure 6.24 shows the overall system integration parameters in solar powered vapour absorption refrigeration system.

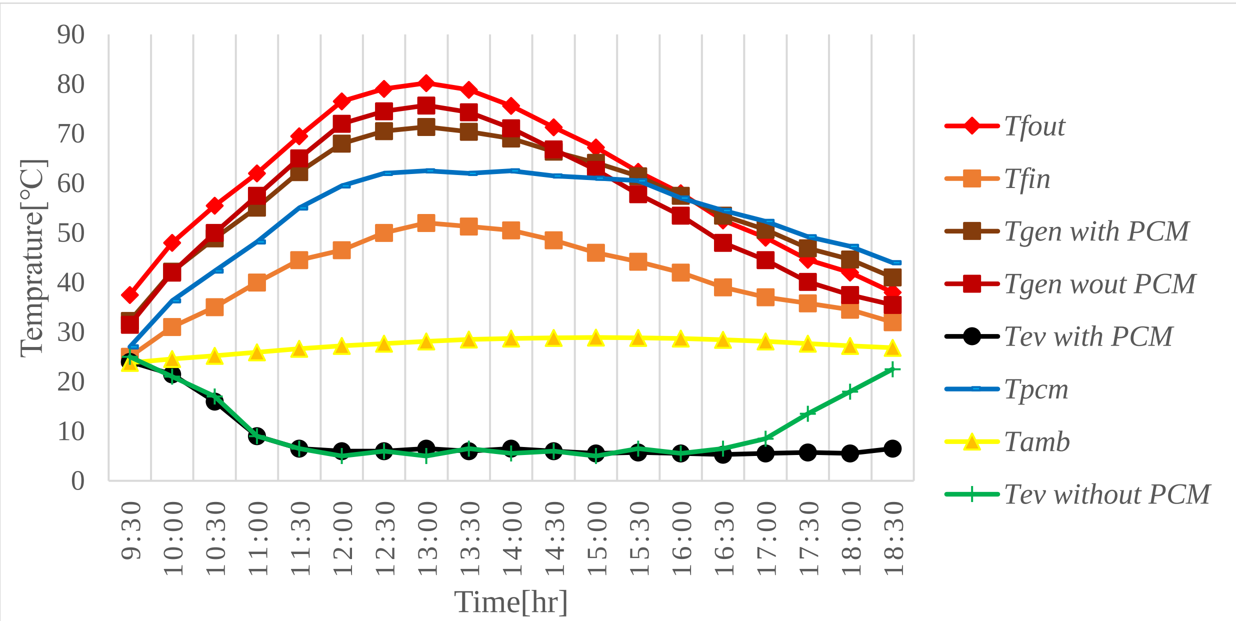

Figure 6.24 The overall description effect of one parameter on the other with time.

CHAPTER 7

CONCLUSIONS AND RECOMMENDATIONS

7.1 Conclusions

A solar powered vapour absorption refrigeration system was designed and fabricated, with NH_3-H_2O as the working fluid for vaccine storage. The following conclusions can be made from the present investigations:

- Based on the data collected from Mukiye Haro rural health center, the cooling capacity of a vapour absorption refrigeration system is determined in this study. From the collected data, 8707.5cm^3 cold chain capacity is required for the number of doses per supply interval. Based on its capacity, a rectangular box 40 cm long, 25 cm wide, and 29 cm high was built from galvanized steel that covering the inside and outside bodies and 4mm thickness of glass wool insulator with 0.023 W/m K thermal conductivity is added between the inside and outside covers on all sides of the box. Using the above data, 0.26 kW cooling capacity or the amount of heat removed from refrigerated space to cool and maintain the required temperature in the refrigerator is determined.
- Depending on the required temperature in the evaporator to store vaccine and determined cooling capacity, the generator and absorber temperature in vapour absorption refrigeration system is determined from analysis made between various absorber temperature (25,28,30 and 32℃) and generator temperature (75,80 and 85℃) that had maximum coefficient of performance. The analyses made shows that maximum coefficient of performance is obtained at 75 and 25℃ generator and absorber temperature respectively, for constant condenser temperature of 30℃ and evaporator temperature of -2℃ which is 0.66. The coefficient of performance was also calculated from the experimental result from the average temperature of system component recorded during the experiment and its value was 0.6.
- A parabolic trough solar collector was designed and fabricated from a 2 m length, 1.3 m aperture width and a 25 mm diameter of stainless-steel receiver for delivering 0.39 kW of the required energy to the generator. From the numerical analysis result, the average outlet temperature of a parabolic trough solar collector on a

representative day of a month in the year is 78.4°C and also, the outlet temperature of the solar collector when the experimental test is performed (June) is 85℃ .From the experimental results 80.2℃ maximum outlet temperature of the day when the experiment has been performed.

- Additionally, from the numerical analysis results, the average useful energy gain from the parabolic trough solar collector in the representative day of the month in the year is 0.414kW, which is input energy for the generator in this system. In this study, the energy required in the generator to evaporate ammonia from the ammonia solution is 0.395kW. So, the sized parabolic trough solar collector is safe to give the required cooling temperature in the system. In addition to this the average thermal efficiency of the parabolic trough solar collector in representative day of the month in the year is (73%) where maximum and minimum thermal efficiency are recorded in February 16 and July 17 respectively.

- Phase change materials are used to store energy from an available source for an unavailable time. In this study, paraffin wax is used for phase change material, which is melted by the energy from the solar collector, especially at maximum solar radiation or at noon. This phase change material is stored in the generators of vapour absorption refrigeration system's components, to transfer heat to the ammonia solution during unavailability and low solar radiation (collector outlet temperature) in order to keep the evaporator (vaccine storage) at required temperatures. The experimental result showed that the phase change material stored in the generator continued to cool the system for three hours after the outlet solar collector temperature is reduced below the required temperature in the system.

7.2 Recommendations

Based on the present study the following ideas are recommended to improve more the system performance.

1. In this study the phase change material is stored in the generator, which have more heat transfer rate to the solution in the generator due to its shape and position. However, additional improvement is needed by increasing the size of phase change material in order to store more heat and discharge it for a more hour to maintain the system at required temperature for a long time. Additionally, adding cold storage phase change material in the evaporator maintain the system at required temperature for a long time.

2. In this study the parabolic trough collector receiver is 2m long and 25mm diameter tube which is enough to get the required temperature for this study. Additional improvement is needed on the receiver tube, rather than using single tube having large diameter, two or three tube of small diameter assembled to each other as one which is important by reducing the mass flow rate and increase the outlet temperature.

3. The tracking system for the solar collector in this study is manual tracking system. But the automatic tracking system have more efficiency than manual, due to that adding automatic tracking system is another improvement needed on this study.

4. This study used two pumps which are powered by electric from electricity due to cost. But using solar panel which is powered by solar energy is recommended rather than using electric from electricity.

SPECIAL ACKNOWLEDGEMENT

This research project is funded by Adama Science and Technology University under the grant number ASTU/SM-R/658/22, Adama, Ethiopia.

REFERENCES

Abdin, Z., Alim, M. A., Saidur, R., Islam, M. R., Rashmi, W., Mekhilef, S., and Wadi, A. (2013). Solar energy harvesting with the application of nanotechnology. *Renewable and sustainable energy reviews*, *26*, 837-852.

Almarshoud, A. F. (2016, June). Sizing of PV array for water pumping application. In *Conference: 32nd European photovoltaic solar energy conference and exhibition, at Munich, Germany* (Vol. 30).

Almultashi, M., Moghiman, M., and Ameer, S. A. A. (2021). *Experimental Study of Using Ethyl Ether-Acetaldehyde Solution in A Solar-Driven Absorption Chiller Integrated with A Parabolic Trough Solar Concentrator, 44*.

Al-Ugla, A. A. (2015). *Development of A Solar Airconditioning System in Saudi Arabia* (Doctoral dissertation, King Fahd University of Petroleum and Minerals (Saudi Arabia)).

Al-Yasiri, Q., and Szabó, M. (2021). Paraffin as a phase change material to improve building performance: an overview of applications and thermal conductivity enhancement techniques. *Renewable Energy and Environmental Sustainability*, *6*, 38.

Amaris, C., Bourouis, M., Vallès, M., Salavera, D., and Coronas, A. (2015). Thermophysical properties and heat and mass transfer of new working fluids in plate heat exchangers for absorption refrigeration systems. *Heat Transfer Engineering*, *36*(4), 388-395.

Arora, C. P. (2000). *Refrigeration and air conditioning*. Tata McGraw-Hill Education.

Arunkumar, S., and Ramesh, K. (2022). Design and optimization of solar parabolic trough collector with evacuated absorber by grey relational analysis. *Current Science*, *122*(4), 410-418.

ASHRAE, A. H. (2006). Refrigeration. *American Society of Heating, Refrigerating and Air Conditioning Engineers (ASHRAE)*.

ASM Handbook Committee. (1978). *Metals Handbook: Heat Treating* (Vol. 4). American Society for Metals.

Bangotra, A. (2017). Design-analysis of generator of vapour absorption refrigeration system for automotive air-conditioning. *Int. J. Eng. Res. Technol.*, *6*, 121-125.

Bekele, A., Alemu, D., and Mishra, M. (2013). Large-scale solar water heating systems analysis in Ethiopia: A case study. *International Journal of Sustainable Energy*, *32*(4), 207-228.

Bergman, T. L., Bergman, T. L., Incropera, F. P., Dewitt, D. P., and Lavine, A. S. (2011). *Fundamentals of heat and mass transfer*. John Wiley and Sons.

Bhowmick, A., and Kundu, B. (2021). Thermo-economic optimization and comparison study of LiBr-H2O and LiCl-H2O working pair in absorption cooling systems based on genetic algorithm. *International Journal of Energy Research*, *45*(3), 3938-3954.

Bose, M., and Modi, A. (Eds.). (2020). *Proceedings of the 7th International Conference on Advances in Energy Research*. Springer Nature.

Çağlar, A. (2016). Design of a parabolic trough solar collector using a concentrator with high reflectivity. *Proc. World Congr. Mech. Chem. Mater. Eng.*, 2-6.

Cao, E. (2010). *Heat transfer in process engineering*. McGraw-Hill Education

Cattin, M., Jonnalagedda, S., Makohliso, S., and Schonenberger, K. (2020). The status of refrigeration techniques for vaccine storage and transportation in low-income settings.

Cengel, Y., and Boles, M. (2010). Thermodynamics: An Engineering Approach with Student Resources DVD.

Chakravarthy, V. S., Shah, R. K., and Venkatarathnam, G. (2011). A review of refrigeration methods in the temperature range 4–300 k. *Journal of Thermal Science and Engineering Applications*, *3*(2).

Chandra, A. R., and Arora, R. C. (2012). *Refrigeration and air conditioning*. PHI Learning Pvt. Ltd.

Christopher, S. S., Santosh, R., Ponrajan Vikram, M., Prabakaran, R., Thakur, A. K., and Xu, H. (2021). Optimization of a solar water heating system for vapor absorption refrigeration system. *Environmental Progress & Sustainable Energy*, *40*(1), e13489.

Dall'Amico, M., and Hornsteiner, M. (2006). A simple method for estimating daily and monthly mean temperatures from daily minima and maxima. *International Journal of Climatology: A Journal of the Royal Meteorological Society*, *26*(13), 1929-1936.

Darwish, N. A., Al-Hashimi, S. H., and Al-Mansoori, A. S. (2008). Performance analysis and evaluation of a commercial absorption–refrigeration water–ammonia (ARWA) system. *International Journal of refrigeration*, *31*(7), 1214-1223.

Devarajan, Y., Nagappan, B., Subbiah, G., and Kariappan, E. (2021). Experimental investigation on solar-powered ejector refrigeration system integrated with different concentrators. *Environmental Science and Pollution Research*, *28*(13), 16298-16307.

Duffie, J. A., and Beckman, W. A. (2013). *Solar engineering of thermal processes*. John Wiley and Sons.

Duffie, J. A., Beckman, W. A., and McGowan, J. (1985). Solar engineering of thermal processes.

Enibe, S. O. (1997). Solar refrigeration for rural applications. *Renewable energy*, *12*(2), 157-167.

Faraj, K., Khaled, M., Faraj, J., Hachem, F., and Castelain, C. (2021). A review on phase change materials for thermal energy storage in buildings: Heating and hybrid applications. *Journal of Energy Storage*, *33*, 101913.

Farid, M. M., Khudhair, A. M., Razack, S. A. K., and Al-Hallaj, S. (2004). A review on phase change energy storage: materials and applications. *Energy conversion and management*, *45*(9-10), 1597-1615.

Fenta, S. M., and Fenta, H. M. (2020). Risk factors of child mortality in Ethiopia: application of the multilevel two-part model. *PLoS One*, *15*(8), e0237640.

Forristall, R. (2003). *Heat transfer analysis and modeling of a parabolic trough solar receiver implemented in engineering equation solver* (No. NREL/TP-550-34169). National Renewable Energy Lab., Golden, CO.(US).

Fudholi, A., and Sopian, K. (2018). Review on solar collector for agricultural produce. *International Journal of Power Electronics and Drive Systems*, *9*(1), 414.

Gandhi, A., and Arakerimath, R. R. (2016). Solar Vapour Absorption Cooling System Using parabolic dish Collector. *IOSR J. Mech. Civ. Eng*, *13*, 9-13

Ge, H., Li, H., Mei, S., and Liu, J. (2013). Low melting point liquid metal as a new class of phase change material: An emerging frontier in energy area. *Renewable and Sustainable Energy Reviews*, *21*, 331-346.

Ghyadh, N. A., Hammadi, S. H., and Shahad, H. A. (2020). Using solar collector unit in a methanol-water vapor absorption cooling system under Iraqi environmental conditions. *Case Studies in Thermal Engineering*, *22*, 100749.

Gomez, J. C. (2011). *High-temperature phase change materials (PCM) candidates for thermal energy storage (TES) applications* (No. NREL/TP-5500-51446). National Renewable Energy Lab. (NREL), Golden, CO (United States).

Green, D. W., and Perry, R. H. (2008). *Perry's chemical engineers' handbook*. McGraw-Hill Education.

Hashim, N. A., and Kassim, M. S. (2021, February). Experimental Study of a LiCl-H_2O Bubble Pump Solar Absorption Cooling System. In *IOP Conference Series: Materials Science and Engineering* (Vol. 1094, No. 1, p. 012017). IOP Publishing.

Hernández-Magallanes, J. A., Domínguez-Inzunza, L. A., Gutiérrez-Urueta, G., Soto, P., Jiménez, C., and Rivera, W. (2014). Experimental assessment of an absorption cooling system operating with the ammonia/lithium nitrate mixture. *Energy*, *78*, 685-692.

Horuz, I., and Callander, T. M. S. (2004). Experimental investigation of a vapor absorption refrigeration system. *International journal of refrigeration*, *27*(1), 10-16.

Huirem, B., and Sahoo, P. K. (2020). Thermodynamic Modeling and Performance Optimization of a Solar-Assisted Vapor Absorption Refrigeration System (SAVARS). *International Journal of Air-Conditioning and Refrigeration*, *28*(01), 2050006.

Ibrahim, I. D. (2020). *Development of Smart Parabolic Trough Solar Collector for Water Heating and Hybrid Polymeric Composite Water Storage Tank* (Doctoral dissertation, Université Paris-Saclay; Tshwane University of Technology).

Itabiyi, O. E., Sangotayo, E. O., Lateef, A. K., and Aminu, I. F. (2021). Experimental Analysis of the Parabolic Trough Solar Concentrator Water Heater. *European International Journal of Science and Technology*, *10*(7), 1-12.

Jejaw, A., and Getnet, A. (2021, August). Performance Evaluation of Locally Fabricated Public Water Cooler. In *International Conference on Advances of Science and Technology* (pp. 233-242). Springer, Cham.

Kakac, S., Liu, H., and Pramuanjaroenkij, A. (2002). *Heat exchangers: selection, rating, and thermal design*. CRC press.

Kalogirou, S. A. (2014). *Solar energy engineering: processes and systems*. Academic press.

Kanabar, B. K., and Ramani, B. M. (2018). Thermodynamic Analysis of Single Effect, Double Effect and Multi Effect LiBr/H2O Vapour Absorption Refrigeration Cycle. *J. Refrig. Air Cond. Heat. Vent*, *4*(1), 43-55.

Karl, K., (2014). Refrigeration systems selections, sizing, and troubleshooting, Kolmetz Handbook of Process Equipment Design.

Ketfi, O., Merzouk, M., Merzouk, N. K., and El Metenani, S. (2015). Performance of a single effect solar absorption cooling system (Libr-H2O). *Energy procedia*, *74*, 130-138.

Kumar, K. S. P., Kumar, A., and Nanduri, P. R. (2015). Analysis of wind speed data for energy production at central Ethiopia, Adama. *Int. J. Recent Res. Sci. Eng. Technol*, *1*(2).

Kumar, S., and Arakerimath, D. R. (2015). Comparative Study on Performance Analysis of Vapour Absorption Refrigeration System Using Various Refrigerants. *PASJ International Journal of Mechanical Engineering (IIJME), 3*(1).

Kurem, E., and Horuz, I. (2001). A comparison between ammonia-water and water-lithium bromide solutions in absorption heat transformers. *International communications in heat and mass transfer*, *28*(3), 427-438.

Li, J. M., Friend, M., Miller, A., and Stone, S. (2016, October). An SDD and PCM solution for vaccine storage and outreach. In *2016 IEEE Global Humanitarian Technology Conference (GHTC)* (pp. 555-562). IEEE.

Lima, A. A., Leite, G. D. N., Ochoa, A. A., dos Santos, C. A., da Costa, J. A., Michima, P. S., and Caldas, A. (2021). Absorption Refrigeration Systems Based on Ammonia as Refrigerant Using Different Absorbents: Review and Applications. *Energies*, *14*(1), 48.

Lingayat, A. B., and Suple, Y. R. (2013). Review on phase change material as thermal energy storage medium: materials, application. *International Journal of Engineering Research and Applications*, *3*(4), 916-921.

Manojprabhakar, S., Ravindranath, R. C., Vinothkumar, R. V., Selvakumar, A., and Visagavel, K. (2014). Fabrication and testing of refrigeration using engine waste heat. *International Journal of Engineering and Innovative Technology, 3.*

Mira-Hernandez, C., and Isaza-Roldan, C. A. (2021). Latent Heat Energy Storage in a Household Refrigerator Powered by Photovoltaic Electricity–Heat Transfer Design and Technical Viability.

Mohanty, D. K., and Padhiary, A. (2015). Thermodynamic Performance Analysis of a Solar Vapour Absorption Refrigeration System. *International Journal of Enhanced Research in Science Technology and Engineering*, *4*(4).

Naidu, P. V. K., and Nair, A. M. (2018). Analysis of paraffin wax as a phase change material. *International Journal of Current Engineering and Technology*, *18*(1).

Natnale, S. (2019). *Numerical Investigation of Solar Vapor Absorption Refrigeration System Integrated with Phase Change Material for Industrial Application* (Doctoral dissertation, ASTU).

Niyas, H., Prasad, S., and Muthukumar, P. (2017). Performance investigation of a lab–scale latent heat storage prototype–Numerical results. *Energy Conversion and Management*, *135*, 188-199.

Oni, T. O. (2018). Cop Analysis of a Vapour Absorption Refrigeration Cycle powered by a solar system. *Gsj*, *6*(6), 189.

Parton, W. J., and Logan, J. A. (1981). A model for diurnal variation in soil and air temperature. *Agricultural meteorology*, *23*, 205-216.

Perry, R. H., and Green, D. W. Perry's Chemical Engineers' Handbook 7th edition (1997). *ISBN-13*, 978-0071834087.

Pirompugd, W., and Wongwises, S. (2016). Helical capillary tube sizing charts for all mixture ratios of R125, R134a and R32. *International Journal of Air-Conditioning and Refrigeration*, *24*(04), 1650022.

Pongtornkulpanich, A., Thepa, S., Amornkitbamrung, M., and Butcher, C. (2008). Experience with fully operational solar-driven 10-ton LiBr/H_2O single-effect absorption cooling system in Thailand. *Renewable Energy*, *33*(5), 943-949.

Praveen, B., Pranay, S., Jhabarmal, S., Mechanical, R. P. B. A., and Group, and O. Institutions. (2018). Fabrication of Portable Solar Thermo Electric Refrigerator by Liquid Cooling. *Int J Sci Resin Sci Technol*, *4*, 248-255.

Raghuvanshi, S., and Maheshwari, G. (2011). Analysis of ammonia–water (NH_3-H_2O) vapor absorption refrigeration system based on first law of thermodynamics. *International journal of scientific & engineering research*, *2*(8), 1-7.

Raghuwanshi, S. S., and Khare, V. (2018). Sizing and implementation of photovoltaic water pumping system for irrigation. *IAES International Journal of Artificial Intelligence*, *7*(1), 54.

Raja, V. B., and Shanmugam, V. (2012). A review and new approach to minimize the cost of solar-assisted absorption cooling system. *Renewable and Sustainable Energy Reviews*, *16*(9), 6725-6731.

Ramesh, J., Kumar, J. K., and Subbareddy, D. E. (2015). Design, Fabrication and Performance Analysis of a Parabolic Trough Solar Collector Water Heater [J]. *International Journal of Innovative Research in Science, Engineering and Technology*, *4*(7), 6038-6043.

Rasul, M., and Murphy, A. (2006, December). Solar powered intermittent absorption refrigeration unit. In *Australasian Power Engineering Conference AUPEC*.

Raut, D., Tiwari, A. K., and Kalamkar, V. R. (2021, May). Theoretical design of solar-powered vapor absorption refrigeration system coupled with latent heat energy storage. In *IOP Conference Series: Materials Science and Engineering* (Vol. 1146, No. 1, p. 012026). IOP Publishing.

Shah, N. (2014). LMTD Correction Factor Chart.

Shah, R. K., and Sekulic, D. P. (2003). *Fundamentals of heat exchanger design*. John Wiley and Sons.

Sharma, D. K., Sharma, D., & Ali, A. H. H. (2020). A state of the art on solar-powered vapor absorption cooling systems integrated with thermal energy storage. *Environmental Science and Pollution Research*, *27*(1), 158-189.

Shukla, A., Mishra, A., Shukla, D., and Chauhan, K. (2015). COP derivation and thermodynamic calculation of ammonia-water vapor absorption refrigeration system. *International journal of mechanical engineering and technology*, *6*(5), 72-81.

Siddharth, R., Jagannath, K., Giridhar, P. K., and Vishnumurthy, K. K. (2018). Design and simulation of a vapour compression refrigeration system using phase change material. In *MATEC Web of Conferences* (Vol. 144, p. 04002). EDP Sciences.

Singh, S. K., Singh, A. K., and Yadav, S. K. (2012). Design and fabrication of parabolic trough solar water heater for hot water generation. *International Journal of Engineering Research & Technology (IJERT)*, *1*(10), 1-9.

Sinha, A., and Karale, S. R. (2013). A review on Solar-Powered Refrigeration and the Various Cooling Thermal Energy Storage (CTES) Systems. *International Journal of Engineering Research &Technology ISSN*, 2278-0181.

Solanki, A., and Pal, Y. (2020). Energy and exergy evaluation of triple-effect H2O/LiBr absorption cooling system. *International Journal of Ambient Energy*, 1-12.

Syed, A., Izquierdo, M., Rodriguez, P., Maidment, G., Missenden, J., Lecuona, A., and Tozer, R. (2005). A novel experimental investigation of a solar cooling system in Madrid. *International Journal of refrigeration*, *28*(6), 859-871.

Tabassum, S., Sharmin, L., Bashar, M. S., Rahaman, M., Debnath, S. C., and Khanam, M. (2019). Design and Analysis of Parabolic Trough Solar Water Heating System. *Journal of Architectural Environment & Structural Engineering Research*, *2*(3).

Tagle-Salazar, P. D., Nigam, K. D., and Rivera-Solorio, C. I. (2020). Parabolic trough solar collectors: A general overview of technology, industrial applications, energy market, modeling, and standards. *Green Processing and Synthesis*, *9*(1), 595-649.

Tetemke, Y., Paramasivam, V., Tadele, F., and Selvaraj, S. K. (2021). Analyzed of vapor absorption refrigeration systems powered by geothermal energy: Site in Ethiopia. *Materials Today: Proceedings*.

Thulukkanam, K. (2000). *Heat exchanger design handbook*. CRC press.

Tiwari, G. N., and Tiwari, A. (2016). *Handbook of solar energy* (Vol. 498). Singapore: Springer.

Torres, H. M., Carrillo, R. A., and Torres, N. M. (2020, December). Design and construction of an experimental parabolic trough collector using low-cost alternative materials. In *AIP Conference Proceedings* (Vol. 2303, No. 1, p. 110004). AIP Publishing LLC.

Upadhyay, B. H. (2020). *Design Optimization and Performance Analysis of Solar Parabolic Trough Collector* (Doctoral dissertation, Gujarat Technological University Ahmedabad).

Uwah, E. (2020). Design and Construction of a Portable Solar Water Heater

Venkatachalam, C., and Solomon, G. (2019). Dataset of solar energy potential assessment for Adama city (Ethiopia). *Data in brief*, *24*, 103879.

Wang, J., Yan, R., Wang, Z., Zhang, X., and Shi, G. (2018). Thermal performance analysis of an absorption cooling system based on parabolic trough solar collectors. *Energies*, *11*(10), 2679.

World Health Organization. (2017). *How to calculate vaccine volumes and cold chain capacity requirements* (No. WHO/IVB/17.06). World Health Organization.

Yadav, A. S., and Agrawal, V. (2018). *Renewable Energy Sources: An Application Guide*. LAP LAMBERT Academic Publishing.

Yadav, M., and Saikhedkar, N. K. (2017). Simulation modelling for the performance of vapor absorption refrigeration system using evacuated tube collector and parabolic disc collector working in the conjugate system. *SIMULATION*, *4*(04).

Yadav, R., and Sharma, M. (2016). Analytical Study of Ammonia–Water (NH3-H2O) Vapor Absorption Refrigeration System Based on Solar Energy. *Imperial Journal of Interdisciplinary Research*, 1245-1250.

Zaki, M. (1999). *Design and Construction of a continuous solar absorption refrigeration Unit* (Doctoral dissertation, University of Khartoum).

APPENDICES

Appendix A

Table A.1 Thermophysical properties of air at atmospheric pressure

The values of μ, k, C_p and Pr are not strongly pressure-dependent and may be used over a fairly wide range of pressures.

T (K)	ρ (kg/m^3)	C_p (kJ/kg K)	μ (kg/m s $\times 10^5$)	v (m^2/s $\times 10^6$)	k (W/mk)	α (m^2/s $\times 10^4$)	Pr
100	3.9010	1.0266	0.6924	1.923	0.009246	0.02501	0.770
150	2.3675	1.0099	1.0283	4.343	0.013735	0.05745	0.753
200	1.7687	1.0061	1.3289	7.49	0.01809	0.10165	0.739
250	1.4128	1.0053	1.488	9.49	0.02227	0.13161	0.722
300	1.1774	1.0057	1.983	15.68	0.02624	0.2216	0.708
350	0.9980	1.0090	2.075	20.76	0.03003	0.2983	0.697
400	0.8826	1.0140	2.286	25.90	0.03365	0.3760	0.689
450	0.7833	1.0207	2.284	28.86	0.03707	0.4222	0.683
500	0.7048	1.0295	2.671	37.90	0.04038	0.5564	0.680
550	0.6423	1.0392	2.848	44.34	0.04360	0.6532	0.680
600	0.5879	1.0551	3.018	51.34	0.04649	0.7512	0.680
650	0.5430	1.0635	3.177	58.51	0.04953	0.8578	0.682
700	0.5030	1.0752	3.322	66.25	0.05230	0.9672	0.684
750	0.4709	1.0856	3.481	73.91	0.05509	1.0774	0.686
800	0.4405	1.0978	3.625	82.29	0.05779	1.1951	0.689
850	0.4149	1.1095	3.765	90.75	0.06028	1.3097	0.692
900	0.3925	1.1212	3.899	99.3	0.06269	1.4271	0.696
950	0.3716	1.1321	4.023	108.2	0.06525	1.5610	0.699
1000	0.3524	1.1417	4.152	117.8	0.06752	1.6779	0.702
1100	0.3204	1.160	4.44	136.6	0.0732	1.969	0.704
1200	0.2947	1.179	4.92	159.1	0.0782	2.251	0.707
1300	0.2707	1.197	4.93	182.1	0.0837	2.583	0.705
1400	0.2515	1.214	5.17	205.5	0.0891	2.920	0.705
1500	0.2355	1.230	5.40	229.1	0.0946	3.262	0.705
1600	0.2211	1.248	5.63	254.5	0.100	3.609	0.705

* From *National Bureau of Standards* (USA), Circ, 564, 1955.

Appendix B

Table B Thermophysical properties of refrigerants

Table B.1 Viscosity of saturated liquid refrigerants in (cP)

Temp. °C	R123	R134a	R22	R290	R717
– 40	.986	.472	.343	.201	.281
– 30	.848	.406	.305	.181	.244
– 20	.735	.353	.272	.164	.214
– 10	.642	.309	.243	.149	.190
0	.565	.271	.218	.137	.171
+ 10	.499	.239	.196	.126	.153
+ 20	.443	.211	.175	.116	.138
+ 30	.394	.186	.157	.101	.126
+ 40	.352	.163	.139	.090	.114
+ 50	.316	.143	.123	.079	.098

Table B.2 Viscosity of saturated vapour refrigerants in (cP)

Temp. °C	R123	R134a	R22	R290	R717
– 40	.0088	.00912	.01013	.0063	.00786
– 20	.0097	.00992	.01074	.00691	.00842
0	.0102	.01073	.01164	.00745	.00906
+ 20	.0108	.01158	.01272	.00809	.00968
+ 40	.0114	.01255	.01354	.00905	.01030

Table B.3 Thermal conductivity of saturated liquid refrigerants in (W/m. K)

Temp. °C	R123	R134a	R22	R290	R717
– 40	.096	.1106	.12	.127	.688
– 20	.090	.1011	.11	.114	.622
0	.084	.0920	.1	.1040	.559
+ 20	.078	.0833	.09	.0961	.410
+ 40	.072	.0747	.08	.0870	.444

Table B.4 Thermal conductivity of saturated Vapour refrigerants in (W/m. K)

Temp. °C	R123	R134a	R22	R290	R717
– 40	.00549	.00817	.00709	.01176	.02065
– 20	.00661	.00982	.00817	.01363	.02177
0	.00774	.01151	.00942	.01574	.02337
+ 20	.00889	.01333	.01095	.01825	.02638
+ 40	.01008	.01544	.01302	.02145	.02838

* *ASHRAE Fundamentals Handbook*, 2005.

Table B.5 Constant pressure specific heat of liquid refrigerants in (kJ/kg. K)

Temp. °C	R123	R134a	R22	R290	R717
– 40	.948	1.255	1.10	2.26	4.414
0	.990	1.341	1.17	2.51	4.617
+ 40	1.038	1.408	1.34	2.93	4.932

Table B.6 Constant pressure specific heat of saturated vapour refrigerants in (kJ/kg. K)

Temp. °C	R123	R134a	R22	R290	R717
– 40	.585	.749	0.608	1.474	2.244
– 20	.617	.816	0.665	1.615	2.425
0	.651	.807	0.739	1.787	2.680
+ 20	.686	1.001	0.84	2.006	3.028
+ 40	.724	1.145	0.997	2.317	3.51

Table B.7 Surface tension of refrigerants in (mN/m)

Temp. °C	R123	R134a	R22	R290	R717
– 40	23.19	17.60	17.94	15.53	42.26
– 30	21.92	16.04	16.34	14.14	43.52
– 20	20.66	14.51	14.76	12.78	39.88
– 10	19.41	13.02	13.21	11.44	36.34
0	18.18	11.56	11.70	10.13	32.91
+ 10	16.97	10.14	10.22	8.84	29.59
+ 20	15.77	8.76	8.78	7.59	26.38

Appendix C

Table C.1 Properties of ammonia solution at different mean temperature and Concentration (Green and Perry,2008).

Mean temperature (°C)	Concentration	Specific heat (C_p) ($kJ/kg.K$)	Thermal conductivity (k) ($W/ m.K$)	Density (ρ) (kg/m^3)	Dynamic viscosity (μ) ($\times 10^{-4}$ $kg/m.s$)	Prandtl number
57.5	0.43	4.6	0.505	813	3.29	2.9
33	0.43	4.437	0.535	844.6	5.51	2.72
52	0.42	4.558	0.513	823.45	3.22	2.86

Table C.2 Properties of ammonia (Manojprabhakar *et al*., 2014)

1	Molecular weight	17
2	Boiling point (°C)	-33 to -35
3	Freezing point (°C)	77.7
4	Critical temperature (°C)	133
5	Critical pressure(bar)	112.8
6	Specific heat ($kJ/kg.K$) 0°C 100°C 200°C	 2.0972 2.2262 2.1056

Appendix D

Table D.1 Thermo physical property of R717(Ammonia)

Temp.	*Pressure*	*Specific Volume* (m^3/kg)		*Enthalpy* (kJ/kg)		*Entropy* kJ/kg.K)	
(°C)	(bar)	$v_f \times 10^3$	v_g	h_f	h_g	s_f	s_g
–60	.2199	1.40	4.685	–69.5	1373.2	–0.1095	6.6592
–55	.3029	1.41	3.474	–47.5	1382.0	–0.0071	6.5454
–50	.4103	1.42	2.617	–25.4	1390.6	0.0926	6.4382
–45	.5474	1.43	2.000	–3.3	1399.0	0.1904	6.3369
–40	.7201	1.45	1.547	18.9	1407.2	0.2865	6.2410
–35	.9349	1.46	1.212	41.2	1415.2	0.3808	6.1501
–30	1.1990	1.48	.961	63.6	1422.8	0.4735	6.0636
–28	1.3202	1.48	.878	72.5	1425.8	0.5101	6.0302
–26	1.4511	1.48	.809	81.5	1428.7	0.5465	5.9974
–25	1.5216	1.49	.770	86.0	1430.2	0.5646	5.9813
–24	1.5922	1.49	.737	90.5	1431.6	0.5827	5.9652
–22	1.7441	1.49	.677	99.6	1434.4	0.6186	5.9336
–20	1.9074	1.50	.622	108.6	1437.2	0.6543	5.9025
–18	2.0826	1.50	.573	117.7	1439.9	0.6898	5.8720
–16	2.2704	1.51	.528	126.7	1442.6	0.7251	5.8420
–15	2.3709	1.52	.508	131.3	1443.9	0.7426	5.8223
–14	2.4714	1.52	.488	135.8	1445.2	0.7601	5.8125
–12	2.6863	1.53	.451	144.9	1447.7	0.7950	5.7835
–10	2.9157	1.53	.417	154.2	1450.2	0.8296	5.7550
–9	3.0360	1.53	.402	158.6	1451.4	0.8469	5.7409
–8	3.1602	1.54	.387	163.2	1452.6	0.8641	5.7269
–7	3.2884	1.54	.373	167.8	1453.8	0.8812	5.7131
–6	3.4207	1.54	.359	172.4	1455.0	0.8983	5.6993
–5	3.5571	1.55	.346	176.9	1456.1	0.9154	5.6856
–4	3.6977	1.55	.334	181.6	1457.2	0.9324	5.6721
–3	3.8426	1.55	.322	186.2	1458.4	0.9493	5.6586
–2	3.9920	1.56	.310	190.8	1459.5	0.9663	5.6453
–1	4.1458	1.56	.299	195.4	1460.6	0.9831	5.6320
0	4.3043	1.57	.289	200.0	1461.7	1.0000	5.6189
1	4.4674	1.57	.279	204.6	1462.7	1.0167	5.6058
2	4.6353	1.57	.269	209.3	1463.8	1.0335	5.5929
3	4.8081	1.57	.260	213.9	1464.8	1.0502	5.5800
4	4.9859	1.58	.251	218.5	1465.8	1.0669	5.5672
5	5.1687	1.58	.243	223.2	1466.8	1.0835	5.5545
6	5.3567	1.59	.235	227.8	1467.8	1.1001	5.5419
7	5.5500	1.59	.227	232.5	1468.8	1.1167	5.5294
8	5.7487	1.59	.219	237.1	1459.7	1.1332	5.5170
9	5.9528	1.60	.212	241.8	1470.7	1.1496	5.5046
10	6.1625	1.60	.205	246.5	1471.5	1.1661	5.4924

(Contd)

Temp.	Pressure	Specific Volume (m^3/kg)		Enthalpy (kJ/kg)		Entropy kJ/kg.K)	
(°C)	(bar)	$v_f \times 10^3$	v_g	h_f	h_g	s_f	s_g
11	6.3778	1.60	.198	251.2	1472.5	1.1825	5.4802
12	6.5989	1.61	.192	255.9	1473.3	1.1988	5.4681
13	6.8259	1.61	.186	260.6	1474.2	1.2152	5.4561
14	7.0588	1.61	.180	265.3	1475.4	1.2314	5.4441
15	7.2979	1.62	.174	270.0	1475.9	1.2477	5.4322
16	7.5431	1.62	.169	274.8	1476.2	1.2639	5.4204
17	7.7946	1.62	.164	279.5	1477.5	1.2801	5.4087
18	8.0525	1.63	.158	284.8	1478.3	1.2963	5.3971
19	8.3169	1.63	.154	289.0	1479.0	1.3124	5.3855
20	8.5879	1.64	.149	293.8	1479.8	1.3285	5.3740
21	8.8657	1.64	.144	298.5	1480.5	1.3445	5.3626
22	9.1503	1.64	.140	303.3	1481.2	1.3606	5.3512
23	9.4418	1.65	.136	308.4	1481.9	1.3765	5.3399
24	9.7403	1.65	.132	312.9	1482.5	1.3925	5.3286
25	10.046	1.66	.128	317.7	1483.2	1.4084	5.3175
26	10.359	1.66	.124	322.5	1483.8	1.4243	5.3063
27	10.680	1.67	.128	327.3	1484.4	1.4402	5.2953
28	11.007	1.67	.117	332.1	1485.0	1.4560	5.2843
29	11.343	1.67	.114	336.9	1485.8	1.4718	5.2733
30	11.686	1.68	.110	341.8	1486.1	1.4876	5.2624
31	12.037	1.68	.107	346.6	1486.7	1.5033	5.2516
32	12.396	1.69	.104	351.5	1487.2	1.5191	5.2408
33	12.763	1.69	.101	356.3	1487.7	1.5348	5.2300
34	13.139	1.70	.098	361.2	1488.1	1.5504	5.2193
35	13.522	1.70	.096	366.1	1488.6	1.5660	5.2086
36	13.915	1.71	.092	370.9	1489.0	1.5816	5.1980
37	14.314	1.71	.090	375.9	1489.4	1.5972	5.1874
38	14.724	1.72	.088	380.8	1489.8	1.6128	5.1768
39	15.143	1.72	.085	385.7	1490.1	1.6283	5.1663
40	15.570	1.72	.083	390.6	1490.4	1.6437	5.1558
41	16.006	1.73	.080	395.5	1490.7	1.6592	5.1453
42	16.451	1.73	.078	400.4	1490.9	1.6747	5.1349
43	16.906	1.74	.076	405.4	1491.2	1.6901	5.1244
44	17.370	1.74	.074	410.4	1491.4	1.7055	5.1140
45	17.843	1.75	.072	415.4	1491.5	1.7209	5.1036
46	18.326	1.75	.070	420.4	1491.7	1.7363	5.0932

Appendix E

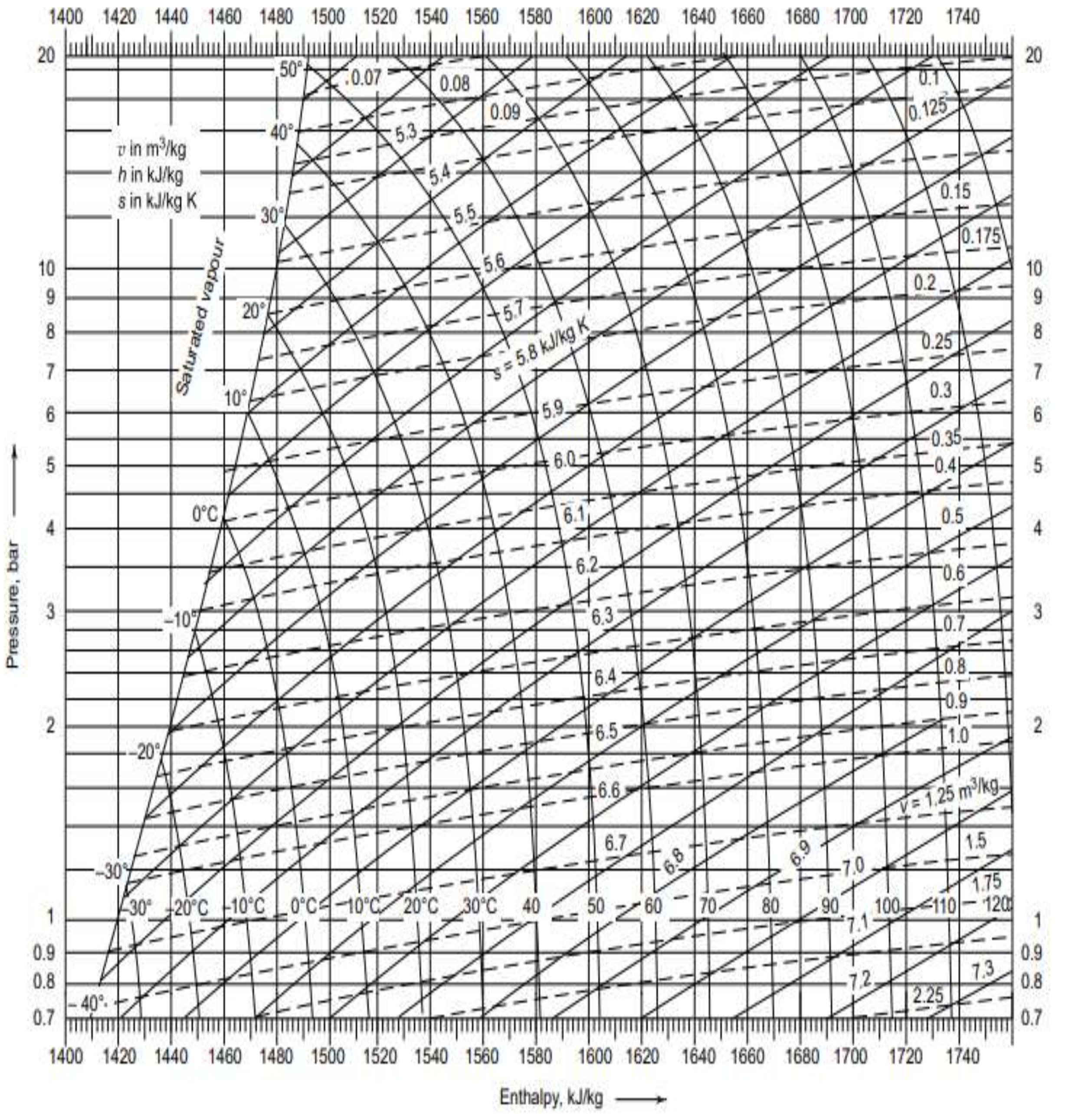

Figure E.1 Pressure Enthalpy Diagram of R717(ammonia) Vapour

Appendix F

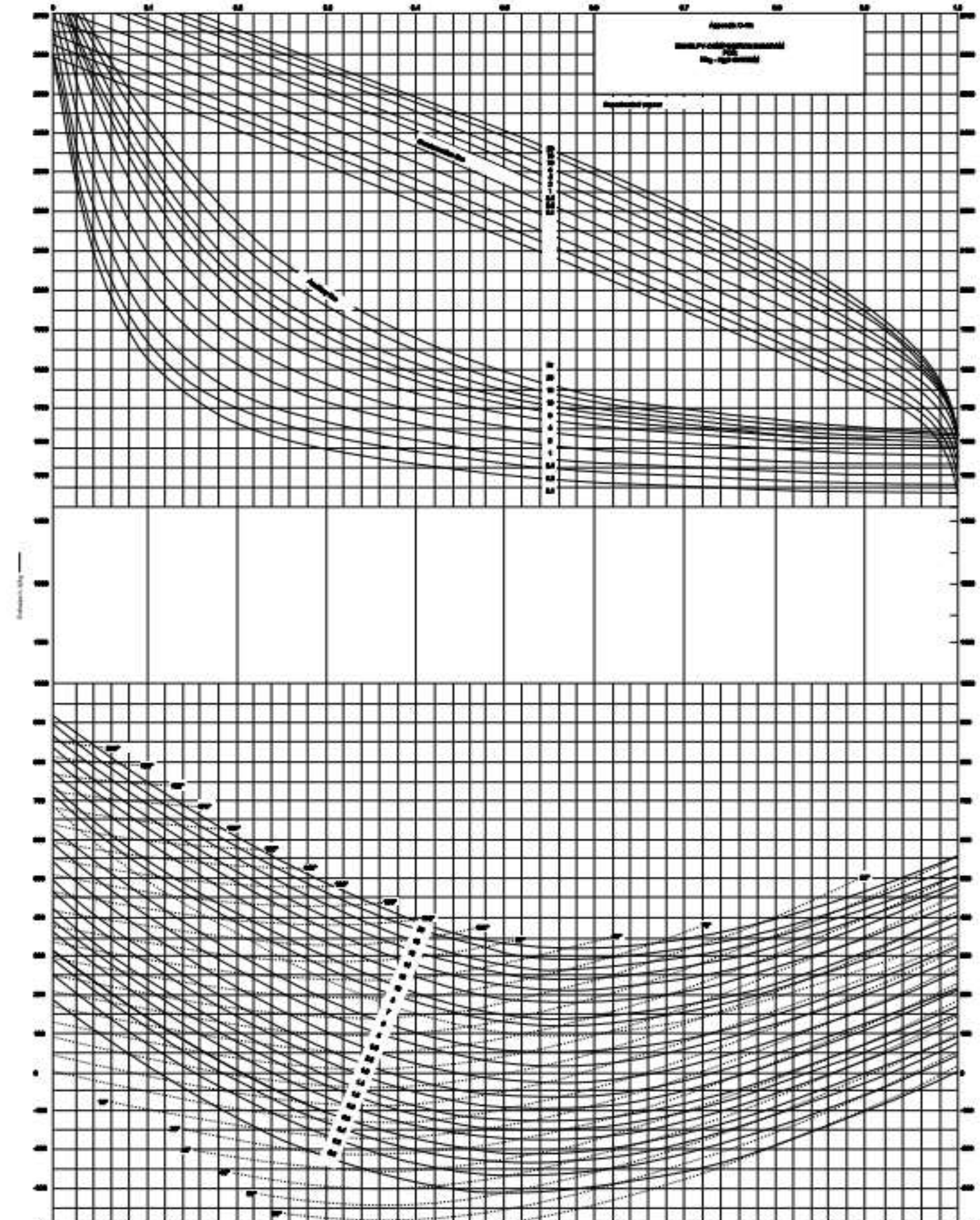

Figure F.1 Enthalpy-Composition Diagram for NH3-H20 System

Appendix G

Table G.1 Enthalpy and concentration at various state point

State point	P bar	T °C	Concentration Kg of NH_3 /kg of solution	Enthalpy, kJ/kg
1	4.6	27	0.47	27
2	11	27	0.47	27
3	11	39	0.47	195
4	11	70	0.43	200
5	11	28	0.43	46
6	4.6	28	0.43	46
7	11	70	0.95	1610
8	11	28	0.95	332.1
9	4.6	2	0.95	332.1
10	4.6	2	0.95	1463.8

Appendix H: Temperature Outlet of Parabolic Trough Solar Collector (PTSC)

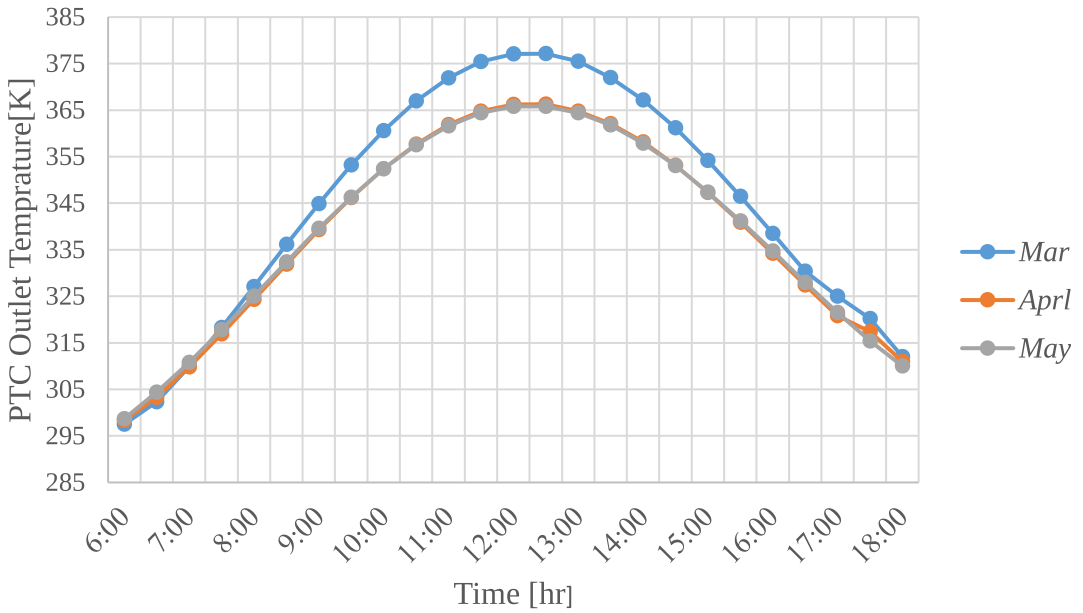

Figure H.1 Hourly outlet temperature of parabolic trough solar collector in representative day of spring seasons.

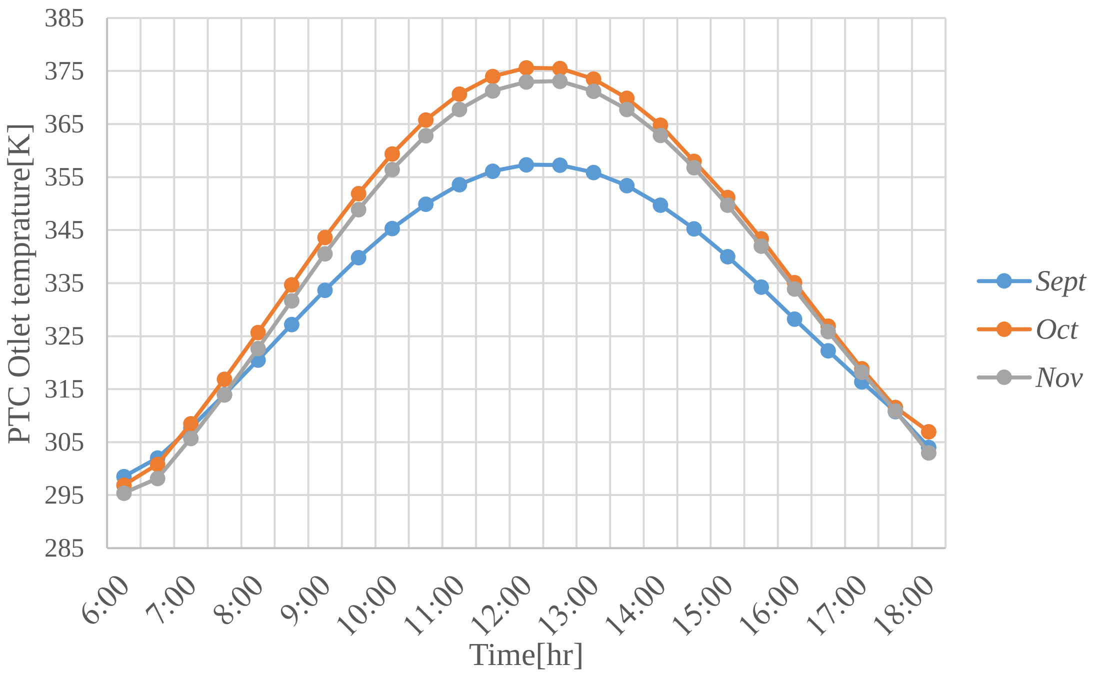

Figure H.2 Hourly outlet temperature of parabolic trough collector in representative day of Autumn seasons.

Appendix I: Useful Energy Gain by Parabolic Trough Solar Collectors

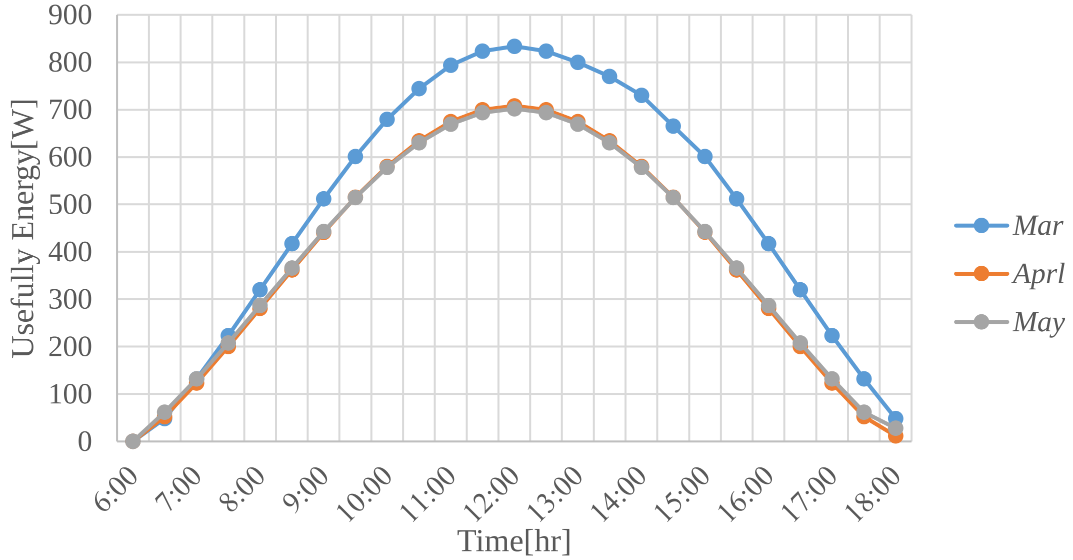

Figure I.1 Hourly useful energy gain of parabolic trough solar collector in representative days of spring seasons

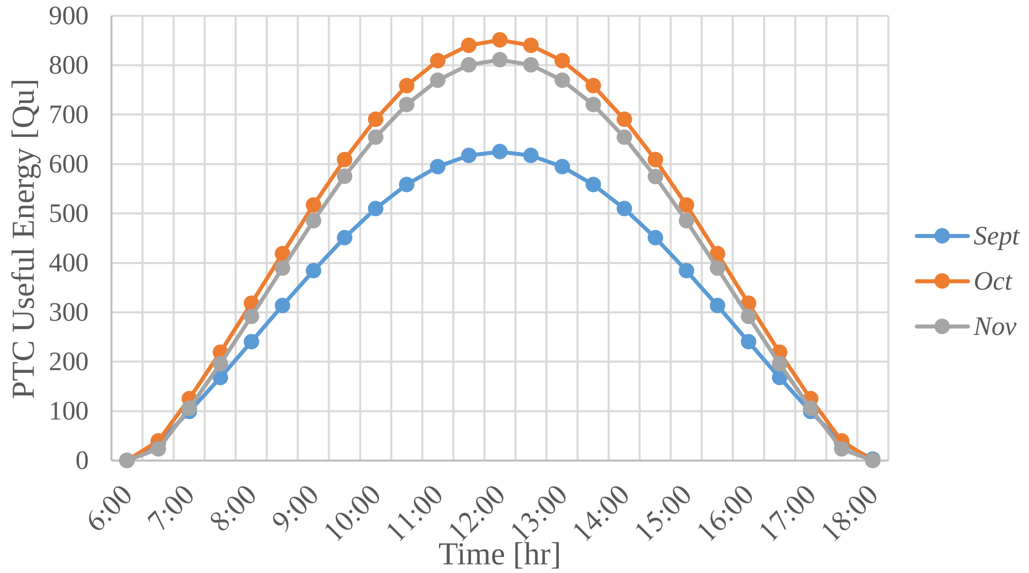

Figure I.2 Hourly useful energy gain of parabolic trough solar collector for representative days of Autumn seasons

Appendix J: Thermal Efficiency of parabolic trough solar collector

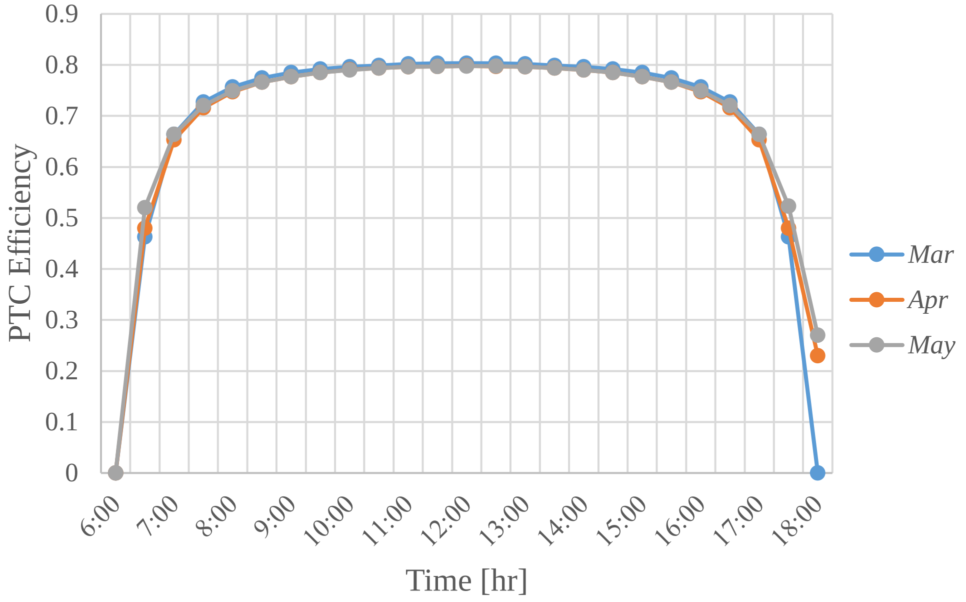

Figure J.1 Thermal efficiency of parabolic trough solar collector in representative days of Spring seasons

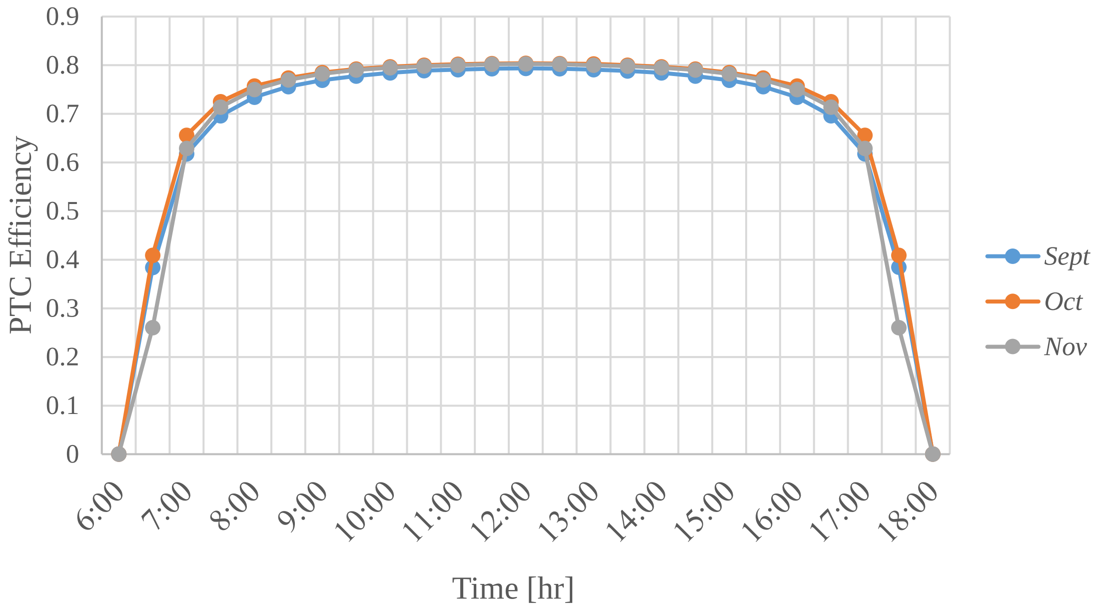

Figure J.2 Thermal efficiency of parabolic trough solar collector in representative days of Autumn seasons

Appendix K: Calibration of thermocouple thermometer

Calibration of thermometer can be carried out by comparing the reading value of the thermometer in parallel with the reading value of a reference thermometer while performing water boiling and cooling test. In this study calibration test for K-type thermometer was conducted in ASTU Thermal laboratory by using digital thermometer as a reference thermometer. For the calibration 1Kg of water is boiled and cooled for 45minutes.

Figure K.1: Calibration set up

Table K.1 Water temperature measuring test by using K-type thermocouples and digital thermometer

Time, t(minutes)	Digital thermometer reading, T_1 (^{0}c)	K-type thermocouple reading, T_2 (^{0}c)	Uncertainty(^{0}c) $T_1 - T_2$	Percentage uncertainty (%) $\frac{T_1 - T_2}{T_1} \times 100\%$
1	26.9	26.6	0.3	1.1
2	29.1	28.9	0.2	0.6
3	30.4	30.2	0.2	0.6
4	32.8	32	0.8	2.4
5	35.4	34.3	1.1	3.1
6	37.6	37	0.6	1.5
7	39.4	38.8	0.6	1.5
8	42	41.1	0.9	2.1
9	45.9	45.5	0.4	0.8

10	51	49.7	1.3	2.5
11	51.5	51.4	0.1	0.2
12	54	53	1	1.8
13	57	56.5	0.5	0.8
14	58.5	57.7	0.8	1.3
15	61.7	61	0.7	1.1
16	62.5	62	0.5	0.8
17	65.6	64.7	0.9	1.3
18	67.4	66.8	0.6	0.8
19	68.7	68.4	0.3	0.4
20	68.7	68.5	0.2	0.2
21	71.4	71.3	0.1	0.1
22	73.7	73.1	0.6	0.8
23	76.2	75.3	0.9	1.1
24	77.7	77.3	0.4	0.5
25	78.9	78.6	0.3	0.3
26	80.5	79.9	0.6	0.7
27	81.3	80.9	0.4	0.4
28	82.4	82	0.4	0.4
29	83.3	83	0.3	0.3
30	84.3	84.2	0.1	0.1
31	85.4	85	0.4	0.4
32	86.5	86	0.5	0.5
33	88.5	88.3	0.2	0.2
34	89.3	89	0.3	0.3
35	90.5	90.4	0.1	0.1
		Average	0.502857	0.9

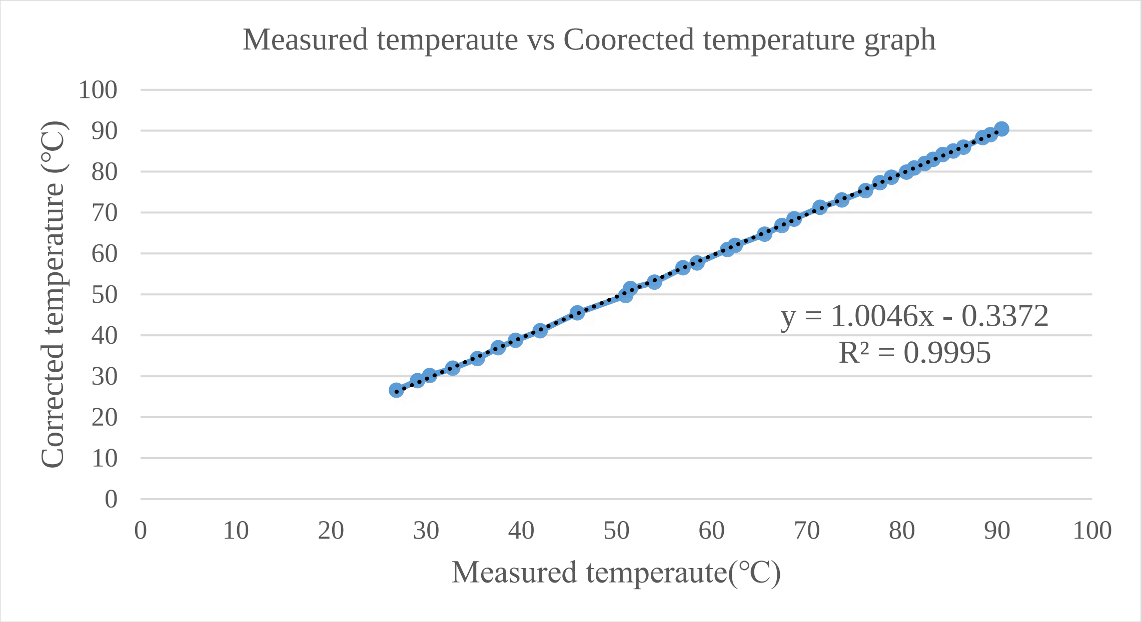

Four-Channel Digital Thermometer Specifications

- Serial number: HT-9815
- Temperature range:0-800℃
- Power supply: 9V
- Weight: approx. 250g

Appendix L: **Photo during the Experimental and development of prototypes**